Trends in Bioprocess Development

ARTICLE COLLECTION

Sponsored by:

WILEY

SARTORIUS

Label Free. Stress Free. Discover the Octet® R Series

Tackle analytical complexity with the Octet® R series, a field-upgradeable, label-free biomolecule analysis platform. With three different models to choose from, users can strike the right balance between throughput needs and budget. All systems offer an advanced, fast, robust and fluidics-free approach for protein-protein and protein-small molecule analysis to make pivotal decisions throughout biologics development, and manufacturing.

Explore more at **www.sartorius.com/octet**

Simplifying Progress

SARTORIUS

Contents

Foreword

Biopharmaceuticals are the hopefuls in the fight against major public diseases and their development is being pursued vigorously worldwide. For the development and production of biopharmaceuticals, the optimization of processes is crucial in order to bring new therapeutics to market as quickly and cost-effectively as possible. In the development of such methods, scientists are dependent on state-of-the-art instruments and technologies, as can be seen from this Article Collection: here you can find cutting-edge research and application articles describing the development of upstream and downstream processes.

Special attention is paid to the development of continuous bioprocesses, which have the potential to significantly improve the product quality as well as profitability. As stated in this collection's first article (page 5), continuous manufacturing is the 'future production method for monoclonal antibodies' (mAbs) – and thus not only of the greatest medical but also of economic relevance. Three of the six drugs worldwide with the highest annual sales (2020) were based on mAbs [1]. In this article, the authors evaluate whether batch and continuous downstream processing lead to comparable results regarding product quality attributes when performing a side-by-side comparability study.

Despite the great advantages of continuous or semi-continuous over batch-based processes, there are some challenges that need to be addressed. In the comprehensive review article on page 15, you can read more about recent advances and ongoing obstacles faced during the use of advanced process analytical technologies, process modeling, and control strategies to enable continuous manufacturing of mAbs. It also discusses how advanced continuous manufacturing approaches that have been adapted by other industries could be implemented for mAbs production in the near future.

Continuous and semi-continuous process are of growing importance in the biomanufacturing of other classes of therapeutic proteins as well. One promising approach is perfusion-based upstream-processes, but the lack of appropriate scale-down models is making the development of these processes more difficult. This problem has been addressed by the authors of the research article which you can find on page 27. Therein, the development of a semi-continuous scale-down procedure for the high-throughput screening and optimization of perfusion bioreactors is described.

Another major challenge in the production of biopharmaceuticals is discussed in the article starting on page 46: The purification of biomolecules to obtain a safe and stable product. In their extensive study of the mechanism of copurification of host cell proteins (HCPs), the authors identified the "difficult to remove" HCPs that are present in marketed mAbs. By elucidating the underlying interactions of mAbs and HCPs, this work can help identifying the crucial residues responsible for mAb-HCPs interaction.

Of utmost importance for a successful biomanufacturing program is efficient and effective cell line screening. In the study presented on pages 59-70, the analysis of a 24-Deep Well Plate based screening strategy for the production of an industrially relevant biopharmaceutical and its comparison to the industry-standard shake flask is reported. The authors demonstrate that this cell line screening strategy can be successfully used to efficiently select cell lines for future production campaigns, while saving development time and reducing costs and labor.

This Article Collection concludes with an application note from Sartorius, in which the utilization of Octet instruments for protein quantitation, cell line development, early clone selection, and for many more applications is presented. It is demonstrated how these versatile instruments, unlike many other bioanalytical tools, offer a combination of structural and functions assessment in the same system. Thus they support many stages of the drug development and manufacturing process. On pages 71-80, you can learn more about how these instruments will help you in enhancing the efficiency in process development and the manufacturing of biotherapeutics.

References

[1] Annika Holzgreve, Roman Skudas: Enhancing the efficiency of pharmaceutical drugs – Glycovariant separation using mixed mode resin, Wiley Analytical Science 2021; https://analyticalscience.wiley.com/do/10.1002/was.0001877.

RESEARCH ARTICLE

BIOTECHNOLOGY PROGRESS

Semi-continuous scale-down models for clone and operating parameter screening in perfusion bioreactors

Jean-Marc Bielser[1,2] | Jakub Domaradzki[1] | Jonathan Souquet[1] | Hervé Broly[1] | Massimo Morbidelli[2]

[1]Biotech Process Sciences, Merck Biopharma, Vevey, Switzerland

[2]Department of Chemistry and Applied Biosciences, Institute for Chemical and Bioengineering, ETH Zürich, Zürich, Switzerland

Correspondence
Jean-Marc Bielser, Biotech Process Sciences, Merck Biopharma
Vevey, Switzerland.
Email: jean-marc.bielser@merckgroup.com
Massimo Morbidelli, Department of Chemistry and Applied Biosciences, Institute for Chemical and Bioengineering, ETH Zürich, Zürich, Switzerland.
Email: massimo.morbidelli@chem.ethz.ch

Perfusion cell culture, confined traditionally to the production of fragile molecules, is currently gaining broader attention in the biomanufacturing of therapeutic proteins. The development of these processes is made difficult by the limited availability of appropriate scale-down models. This is due to the continuous operation that requires complex control and cell retention capacity. For example, the determination of an optimal perfusion and bleed rate for continuous cell culture is often performed in scale-down bioreactors and requires a substantial amount of time and effort. To increase the experimental throughput and decrease the required workload, a semi-continuous procedure, referred to as the VCD_{max} (viable cell density) approach, has been developed on the basis of shake tubes (ST) and deepwell plates (96-DWP). Its effectiveness has been demonstrated for 12 different CHO-K1-SV cell lines expressing an IgG1. Further, its reliability has been investigated through proper comparisons with perfusion runs in lab-scale bioreactors. It was found that the volumetric productivity and the $CSPR_{min}$ (cell specific perfusion rate) determined using the ST and 96-DWP models were successfully (mostly within the experimental error) confirmed in lab-scale bioreactors, which then covered a significant scale-up from the half milliliter to the liter scale. These scale-down models are very useful to design and scale-up optimal bioreactor operating conditions as well as screening for different media and cell lines.

KEYWORDS
cell culture, perfusion, scale-down, screening, semi-continuous

1 | INTRODUCTION

Although fed-batch remains the most widely used bioreactor operating mode in the biomanufacturing industry, perfusion-based upstream processes are receiving increasing consideration.[1–5] The main characteristic of perfusion is continuous media addition and toxic waste removal, which coupled with an appropriate cell retention device, allow reaching higher cell densities compared to traditional fed-batch systems. Continuous operation of a production bioreactor is interesting for its process intensification potential, but also for its stable operation and low-residence time that lead to more consistent product quality.[3,6] Hence, perfusion is more and more widely considered and, in addition, continuous manufacturing is encouraged by the regulatory authorities such as FDA.[4,7,8] Nevertheless, many practical factors such as acceptance for change, long-term operation, and development timelines are still limiting the establishment of this technology.[5,9]

Process design and development is supported in the case of fed-batch by various screening procedures, which are by now consolidated and widely accepted.[10–14] Similar tools are needed for the development of perfusion bioreactors. This refers particularly to scale-down models, which are complicated by technical limitations, specifically related to the realization of continuous flow and cell retention in the milliliters scale and even smaller. Semi-continuous operations have been proposed to approximate continuous flows and to evaluate the performance of

high-density perfusion cultures in shake flasks and shake tubes[15–18] in the milliliters scale. In this work, we make a further step in this direction and develop a scale-down semi-continuous procedure for predicting growth and productivity in perfusion systems, which is also extended to the 96-DWP unit in the microliters scale.

The developed procedure mimics a perfusion process at constant perfusion rate. In particular, the viable cell density (VCD) is first measured, then the supernatant is separated from the cells to remove a certain fraction of it and replace it with fresh media, before resuspending the cells as schematically illustrated in Figure 1. This is repeated on a daily basis until reaching the maximum VCD that can be sustained by the system. This procedure, in the following referred to as the VCD_{max} experiment, can, for example, be applied to various scale-down models or high throughput units such as ST or 96-DWP, thus significantly increasing the experimental throughput for screening applications.

To demonstrate the reliability of this procedure, we have applied it to a set of 12 CHO-K1-SV cell lines expressing an IgG1, issued from a previous screening based on fed-batch mode,[12] using both 96-DWP and ST. The results are compared, with respect to clone screening, in terms of the VCD_{max} and the corresponding volumetric productivities. These values should be similar to the corresponding quantities in a continuous system, with the assumption that the cells behave similarly in a controlled steady state at VCD_{max} and during the 24 hr before the sampling at VCD_{max} in the semi-continuous experiment.

Next, we tested the reliability of the above results obtained at the milliliters- and microliters-scale at the larger L scale using perfusion lab-scale bioreactors. For this, we selected four clones for illustrative purposes: two are among the top performing ones and two are selected because exhibiting some different phenotypic characteristics in terms of growth and/or productivity. With these clones, a *push-to-low* approach with a fixed perfusion rate was performed in 3.5 L bioreactors to identify the maximum achievable cell density for the different cell lines for the fixed medium and perfusion rate.[19] The obtained $CSPR_{min}$ values were then compared to those found above with the scale-down model experiments (96-DWP and ST). Finally, to confirm the feasibility of the operating conditions defined in this experimental approach, two of the four clones were selected for a production, run to demonstrate stable operation for 15 days.

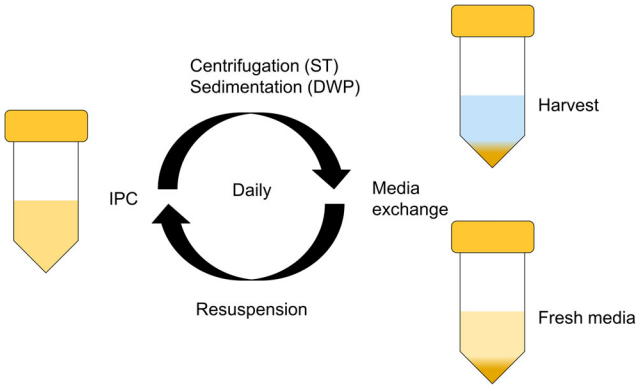

FIGURE 1 Schematic of small-scale semi-continuous cell culture to mimic perfusion at constant perfusion rate. In process control (IPC) is made on a daily basis to determine the cell density. In particular, the shake tubes (ST) or deepwell plates (96-DWP) are centrifuged or sedimented to separate the cells from the depleted media that can be removed and is considered as the harvest. The mAb concentration is measured in this fraction. Then, fresh media is added to the original volume, and the cell resuspended. This set of operation was performed on a daily basis with a total media exchange for ST, and a 50% media exchange for the 96-DWP

The outcome of this experimental study is twofold. First, it shows that the VCD_{max} experiment described here can be used to design appropriate process conditions, using the $CSPR_{min}$ concept, and scale them up at the bioreactor scale. Second, the procedure at small scale offers significant advantages in terms of experimental throughput. Potentially, hundreds of conditions can be tested in 96-DWP. This offers a new tool for screening media and cell lines appropriate for perfusion processes. Although ST allow lower throughput than 96-DWP because the handling is manual, they can be very convenient due to their simplicity and availability in any cell culture lab, particularly for smaller experimental designs.

2 | MATERIAL AND METHODS

2.1 | Cell culture media

The perfusion cell culture medium used in this study was derived from a proprietary chemically defined fed-batch platform medium that was itself derived from DMEM/F12 medium. Several components were enriched based on the consumption rates observed in prior experimental campaigns.

2.2 | Cell line

Twelve CHO-K1-SV cell lines expressing an IgG1 (Immunoglobuline G, subclass 1) were used in this study. They are issued from a single transfection pool and were selected for their differences in terms of growth and productivity as described in a previous study.[12]

2.3 | Semi-continuous cell culture

Fifty milliliter shake tubes (TubeSpin Bioreactor 50 by TPP, Switzerland) were used at a working volume of 15 ml. During cultivation, the shake tubes were incubated at 36.5°C, 5% CO_2, and 320 rpm agitation (ISF1-X, Adolf Kuhner, Birsfleden, Switzerland). Daily operations included the following: a sample was taken for cell quantification, the shake tubes were centrifuged (5 min, 200*g*), the supernatant was removed and filtered for mAb quantification. Fresh medium was then added to the culture to recover the initial working volume and the pellet was resuspended (Figure 1). The exchange volume was mimicking a perfusion rate of 1 volume media/volume culture/day (VVD). The shake tube was then placed back in the initial cell culture conditions. It is worth noting that in this way the average volume exchange rate in the two units is the same, however the compositions are different as in the shake tube, they obviously change in time.

Cell cultures in 96-DWP (Greiner Bio-One, Austria) were incubated in the same conditions as the shake tubes. Each well contains

450 µl of cell suspension. Liquid handling was performed using a robotic platform (Biomek FX, Beckman-Coulter, Fullerton, CA). Daily operations included the following: a sample was taken for cell quantification. Prior to medium exchange, the cells were settled for 30 min in static conditions at 36.5°C, 5% CO_2, then the clarified supernatant was removed by aspiration and kept aside for mAb quantification. Fresh medium was then added to the culture to recover the initial working volume (Figure 1). The exchange volume used here was half the culture volume, thus mimicking a perfusion rate of 0.5 VVD. The reason for using a lower exchange volume than in shake tubes is the difficulty in controlling the height of the pipetting tip which could lead to cells removal by aspiration. In addition, the cell pellet is less dense than the one issued by centrifugation and can also be of different volume depending on the condition.

The duration of the experiment might vary depending on the cell line and media. The parameter VCD_{max} is identified as the highest cell density reached before the first decay. After this first maximum, due to the continuous media exchange, the cell culture typically starts oscillating between higher and lower cell densities, which however are not related to the maximum value that can be achieved by the culture. In general, a duration between 10 and 14 days was enough to determine the VCD_{max}. It is worthwhile to note that the sampling for cell count corresponds to a certain amount of cell removal which somehow mimics the bleed stream in the continuous set-up. In this case, this corresponds to about 6 and 10% culture volume for ST and 96-DWP, respectively.

2.4 | Perfusion bioreactors

A total of 3.5 L perfusion bioreactors (Biostat B, Sartorius, Goettingen, Germany) were operated using a fixed medium inlet flow (perfusion rate), as shown in Figure 2. Alternating tangential flow filtration (ATF, Repligen, Waltham, MA) was used for cell retention. The bioreactor volume was controlled with a feedback from the bioreactor weight to the harvest pump. An online biocapacitance signal (Incyte, Hamilton, Bonaduz, Switzerland) was used to control the bleed stream and, therefore, maintain the cell biomass at the target set-point.[20,21] A 15 ml sample was collected daily for cell count and mAb quantification.

2.5 | Perfusion screening runs

To find the optimal operating conditions for the four clones in a perfusion set-up, a *push-to-low* approach was used, meaning that the CSPR was sequentially decreased by increasing the VCD at a constant perfusion rate.[18,21] The perfusion rate was controlled by fixing the pump speed (rpm) and led to slightly different values for the four clones: 1.24 ± 0.07, 1.30 ± 0.10, 1.14 ± 0.11, and 1.16 ± 0.23 VVD, respectively. The biocapacitance set-points were each maintained for 4 days and were increased stepwise until the bleed flow was near or below 15% of the total perfusion rate. The capacitance set-points were fixed at 40, 50, 60, and finally 70 pF/cm. These four steps are referred in the following as set-points 1–4 (or SP1 to SP4), respectively. The perfusion rate was kept in the order of 1 VVD so as to create a fair amount of biomass, without overtaking operational limitations such as insufficient oxygen supply.[18,20]

2.6 | Perfusion confirmation runs

Clones 1 and 2 were selected to perform a longer perfusion run to check the system's stability. The set-up was similar to the screening bioreactors, and the biocapacitance target was directly set to 70 pF/cm and kept constant for about 15 days. The growth phase lasted about 10 days and the stable steady-state operating phase, or production phase, lasted from day 10 to 25.

2.7 | Analytical methods for cell culture

For experiments performed in 96-DWP, cell counts and cell viability were determined using a Guava easyCyte (Merck Millipore, Darmstadt, Germany) and mAb quantification was performed with an Octet QK system (Pall ForteBio, Portsmouth, United Kingdom). For experiments

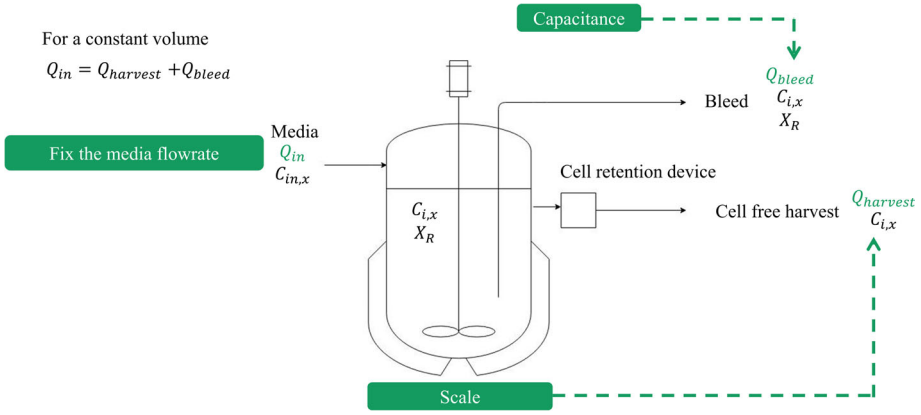

FIGURE 2 Schematic of a perfusion bioreactor and the corresponding control system. The media inlet flowrate (Q_{in}) was fixed based on the set-point of a volumetric pump. The harvest stream ($Q_{harvest}$) was controlled to keep constant the overall bioreactor weight. The bleed stream (Q_{bleed}) was controlled based on the capacitance sensor. With the assumption, the bioreactor is a perfectly mixed system and that the cell retention device retains only the cells, the concentrations inside the bioreactor, in the bleed stream and in the harvest stream are the same. The cell concentration in the bioreactor and in the bleed stream is also equivalent

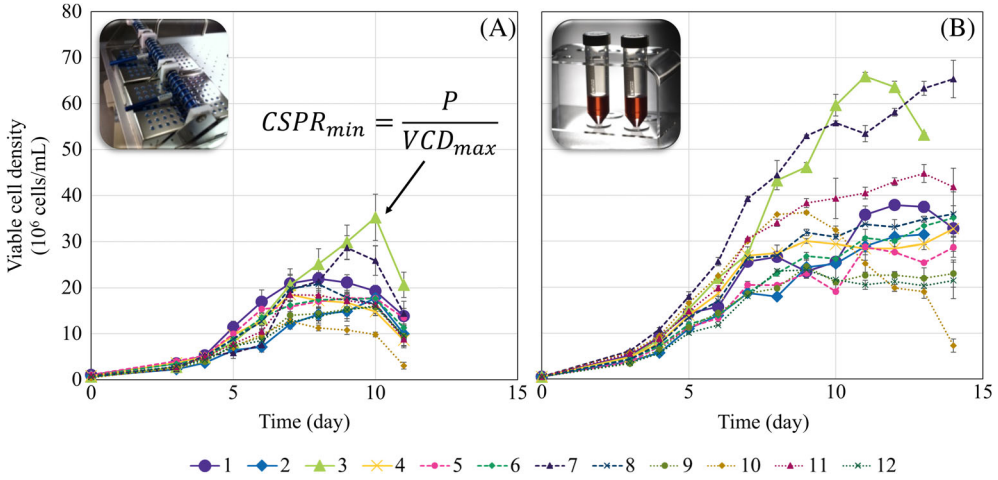

FIGURE 3 Viable cell density profiles of 12 different clones during a VCD_{max} experiment in deepwell plates (a) with 0.5 VVD (n = 8) and in shake tubes (b) with 1 VVD (n = 2). For each clone, the $CSPR_{min}$ was calculated when the VCD_{max} was reached, by dividing the perfusion rate by the cell density, as indicated in (a)

performed in shake tubes and 3.5 L bioreactors, cell counts and viability were performed using a Vi-Cell analyzer (Beckman Coulter, Brea, CA) and mAb quantification was performed with a Biacore C instrument (GE Healthcare, Waukesha, WI). Protein quality was measured on Phytips eluates (Phytips, PhYNexus, San Jose, CA). Charge variants were analyzed by capillary isoelectric focusing (iCE280 analyzer, ProteinSimple, Santa Clara, CA) which identifies six clusters of possible charge isoforms, glycosylation via capillary gel electrophoresis with laser-induced fluorescence detection (CGE-LIF, DNA genetic analyzer, 3130XL, Life Technologies, Darmstadt, Germany), fragments with Caliper's LabChip GXII system (Caliper LabChip GXII, Perkin Elmer, Waltham, MA), and aggregation by size exclusion high-performance chromatography (SE-HPLC, Waters, Baden-Wättwil, Switzerland).

3 | RESULTS

3.1 | Semi-continuous screening application: VCD_{max} experiments

VCD_{max} experiments were performed using the 12 clones in 96-DWP (eight replicates each) and ST (two replicates each) with daily media exchange as described in Section 2.3. As expected, the clones responded differently to the culture conditions which resulted in different growth profiles. Because the exchange rate was only 0.5 VVD in 96-DWP and 1 VVD in ST the VCD_{max} reached in 96-DWP was lower than in the ST as shown in Figure 3. From these values, and for the corresponding perfusion rate (P, expressed in day^{-1}), the $CSPR_{min}$ (expressed in pL/cell/day) was calculated as follows:

$$CSPR_{min} = \frac{P}{VCD_{max}} \quad (1)$$

and from the measured antibody concentration C_{mAb} (g_{mAb}/L) at the VCD_{max} point, the volumetric productivities normalized with respect to the reactor volume (expressed in g_{mAb}/L_R/day) were computed:

$$\text{Volumetric Productivity} = C_{mAb} \cdot P \quad (2)$$

Using these values, the 12 clones are ranked in Table 1 for both scale-down models. It is seen that three groups can be identified. Clones 1 and 5 shared the top 2 position in both screenings. Ranks 3–5 were occupied by clones 2, 6, and 7. The rest of the clones shared lower ranking positions. In addition, it is seen that the two top performers produced, based on the ST screening, more than 1 g/L/day, while clones 2, 6, and 7 share productivity values in the range of 0.67–0.85 g/L/day. All the other clones exhibited lower productivity that are close to each other (in the range 0.27–0.51 g/L/day). This explains the strong variability in the ranking of positions 6–12. Nevertheless, the same top producers were clearly identified using the VCD_{max} experiment in ST and 96-DWP.

TABLE 1 Ranking of clones 1–12 based on the volumetric productivity values computed from the corresponding mAb concentrations reached at VCD_{max} in ST and 96-DWP using Equation 2, clones 1 and 5 are highlighted in bold because they were identified as the two top producers in both screening methods

Clone #	Volumetric productivity in ST ($g\ L_R^{-1}\ day^{-1}$)	Volumetric productivity in 96-DWP ($g\ L_R^{-1}\ day^{-1}$)	Rank in ST	Rank in 96-DWP
#1◆	**1.14**	**0.59**	**1**	**2**
#5	**1.01**	**0.67**	**2**	**1**
#6	0.85	0.51	3	4
#7	0.82	0.47	4	5
#2◆	0.67	0.53	5	3
#4◆	0.51	0.28	6	9
#8	0.49	0.18	7	11
#9	0.46	0.45	8	6
#3◆	0.45	0.36	9	7
#10	0.43	0.25	10	10
#11	0.36	0.10	11	12
#12	0.27	0.33	12	8

The four clones selected for further investigation in bioreactors are marked with symbol (◆).

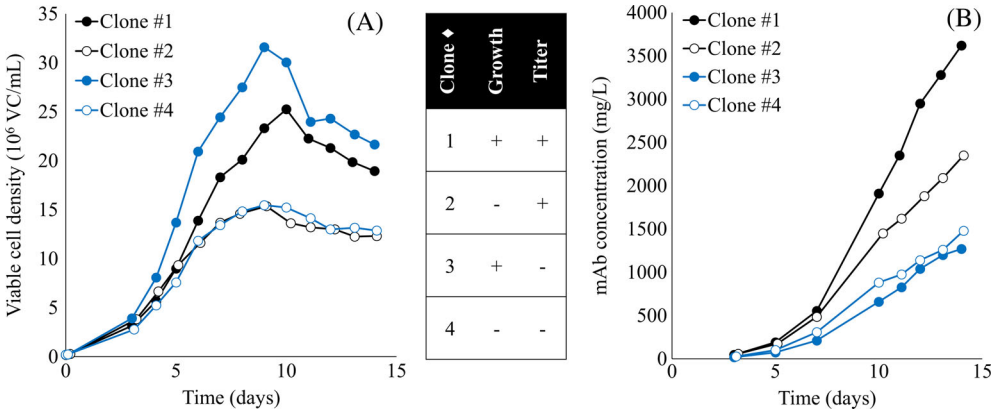

FIGURE 4 Viable cell density (a) and mAb concentration (b) of a fed-batch platform process for four selected clones that exhibit high/low growth and high/low productivity phenotypes. Clones 1 and 3 reached significantly higher cell densities than clones 2 and 4. In terms of product concentration, it is clones 1 and 2 that performed the best

To confirm these results, the $CSPR_{min}$ and the volumetric productivity were determined in lab-scale bioreactors. Because of throughput limitations, the following exercise was made only with clones 1–4 marked by a diamond in Table 1. They were selected for their differences in terms of growth and productivity performances. For comparison, the behavior of these four clones in a typical fed-batch experiment is illustrated in Figure 4.

3.2 | Perfusion screening

The behavior of clones 1–4 in a 3.5-L perfusion bioreactor, operated as described in Section 2.5, is illustrated in Figure 5. The permittivity signal was used to control the biomass at four different set-points SP1 to SP4 at 40, 50, 60, and 70 pF/cm, respectively, as shown in Figure 5a. The first capacitance value was chosen to have a cell density that was below the ones obeserved in the scale-down model systems, so as to make sure to have a stable perfusion. It was then increased stepwise to reduce the CSPR progressively. Observed disturbances in the biocapacitance signal are due to antifoam additions that probably affected the signal for a short time before going back to normal. Ideally such disturbances should not appear or should be minimized, but they were regarded as tolerable for the present study. The corresponding VCD data in Figure 5b indicate that clones 1–4 reached at SP4 VCD values of 55.4 ± 0.2, 42.7 ± 2.2, 72.7 ± 1.4 and 50.7 ± 3.0 (10^6 viable cells/ml), respectively. Note that the growth behavior from one set point to the next one of the four clones is very similar to that observed in fed-batch mode (Figure 4). In particular, clones 2 and 4 grew to similar cell densities, clone 1 grew slightly more, and finally clone 3 was the best grower.

From the data above at fixed perfusion rate and VCD increasing from SP1 to SP4, the values of bleed flow rate and CSPR in Figures 6 can be computed for each clone. It is seen (Figure 6a) that at SP4 the bleed flow rate was close to or below 15% of the total perfusion rate for all clones, which can be regarded as reasonable target with respect to product yield. No attempt was made to further increase the VCD, and the CSPR calculated at this fourth set-point was taken as the $CSPR_{min}$ for the bioreactor scale, also because the residual bleed was in all cases below 15%, as shown in Figure 6. In a process optimization perspective, this decision is not optimal for all clones because, for some of them, the bleed fraction could be further decreased. In the present case, this is especially true for clone 3 for which the bleed flow rate at SP3 is still 15% of the total perfusion rate. Nevertheless, in the frame of this study, the decision to fix the conditions at similar capacitance signal for each clone simplified the operations. Therefore, the VCD and CSPR at SP4 were defined as being the VCD_{max} and $CSPR_{min}$, respectively. It may also be noted that the CSPR of clone 3 was unexpectedly similar at the different SP (Figure 6b). This can be explained by the slightly lower perfusion rate values at SP1 and SP2

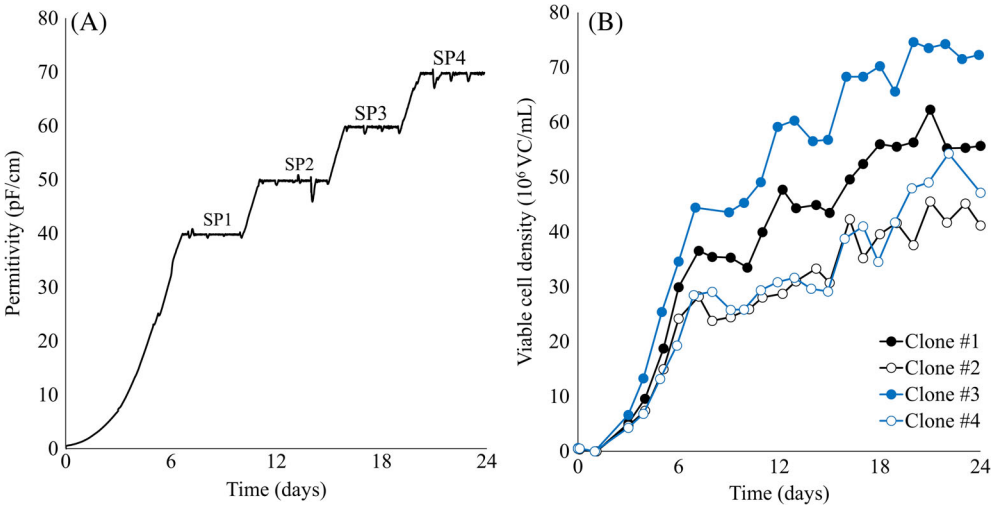

FIGURE 5 Permittivity or biocapacitance (a) and viable cell density (b) profiles of perfusion runs for the four selected clones. The permittivity signal was used to control the biomass at four different set-points SP1–SP4 at 40, 50, 60, and 70 pF/cm, respectively

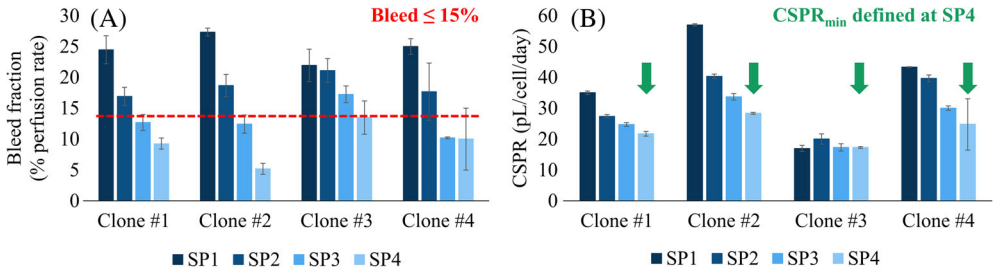

FIGURE 6 Average value per set-point of bleed fraction (a) and CSPR (b) for clones 1–4. With the increasing cell density set-point, the bleed fraction decreases with each new SP. Because the perfusion rate is maintained constant during this experiment, the CSPR also decrease with each set-point, as the cell density increases. Error bars are one standard deviation calculated with each data point of the steady states

for this particular clone. This unwanted misalignment highlights the need for robust and precise control of the experimental operating conditions.

The $CSPR_{min}$ values estimated with the bioreactors are compared in Figure 7 with the corresponding values obtained from the ST and 96-DWP scale-down models. The differences are very close to the estimated experimental errors which is indeed a remarkable result considering that the experiments span from milliliter to liter scale.

The last phase of this study was to confirm these findings in the same bioreactor, with clones 1 and 2, in which the defined state (VCD_{max} using $CSPR_{min}$ and 1 VVD) was maintained for a longer time period.

3.3 | Perfusion confirmation

The results of the confirmation runs described in Section 2.6 are shown in Figure 8. It is seen that the cell viability could be maintained above 94% for clone 1 and above 90% for clone 2 throughout the entire run. During the production phase, the biomass (calculated with the cell diameter, assuming spherical shape of the cell) was very stable

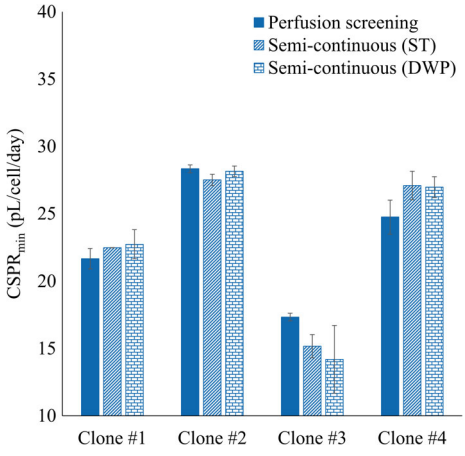

FIGURE 7 Comparison of the $CSPR_{min}$ values estimated for clones 1–4 calculated using the screening bioreactors and the semi-continuous VCD_{max} experiments in deepwell plates (96-DWP) and shake tubes (ST). Error bars are one standard deviation calculated with each data point for the bioreactor steady states, and with two and eight replicates for the semi-continuous experiments ST and 96-DWP, respectively

for both clones (Figure 8b). The VCD nevertheless behaved differently. For clone 1, it decreased slowly from 62.8 to $42.1 \cdot 10^6$ viable cells/ml, although the biomass stayed constant. On the contrary, the VCD of clone 2 was stable at around $40 \cdot 10^6$ viable cells/ml (Figure 8c). During the production phase, the mAb concentration was also stable at 0.95 ± 0.04 and 0.64 ± 0.03 g/L for clones 1 and 2, respectively (Figure 8d).

The minimum CSPR values achieved in the confirmation runs were again very close to the $CSPR_{min}$ defined in the preliminary screening procedures, as shown by the comparison in Figure 9. The largest difference was found between a confirmation run and a ST experiment for clone 2 and was 4 pL/cell/day, corresponding to a difference of 0.08 VVD for a system targeting $50 \cdot 10^6$ cells/ml/day. The same conclusion can be drawn for the volumetric productivities predicted in the ST VCD_{max} experiment and in the screening and confirmation bioreactor runs, as shown by the comparison in Figure 10. Here, only experiments operated at the same perfusion rate of about 1 VVD were considered, thus excluding the results of the 96-DWP VCD_{max} experiments. Again taking into account the bleed, the volumetric productivities for clones 1 and 2, respectively, were 1.08 ± 0.09 and 0.77 ± 0.06 g/L/day in the confirmation run, 0.98 ± 0.08 and 0.53 ± 0.02 g/L/day at SP4 in the screening bioreactor and 1.08 ± 0.01 and 0.69 ± 0.01 g/L/day in the ST VCD_{max} experiment.

Figure 8e,f show that the glucose concentration and osmolality were constant during the production phase for both clones. The bioreactor was operated in batch mode from day 0 to 3, thus explaining the initial decrease in concentration. The perfusion rate was started on day 3 and then the concentration increased and stabilized around day 10, when the biomass set-point was reached. This was the case for all metabolites, amino acids, and other media compounds measured during these runs (data not shown).

Other critical attributes like charge variants were also found to be very stable during the steady state as shown in Figure 11a,d for the two clones, respectively: five clusters extracted from the analytical chromatogram and representing different types of (group) charge variants are shown as a function of time. Fragment and aggegates, also known as low- and high-molecular weight species (LMW and HMW, respectively) remained also very stable during the runs as shown for the two clones shown in Figure 11b,e, respectively. HMW were below 1% in both cases during the entire steady state, whereas LMW levels were slightly higher for clone 1. Glycosylation was also quantified but

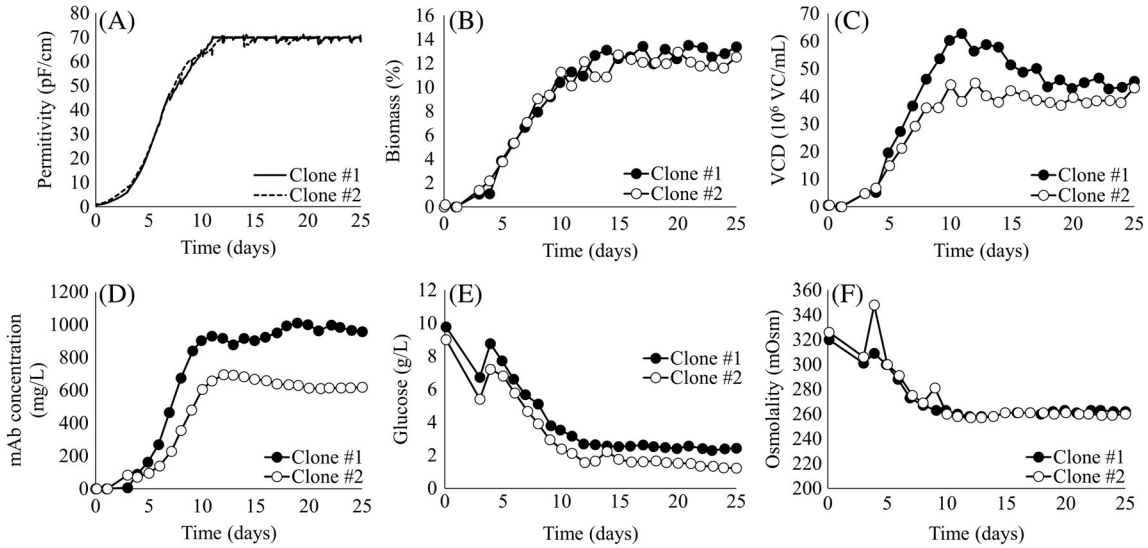

FIGURE 8 Permittivity (a), biomass (b), viable cell density (c), mAb concentration (d), glucose concentration (e), and osmolality (f) in the confirmation perfusion bioreactor runs as a function of time for clones 1 and 2

seemed to need more time to stabilize. For clone 1, complex forms tend to increase slightly with time, while for clone 2, all glycoforms were stable after day 14, as shown in Figure 11c,f.

4 | DISCUSSION

The described semi-continuous procedure was applied, with illustrative purposes, to screen 12 CHO-K1-SV cell lines producing an IgG1 but having different growth/productivity performances. We have shown that the proposed semi-continuous procedure based on 96-DWP and ST scale-down models is able to predict the $CSPR_{min}$ in perfusion bioreactors, with an accuracy very close to the experimental error, in spite of the significant scale change from 0.5 ml to a few liters. The comparisons in Figures 7 and 9 show that the largest $CSPR_{min}$ difference observed between a bioreactor and a semi-continuous experiment was 3 pL/cell/day, which corresponds to an error of about 6% in the perfusion rate for a target density of $50{\cdot}10^6$ cells/ml. This is a very reasonable error particularly when considering the benefit, these methods could provide to accelerate the process development of a perfusion process, particularly at the media and cell line screening stage.

With ST and 96-DWP scale-down models, the experimental throughput is significantly increased compared to lab-scale bioreactors (up to hundreds of different operating conditions in 96-DWP). Table 1 shows that the performance assessment in ST and DWP identified the same clones as being the highest producers. Moreover, the

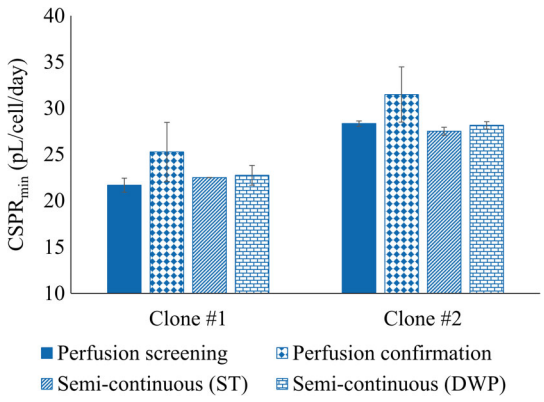

FIGURE 9 Comparison of the $CSPR_{min}$ values estimated for clones 1 and 2 from the screening and confirmation bioreactor runs and from the semi-continuous VCD_{max} experiments in shake tubes (ST) and deepwell plates (96-DWP). Error bars are one standard deviation calculated with each data point for the bioreactor steady states, and with two and eight replicates for the semi-continuous experiments ST and 96-DWP, respectively

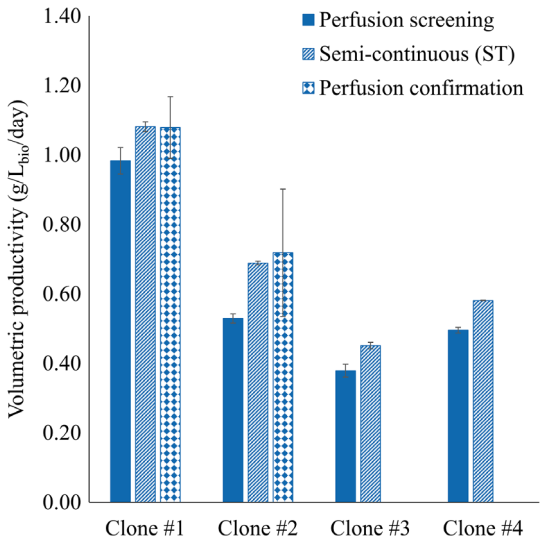

FIGURE 10 Comparison of the volumetric productivity values estimated for clones 1 and 2 from the screening and confirmation bioreactor runs, and from the shake tubes (ST) VCD_{max} experiments, at the same perfusion rate of about 1 VVD. Error bars are one standard deviation calculated with each data point for the bioreactor steady states, and with two replicates for the semi-continuous ST experiment

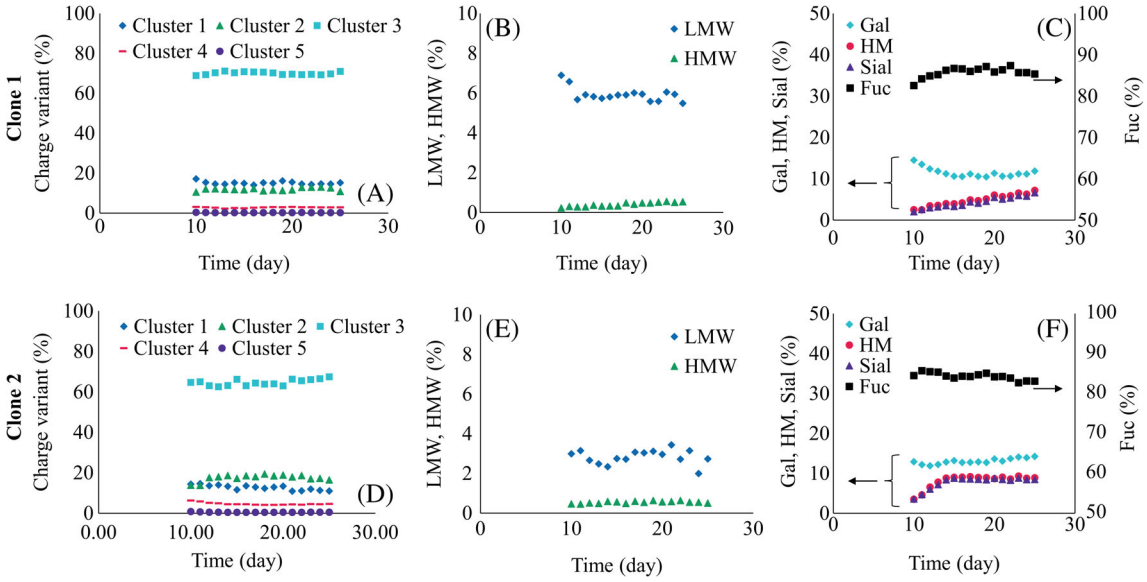

FIGURE 11 Critical quality attributes (CQAs) as a function of time during the steady state of the confirmation runs for clone 1 (a–c) and 2 (d–f) and showing charge variants (a, d), fragments or low-molecular weights (LMW), aggregate or high-molecular weights (HMW; b, e), and glycoforms (c,f) with galactosylated (Gal), high mannose (HM), sialylated (Sial), and fucosylated (Fuc) forms

predictions obtained with the ST semi-continuous experiment, that was mimicking a perfusion rate of 1 VVD similar to the confirmation runs, were very close to the productivities of the perfusions set-up (Figure 10). Therefore, we can claim that the procedure in ST and 96-DWP can be used to screen for high-performance cell lines adapted to a perfusion process.

An additional advantage of these systems compared to the use of bioreactors is that the workload in terms of media preparation, equipment preparation, and experiment monitoring is significantly reduced.

The fact that the $CSPR_{min}$ can be extracted by these high throughput models is a relevant result as it is a very important parameter in perfusion operation, that can be used both at the level of screening for the best media-cell line combination,[22,23] and later when searching for the best operating conditions for perfusion bioreactors.[15,18] It is also interesting to note that the $CSPR_{min}$ does not depend on the adopted perfusion rate, as confirmed by the results of the ST and 96-DWP experiments conducted with 1 and 0.5 VVD, respectively. The relation between cell density and media requirement is linear as long as no other limitation perturbs the system. For example, if a cell line and media combination allows for extraordinary cell densities already at 1 VVD, it could be preferred to lower the tested perfusion rate in a semi-continuous set-up, to avoid, for example, oxygen limitations that would affect the experimental output.

The experimental procedure described here was illustrated using a clone screening application. The procedure can nevertheless be applied to any cell line/media combination. Media formulation for example could be investigated by doing media blending, as it was already reported for fed-batch.[11,24,25] It can also be used for the screening of a large number of clones (several hundreds in DWP), and to identify the best candidates for perfusion cell culture. An aspect of clone selection that was not addressed here is the stability of the clone, which is of particular importance for continuous integrated processing. To address this aspect, the proposed experimental procedure could be repeated using an ageing cell expansion.

The confirmation runs were successful in the sense that they confirmed the applicability of the $CSPR_{min}$ that was estimated from the scale-down models. The bleed was started as the maximum expected cell density with the applied perfusion rate (calculated using the $CSPR_{min}$) was reached. The bleed was controlled using an online biocapacitance probe and it was observed that the relation between the VCD and the biocapacitance signal was not linear over time for both clones, similarly to what was indicated in previous reports. The relation between VCD and biocapacitance measurement depends on different factors such as the conductivity of the medium, the cell size, shape, and metabolism. When these parameters change in one direction or the other, there is a drift in the relation between the VCD and the capacitance signal.[26–29] In the present case, some cells tend to become larger once the steady state is reached, thus explaining the observed drift with the VCD (Figure 8). Further studies are needed for a more detailed understanding of how the capacitance signal and/or the viable cell count should be used for the monitoring and control of perfusion cell cultures are necessary to fully understand the implication of these observations. Despite this, the operating conditions between day 10 and 25 were very stable as shown by the concentration of product, glucose, and osmolality (Figure 8d–f). Charge variant, LMW and HMW levels were also very stable during the confirmation runs (Figure 11a,b,d,e). Despite this, glycosylation seemed to need more time to stabilize. For clone 2, for example, the glycoforms stabilize after day 15 (Figure 11f). This lag time between cell culture steady state and glycosylation steady state was already reported by Karst et al.[30] For clone 1, high mannose and sialylated (Sial) forms seem to accumulate over time whereas galactosylated (Gal) forms tend to decrease. The general trend seems to favor complex glycoforms while the run is progressing in time (Figure 11c). This observation goes beyond the scope of this

article, but it highlights the need for extra care in a real clinical development project.

5 | CONCLUSION

A scale-down procedure for the high-throughput screening and optimization of perfusion bioreactors has been developed. This is based on the so called VCD_{max} experiments performed on semi-continuous cell cultures in ST or in 96-DWP. The concept is to exchange media on a daily basis using sedimentation or centrifugation to retain the cells in the system. Then, at the VCD_{max} point, the $CSPR_{min}$ and the corresponding volumetric productivity were calculated.

The 96-DWP and ST semi-continuous cell culture procedure delivered a good estimation of the $CSPR_{min}$. This parameter is crucial for perfusion operation as it can be used for defining a target cell density for a given perfusion rate, or a given perfusion rate for a desired cell density, at the very early stage of the manufacturing process design. Another output is the ranking and assessment of volumetric productivity for, in that case, a set of different clones. In the present study, the quantification in ST was used to predict successfully the productivity expected in a bioreactor system. For 96-DWP, the productivity quantification was used only for ranking purposes, because the applied perfusion rate was not the same one used in the bioreactors.

In conclusion, the semi-continuous procedure based on 96-DWP and ST scale-down models allows a reliable screening of media and cell line performances, as well as predicting an accurate design of perfusion conditions in bioreactors.

ORCID

Jean-Marc Bielser https://orcid.org/0000-0002-9931-5920
Massimo Morbidelli https://orcid.org/0000-0002-0112-414X

REFERENCES

1. Langer ES. Trends in perfusion bioreactors: the next revolution in bioprocessing? *Bioprocess Int*. 2011;9(10):18-22.
2. Sawyer D, Sanderson K, Lu R, et al. Biomanufacturing technology roadmap—executive summary. 2017. https://www.biophorum.com/category/resources/technology-roadmapping-resources/roadmap/#
3. Konstantinov KB, Cooney CL. White paper on continuous bioprocessing May 20-21, 2014 continuous manufacturing symposium. *J Pharm Sci*. 2015;104(3):813-820.
4. Langer ES, Rader RA. Continuous bioprocessing and perfusion: wider adoption coming as bioprocessing matures. *BioProcess J*. 2014;13(1):43-49.
5. Croughan MS, Konstantinov KB, Cooney C. The future of industrial bioprocessing: batch or continuous? *Biotechnol Bioeng*. 2015;112(4):648-651.
6. Bonham-Carter J, Shevitz JA. Brief history of perfusion. *Bioprocess Int*. 2011;9(9):24-30.
7. Allison G, Cain YT, Cooney C, et al. Regulatory and quality considerations for continuous manufacturing May 20-21, 2014 continuous manufacturing symposium. *J Pharm Sci*. 2015;104(3):803-812.
8. Chatterjee S. FDA perspective on continuous manufacturing. In: IFPAC Annual Meeting, Baltimore, Maryland, USA; 2012.
9. Bielser J, Wolf M, Souquet J, Broly H, Morbidelli M. Perfusion mammalian cell culture for recombinant protein manufacturing—a critical review. *Biotechnol Adv*. 2018;36:1328-1340.
10. De Jesus MJ, Girard P, Bourgeois M, et al. TubeSpin satellites: a fast track approach for process development with animal cells using shaking technology. *Biochem Eng J*. 2004;17(3):217-223.
11. Rouiller Y, Périlleux A, Collet N, Jordan M, Stettler M, Broly H. A high-throughput media design approach for high performance mammalian fed-batch cultures. *MAbs*. 2013;5(3):501-511.
12. Rouiller AY, Bielser J, Brühlmann D, Jordan M, Broly H. Screening and assessment of performance and molecule quality attributes of industrial cell lines across different fed-batch systems. *Biotechnol Prog*. 2015;32(1):160-170.
13. Villiger TK, Roulet A, Périlleux A, et al. Controlling the time evolution of mAb N-linked glycosylation—part I: micro-bioreactor experiments. *Biotechnol Prog*. 2016;32(5):1123-1134.
14. Bareither R, Pollard D. A review of advanced small-scale parallel bioreactor technology for accelerated process development: current state and future need. *Biotechnol Prog*. 2011;27(1):2-14.
15. Villiger-Oberbek A, Yang Y, Zhou W, Yang J. Development and application of a high-throughput platform for perfusion-based cell culture processes. *J Biotechnol*. 2015;212:21-29.
16. Gomez N, Ambhaikar M, Zhang L, et al. Analysis of Tubespins as a suitable scale-down model of bioreactors for high cell density CHO cell culture. *Biotechnol Prog*. 2017;33(2):490-499.
17. Henry O, Kwok E, Piret JM. Simpler noninstrumented batch and semi-continuous cultures provide mammalian cell kinetic data comparable to continuous and perfusion cultures. *Biotechnol Prog*. 2008;24:921-931.
18. Wolf MKF, Lorenz V, Karst DJ, Souquet J, Broly H, Morbidelli M. Development of a shake tube-based scale-down model for perfusion cultures. *Biotechnol Bioeng*. 2018;115(11):2703–2713.
19. Konstantinov K, Goudar C, Ng M, et al. The "push-to-low" approach for optimization of high-density perfusion cultures of animal cells. *Adv Biochem Eng Biotechnol*. 2006;101:75-98.
20. Davey CL, Davey HM, Kell DB, Todd RW. Introduction to the dielectric estimation of cellular biomass in real time, with special emphasis on measurements at high volume fractions. *Anal Chim Acta*. 1993;279(1):155-161.
21. Dowd JE, Jubb A, Kwok KE, Piret JM. Optimization and control of perfusion cultures using a viable cell probe and cell specific perfusion rates. *Cytotechnology*. 2003;42(1):35-45.
22. Jacquemart R, Vandersluis M, Zhao M, Sukhija K, Sidhu N, Stout J. A single-use strategy to enable manufacturing of affordable biologics. *Comput Struct Biotechnol J*. 2016;14:309-318.
23. Heidemann R, Zhang C, Qi H, et al. The use of peptones as medium additives for the production of a recombinant therapeutic protein in high density perfusion cultures of mammalian cells. *Cytotechnology*. 2000;32(2):157-167.
24. Jordan M, Voisard D, Berthoud A, Tercier L. Cell culture medium improvement by rigorous shuffling of components using media blending. *Cytotechnology*. 2012;65(1):31-40.
25. Brühlmann D, Sokolov M, Butté A, et al. Parallel experimental design and multivariate analysis provides efficient screening of cell culture media supplements to improve biosimilar product quality. *Biotechnol Bioeng*. 2017;114(7):1448-1458.
26. Carvell JP, Dowd JE. On-line measurements and control of viable cell density in cell culture manufacturing processes using radio-frequency impedance. *Cytotechnology*. 2006;50(1–3):35-48.
27. Ansorge S, Esteban G, Schmid G. On-line monitoring of responses to nutrient feed additions by multi-frequency permittivity measurements in fed-batch cultivations of CHO cells. *Cytotechnology*. 2010;62(2):121-132.
28. Ducommun P, Kadouri A, Von Stockar U, Marison IW. On-line determination of animal cell concentration in two industrial high-density culture

processes by dielectric spectroscopy. *Biotechnol Bioeng*. 2001;77(3): 316-323.
29. Opel CF, Li J, Amanullah A. Quantitative modeling of viable cell density, cell size, intracellular conductivity, and membrane capacitance in batch and fed-batch CHO processes using dielectric spectroscopy. *Biotechnol Prog*. 2010;26(4):1187-1199.
30. Karst DJ, Scibona E, Serra E, et al. Modulation and modeling of monoclonal antibody N-linked glycosylation in mammalian cell perfusion reactors. *Biotechnol Bioeng*. 2017;114(9):1978-1990.

RESEARCH ARTICLE

BIOTECHNOLOGY PROGRESS

Understanding the mechanism of copurification of "difficult to remove" host cell proteins in rituximab biosimilar products

Sumit K. Singh | Avinash Mishra | Divyanshi Yadav | Niharika Budholiya | Anurag S. Rathore

Department of Chemical Engineering, Indian Institute of Technology, Hauz Khas, New Delhi, India

Correspondence
Anurag S. Rathore, Department of Chemical Engineering, Indian Institute of Technology, Hauz Khas, New Delhi 110016, India.
Email: asrathore@biotechcmz.com

Funding information
Department of Biotechnology, Ministry of Science and Technology, Grant/Award Number: BT/COE/34/SP15097/2015

Peer Review
The peer review history for this article is available at https://publons.com/publon/10.1002/btpr.2936.

Host cell proteins (HCPs) are considered a critical quality attribute and are linked to safety and efficacy of biotherapeutic products. Researchers have identified 10 HCPs in Chinese hamster ovary (CHO) that exhibit common characteristics of product association, coelution, and age-dependent expression and therefore are "difficult to remove" during downstream purification. These include cathepsin D, clusterin, galectin-3-binding protein, G-protein coupled receptor 56, lipoprotein lipase, metalloproteinase inhibitor, nidogen-1 secreted protein acidic and rich in cysteine (SPARC), sulfated glycoprotein, and insulin-like growth factor-2 RNA-binding protein. While the levels of HCPs in the investigated biosimilars were within the acceptable range of <100 ppm, certain "difficult to remove" HCPs were found in the biosimilar samples. This article aims to elucidate the underlying interactions between these "difficult to remove" HCPs and the mAb product. Surface study of rituximab exhibited unstable discontinuous patches of residues on the protein surface that have high propensity to get buried and lower the solvent exposed area. The higher order structure and the receptor binding were not affected, except for one of the biosimilars, owing to extremely low-HCP levels in its final drug product. Finally, based on the combined experimental and computational data from this study, a probable mechanism of retention for the 10 HCPs is proposed. The results presented here can guide downstream process design or avenues for protein engineering during product discovery to achieve more effective removal of the impurities.

KEYWORDS

ELISA, host cell proteins, mass spectrometry, molecular homology modeling, protein–protein docking

1 | INTRODUCTION

A primary prerequisite in biotherapeutic development using cell-based systems is to ensure safety, efficacy, and quality of these products.[1] Target biotherapeutic product must be purified from the myriad of host cell impurities that are present in the cell culture broth. Similarly, it should be free from product related impurities and variants to an acceptable level before being administered to the patients. Clearance of host cell proteins (HCPs), in particular, has often been highlighted as a major process development challenge.[2]

Broadly, protein A chromatography followed by anion exchange chromatography as polishing step are used in a typical mAb purification platform to achieve ~99% removal of the HCPs (~ng/ml concentration).[3] Monitoring of HCP removal is typically performed using enzyme linked immunosorbent assay (ELISA), which provides data with regard to the cumulative amount of HCPs present in the given

sample. More recently, the industry has been performing measurement and characterization of HCPs using orthogonal analytical methods (prominently mass spectrometry) both for identification and quantification of the individual HCPs.[4] This is primarily because some of the HCPs fail to elicit immune response and thereby are not detected by the polyclonal primary antibodies.[5] Another possibility is that some HCPs are detected by multiple antibodies, resulting in a larger than accurate signal.[6] A side-by-side comparison of four different ELISA based measurements yielding varying results bears testimony to the inadequacy of ELISA as a sole analytical method for HCP analysis.[5]

Another driver for this shift is the risk posed in multiple forms including immunogenicity and proteolytic cleavage of the target protein by some of the individual HCPs. For example, investigational intravenous recombinant factor IX (rFIX) therapy (produced in Chinese hamster ovary [CHO] cells) for the treatment and prevention of bleeding episodes in people with hemophilia B had to be placed on clinical hold (Phase III trials) on account of higher than expected rate of anti-CHO antibody response in patients administered.[7] While the HCP level in the product was well within the prescribed limits, enzymatically active HCPs like lipoprotein lipases adversely affected product quality during processing and long-term storage.[8] These observations underscore the need for a comprehensive analysis of HCPs, both in terms of their identity and quantity. Given the specie-specific impact of the HCPs, it is desirable to generate a detailed understanding of the underlying mechanism that lead to their copurification. Understanding the interaction profiles of the HCPs with the target mAb by looking for common characteristics either with respect to the mAb or the HCP may shed some light on the coelution.

Previous studies have proposed shortlisting of certain HCPs that exhibit high propensity of retention with the target product during downstream purification, tagged as "difficult to remove" HCPs. These HCPs broadly belong to three categories: product associated HCPs, coeluting HCPs, and HCPs with varying expression as CHO cells age.[7] HCPs belonging to any of these classes are likely to enter the product fraction of the protein A affinity step or any of the later polishing steps. It has been previously established that product association mode of HCP retention is more common than the coelution or variable age expression mechanism of retention.[9] Despite different therapeutic targets, a considerable sequence homology has been found across different mAbs, and this results in a similar group of associating HCPs.

While the product associated HCPs have strong interactions with the target product, coeluting HCPs share interactions with the chromatographic ligand or the resin backbone and thus end up into the final product pool. Till now, 118 out of 23,884 CHO HCPs have been identified and they belong to either of these two classes.[10-12] The third class of HCPs have varying expression due to extended culture durations.[10] Another 92 CHO HCPs have been identified in this class, particularly important where continuous bioprocessing is being adopted for production of biopharmaceuticals.[10] However, it was found that 10 CHO HCPs have common characteristics to all the three classes of "difficult to remove" HCPs[8] (Figure 1).

In this work, we have analyzed three biosimilars of rituximab for the presence of these 10 "difficult to remove" HCPs. Further, in silico modeling and docking studies were performed to understand the underlying factors that lead to copurification of these HCPs with the target product. It was found that discontinuous patches of aminoacids on the mAb surface are relatively unstable and prefer to bury themselves from the solvent environment. Interactions of the "difficult to remove" HCPs with these surface unstable patches explain their coelution with the product.

2 | MATERIALS AND METHODS

Three biosimilars of rituximab marketed in India, Retuxirel (Reliance Life Sciences), Maball (Hetero Drugs), and Cytomab (Alkem Laboratories formulated at 10 mg/ml), were purchased from local authorized distributor (Sai Distributors, New Delhi, and Vardhman Health Specialties, Bangalore). These have been referred to as Biosimilars 1–3 in no particular order. All three biosimilars were formulated at a concentration of 10 mg/ml comprising of the following components: sodium citrate dihydrate (7.35 mg), sodium chloride (9 mg), polysorbate

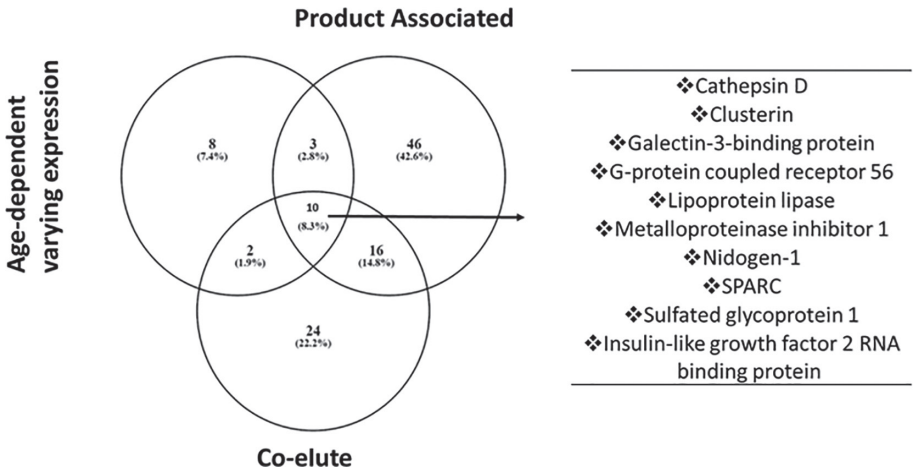

FIGURE 1 Classification of HCPs impurities that exhibit characteristics of product association, coelution, and age related variable expression. A small subset of 10 HCPs have common properties which show all the three behaviors that makes them difficult to remove during downstream purification and hence are termed as "difficult to remove" HCPs

80 (0.7 mg), pH 6.5. The necessary analysis pertinent to this study was performed well before the expiry of each of the biosimilar.

2.1 | Analysis of HCPs using octet

The level of HCP in the three biosimilars were assessed using dip and read CHO HCP detection kit (Pall Fortebio LLC, CA) on RED96 Octet system (Pall Fortebio LLC, CA). The samples and the HCP standard were prepared by diluting in sample diluent from Pall Fortebio LLC, CA. Other reagents and buffers necessary for the assay were prepared according to the manufacturer's protocol.[13] Briefly, the CHO HCP sensors were hydrated in sample diluent for 10 min followed by their incubation in samples and standards for 30 min. Next, the sensors were again washed with the sample diluent and incubated in fluorescein anti-CHO antibody for 30 min. Finally, the HCPs in the biosimilar samples were detected by sequential incubation of the prepared sensors in sample diluent for 30 s, anti-FITC HRP antibody (60 s), stable peroxide buffer (30 s) and metal enhanced DAB solution for 60 s. The acquired binding rate data were analyzed using the Octet data analysis software. Using the binding rate for each biosimilar, a calibration curve was plotted using a five parametric fit and this was further used for calculating the HCP concentration in the samples.

2.2 | Analysis of HCPs by MALDI-TOF-MS/MS

LC–MS/MS of the biosimilar samples was performed for identification of the HCP species present in the final drug product. The sample preparation involved HCP enrichment so as to overcome the limitations of dynamic range owing to orders of magnitude concentration difference between target product and the associated HCPs. HCP enrichment was achieved using protein A and protein L chromatography performed on AKTA® Purifier (GE Healthcare Life Sciences, Stockholm, Sweden). Protein A/L resins (MabSelect SuRe and Capto L, from GE Healthcare, Hatfield, UK) were packed in 1 ml HiTrap columns, and equilibrated with 50 mM phosphate and 150 mM NaCl, pH 7.5 (5CV, 500 cm/hr). The biosimilar samples diluted in ×1 PBS was loaded at 500 cm/hr onto the column to 20 mg of rituximab product/ml of resin. Elution was performed with 100 mM glycine, pH 3 (10 CV, 250 cm/hr). The elute was collected and loaded onto a protein L column equilibrated with 50 mM phosphate + 150 mM NaCl, pH 7.5 (5CV, 500 cm/hr). The flow-through fraction of the protein L eluent represented enriched HCP species that otherwise coeluted with the target product.[14] Product elution was achieved using step conditions with 100 mM glycine, pH 3 (10CV, 250 cm/hr).

The flow-through fractions of the three biosimilars from protein L chromatography were subjected to cold acetone precipitation, dried, and stored at −80°C, until use. Further, tryptic digestion was performed by resuspending the dried pellet in 6 M urea, 100 mM tris buffer. This was followed by reduction and alkylation using DTT and iodoacetamide. After incubation at room temperature for 1 hr, urea concentration was reduced to 0.6 M by dilution with water. Further, digestion was performed by adding trypsin to the protein in the ratio 1:50 and incubated at 37°C overnight.

Digestion was stopped by adjusting the pH of the solution to <6 by adding concentrated acetic acid as needed. The tryptic digests were desalted using C18 ZipTip™ (Millipore Corporation) before performing MALDI-TOF-MS/MS. For mass spectrometry analysis, the digested peptides were mixed with matrix solution and spotted on the MALDI target plate. Analysis was performed using the UltrafleXtreme MALDI-TOF/TOF Mass Spectrometer (Bruker Daltonik, Germany) using sinapinic acid matrix. Data were acquired in positive ion MS reflector mode and MS/MS. The resultant spectra was searched on Mascot v2.2 (Matrix Science Ltd., London, UK) against UniProt database with taxonomy as *Cricetulus griseus* (Chinese hamster; www.uniprot.org; Proteome ID UP000001075). Parameters for database searching included full tryptic digestion with up to two missed cleavages, the precursor mass tolerance was set at 10 ppm, and fragment mass tolerance was 0.5 Da. Carbamidomethylation (C) was set as fixed modifications as the samples were alkylated during tryptic digestion. Oxidation (M) and deamidated (NQ) were set as variable modifications. Hits with 95% or greater confidence interval were selected.

2.3 | Homology modeling of the "difficult to remove" CHO HCPs

The sequences of the 10 "difficult to remove" CHO HCPs were collected from the UniProt database with taxonomy as *C. griseus* (Chinese hamster; www.uniprot.org; Proteome ID UP000001075). None of the collected sequences had solved 3D structure in PDB. Therefore, they were homology modeled using consensus based approach. Five different homology-modeling suites (I-Tasser, Bhageerath H, Phyre 2, Robetta and RaptorX) were chosen and the sequences submitted.[15-19] Structures obtained from these servers were validated for their backbone conformation geometry, residue contact, and energy profile using both individual servers such as PROCHECK, VERIFY 3D, and ERRAT, as well as, Meta-Servers such as through the NIH-SAVES server (https://services.mbi.ucla.edu/SAVES/). The shortlisted models were further subjected to structural refinement using 3D refine server (http://sysbio.rnet.missouri.edu/3Drefine/) and Galaxy WEB server (galaxy.seoklab.org/). The resultant high-quality models were used for further analysis.[20-22]

2.4 | Protein–protein molecular docking and interaction profiling

Keeping the aim of predicting the molecular interaction profile of these "difficult to remove" HCPs with the target mAb, a crystal structure of mAb (PDB ID: 4KAQ) having a resolution of >2.48 Å for enhanced accuracy of docking results was retrieved from the RCSB protein data bank.[23] Protein–protein molecular docking of the high quality and structurally refined HCPs with the model mAb were performed using the ClusPro server version 2.0 (http://cluspro.bu.edu/

login.php), with the parameter of balanced coefficients. ClusPro performs rigid body search based on the fast Fourier transform (FFT) correlation techniques. The docked structures were filtered using distance-dependent electrostatics and an empirical potential representing desolvation. The 2,000 conformations retained after the filtering were clustered based on the pairwise RMSD. Finally, representative conformations from the 30 largest clusters were selected and refined using brief CHARMM minimization.[24,25] Among the top 10 docking results, the models with lowest binding energy were selected for further analysis. The final docked HCP-mAb structures were further validated using Ramchandran plots to evaluate if all the residues in the structure are stereo chemically feasible. Aggregation server A3D (22) was used to find the unstable surface residue of mAb that may participate in HCPs interaction. PRODIGY server (27) was used for estimating binding energies of docked complexes. Interaction profile of HCP-mAb including hydrogen bond was calculated using CoCoMaps server (28).

2.5 | Structural and functional analysis

Structural analysis included examination of the secondary and tertiary structure using far-UV CD and fluorescence spectroscopy of the mAb biosimilars. Far-UV CD spectra were recorded in the range of 200–250 nm at 25°C on a JASCO J-815 spectropolarimeter according to Reference 26.

For functional assessment, kinetics of binding affinity between mAb biosimilars (analyte) and human FcRγIIIa (ligand) receptor (R&D systems) was examined with Octet RED96 (Pall ForteBio) using biotin-streptavidin chemistry. FcRγIIIa (CD16a) was biotinylated using the EZ-Link biotinylation kit (ThermoScientific) with biotin: antibody molecular coupling ratio of 1:3. Streptavidin kinetic grade biosensors (Pall ForteBio) were hydrated in 1X kinetic buffer (Pall ForteBio part no. 18-5032) prior to analysis. Assay steps included equilibration for 60 s, 300 s of biotinylated-CD 16a loading (10 μg/ml), 120 s of baseline stabilization, 300 s of ligand-analyte association, and 600 s of ligand: analyte dissociation. Analyte concentration used were 60, 50, 25, 15 and 7 μM. Kinetic buffer (1X) was used as the matrix throughout and the assay temperature was 30°C with a shaking speed of 1,000 rpm. Data were analyzed and kinetic parameters determined from the acquired data using Global (Full) fitting, specifying 1:1 kinetic model. Subsequent analysis of other Rituximab biosimilars were performed using the same protocol with an intermittent step of sensor regeneration and neutralization. Regeneration was performed using 3 cycles of 30 s incubation in 10 mM glycine, pH 2.0 followed by neutralization in PBS for 30 s.

3 | RESULTS

3.1 | Quantitative analysis of HCPs

Figure 2 shows the levels of HCPs in the investigated mAb biosimilars. All the three products have HCP levels <100 ppm as per the current regulatory requirements of acceptable level of process related impurities for biosimilars. Figure 2a represents the standard curve depicting the known HCP concentration to the binding rate observed in the

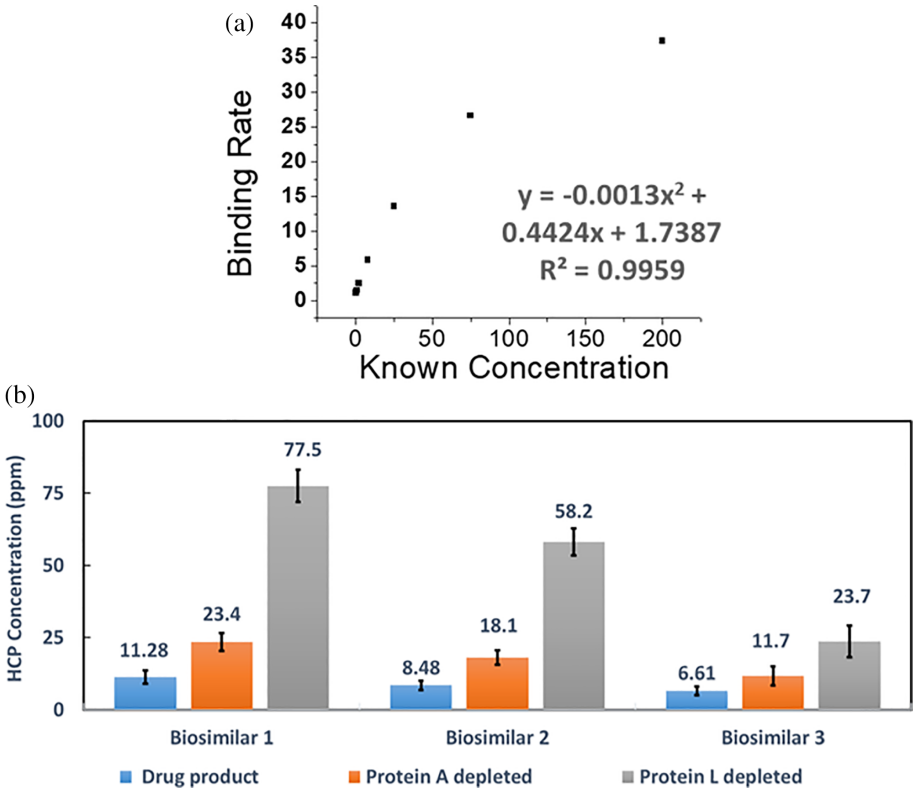

FIGURE 2 Quantification of CHO host cell proteins using biolayer interferometry based assay. (a) Standard curve correlating the binding rate to the known HCP concentration. (b) Depicting the effect of HCP enrichment using protein A/L chromatography

TABLE 1 List of HCP species identified in the flow-through fractions (coeluting HCPs) from protein L chromatography of the three rituximab biosimilars

	Biosimilar 1	Biosimilar 2	Biosimilar 3
60S ribosomal protein L29-like	+	–	–
Actin-related protein T2	+	–	–
ADP-ribosylation factor-like protein 3	–	+	–
Alpha enolase	–	–	+
Ankyrin-3-like	+	–	–
ATP synthase subunit beta	–	–	+
Cathepsin D	+	+	+
Clusterin	+	+	+
Dynein heavy chain 8	+	–	–
Dystonin isoform 1	+	–	–
Extracellular calcium-sensing receptor	+	–	–
Galectin-3-binding protein	–	–	+
G-protein coupled receptor 56	+	+	+
Histone deacetylase complex subunit SAP30L	+	–	–
Histone-lysine N-methyltransferase MLL3	+	–	–
Insulin-like growth factor-binding protein 3	+	–	+
Lactadherin	+	–	–
Laminin subunit alpha-4	+	–	–
Lipoprotein lipase	–	+	+
Lipoxygenase homology domain-containing protein 1	+	–	–
Metalloproteinase inhibitor 1	+	+	–
Metalloproteinase inhibitor 2	+	–	–
Microtubule-actin cross-linking factor 1 isoform 2	+	–	–
Nidogen-1-like, partial	+	–	–
Peroxirodoxin 1	–	–	+
Phosphatidylinositol N-acetylglucosaminyltransferase	–	+	–
Procollagen galactosyltransferase 2	+	–	–
Regulator of G-protein signaling 9	+	–	–
RNA-binding protein 6-like isoform 1	+	–	–
SPARC	+	–	–
Sulfated glycoprotein 1	–	+	–
Synaptotagmin-like protein 2 isoform 3	–	+	–
Transcription initiation factor	–	+	–
U3 small nucleolar RNA-associated protein	–	–	+
Zinc finger protein 120	–	+	–

Abbreviation: HCP, host cell protein.

Octet. In order to gain insights about the identity of the HCPs, with a view to verify the presence/absence of "difficult to remove" HCPs in commercial mAb biosimilar products, mass spectrometry based identification was performed. However, owing to dynamic range limitations of mass spectrometry, the HCPs in the biosimilar mAb had to be enriched using established technique of protein A and protein L chromatography.[27] In this case, all the three biosimilars were protein A purified by their corresponding manufacturers.

To enrich the HCPs that copurified with mAb, an additional protein L depletion step was employed. While Protein A resin effectively binds to the Fc region in the heavy chain of the mAbs, Protein L resins bind to the kappa region in the light chain of the mAb product. The underlying reason for using protein L after protein A was that the former does not have the same affinity as the latter, and therefore should effectively deplete HCPs from most of the protein A purified biotherapeutics. Figure 2b supports this assumption as it is evident that the flow-through fraction of the protein L elute is enriched with the HCPs that otherwise copurified with the rituximab biosimilars. Table 1 shows the list of HCPs that were found to be associated with the tested three mAb biosimilar. It is seen that even though all the three biosimilars are nearly equivalent in terms of HCP count, there is significant difference in the distribution of the HCPs species. For

instance, 23 HCPs were found in Biosimilar 1, but Biosimilars 2 and 3 contained 12 and 10 HCPs, respectively (Figure 3). Further investigation revealed that of the 10 "difficult to remove" HCPs, 7 were present in Biosimilar 1, 6 in Biosimilar 2, and 5 in Biosimilar 3. Specifically, G-protein coupled receptor 56, cathepsin D and clusterin were common HCPs to all the three biosimilars. Metalloproteinase inhibitor 1 was present in Biosimilars 1 and 2 and lipoprotein lipase was present in Biosimilars 2 and 3. Moreover, nidogen-1, SPARC, and insulin-like growth factor binding protein were present exclusively in Biosimilar 1, sulfated glycoprotein 1 in Biosimilar 2, and galectin-3-binding protein in Biosimilar 3.

3.2 | Surface study of rituximab

The mAb structure was analyzed to understand its surface stability in context to water solvent. Aggrescan3D (A3D) server detects the aggregation prone patches based on chemical nature of residue and solvents exposed surface area of given residue along with its neighbors.[28] These aggregation prone detected patches are considered unstable on protein surface and prone to involvement in fibril formation. These patches are unfavorably exposed to solvent and are relatively more susceptible toward interaction with other molecules (e.g., proteins). A3D score was used to detect these unstable patches on the surface of mAb. Figure 4a shows the surface of mAb where red gradient indicates unstable or aggregation prone patches while blue gradient shows stable or soluble patches. It shows that there are a few small unstable patches (shown in red color) detected on the mAb surface, likely to promote interaction with different HCPs. Figure 4b,c show the A3D scores of all residues in heavy and light chains of mAb. A score greater than 0 indicates instability while negative scored residues are soluble on the surface. It is evident that ~10% of residues in heavy and light chains are prone to interactions with other molecules including HCPs. Further, structures of HCPs were modeled using in silico approach and docked with mAb to investigate the coverage of these relatively unstable residues and their participation with HCPs.

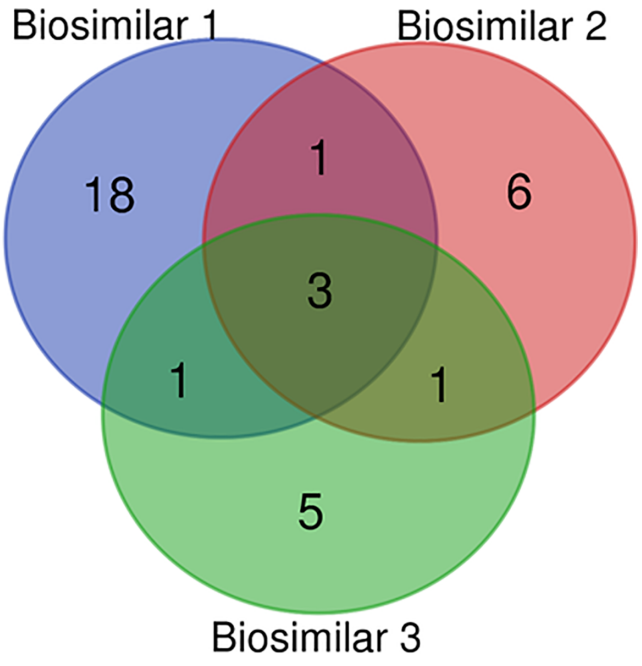

FIGURE 3 Venn-diagram showing distribution of copurifed HCPs in the three biosimilar products

3.3 | Structure modeling of HCPs

The presence of "difficult to remove" HCPs in the investigated biosimilars observed in this study, in conjugation to findings with previous studies, motivated us to understand the prevailing mechanism of retention. In silico protein structure modeling was performed for these HCPs that later docked with mAb to gain insight into their interactions (Supporting Information Figure S1). Multiple protein structure modeling servers were used to model HCPs structures: I–Tasser, Bhageerath H, Phyre 2, Robetta and RaptorX. Later, these models were scored with 3D refine and galaxyWEB servers.[15-19,21,22] In addition, ProTsav server was used to score quality of model structure. Few modeling servers could not process the input sequences of certain HCPs and thus did not produce the output model structures. A total of 151 model structures were generated for the targeted 10 HCPs. Modeled structures of HCPs showed high content of β-strands and loops (>50%) except for clusterin, insulin-like growth factor, 2 RNA-binding protein, and sulfated glycoprotein-1, where helices dominated. Further, quality of models was assessed using NIH-SAVES and ProTsav server. ProTsav is a meta-server combined eight individual servers (DDFIRE, ERRAT, NACCESS, PROSA, PROCHECK, VERIFY 3D, MOLPROBITY and D2N)[20] and assigns a cumulative score on a scale of 0–1. Any structure with a ProTsav score ≤ 0.4 is considered acceptable. However, modeled HCPs have ProTsav score > 0.4, indicating relatively low quality. Therefore, the models with low ProTsav score (highest quality) were subjected to structural refinement program using 3D refine and galaxy WEB servers. Final goal of refinement is to improve ProTsav score and thus enhance the quality of model. Here, galaxy WEB server generated refined models with ProTsav scores less than the original model. Therefore, the refined models from galaxy WEB servers were used for docking with target mAb (Table 2). However, structure model of nidogen-1 HCP was deteriorated during refinement as per ProTsav score, thus original model was used to docking. The final best quality models used for docking are represented in Supporting Information Figure S2.

3.4 | Molecular docking

The aim of performing HCP-mAb docking was to investigate the interaction of all 10 HCPs with mAb. Modeled HCPs were docked with mAb using ClusPro 2.0 server[29] and best docked pose as per ClusPro scoring was examined to study protein–protein interaction. Binding

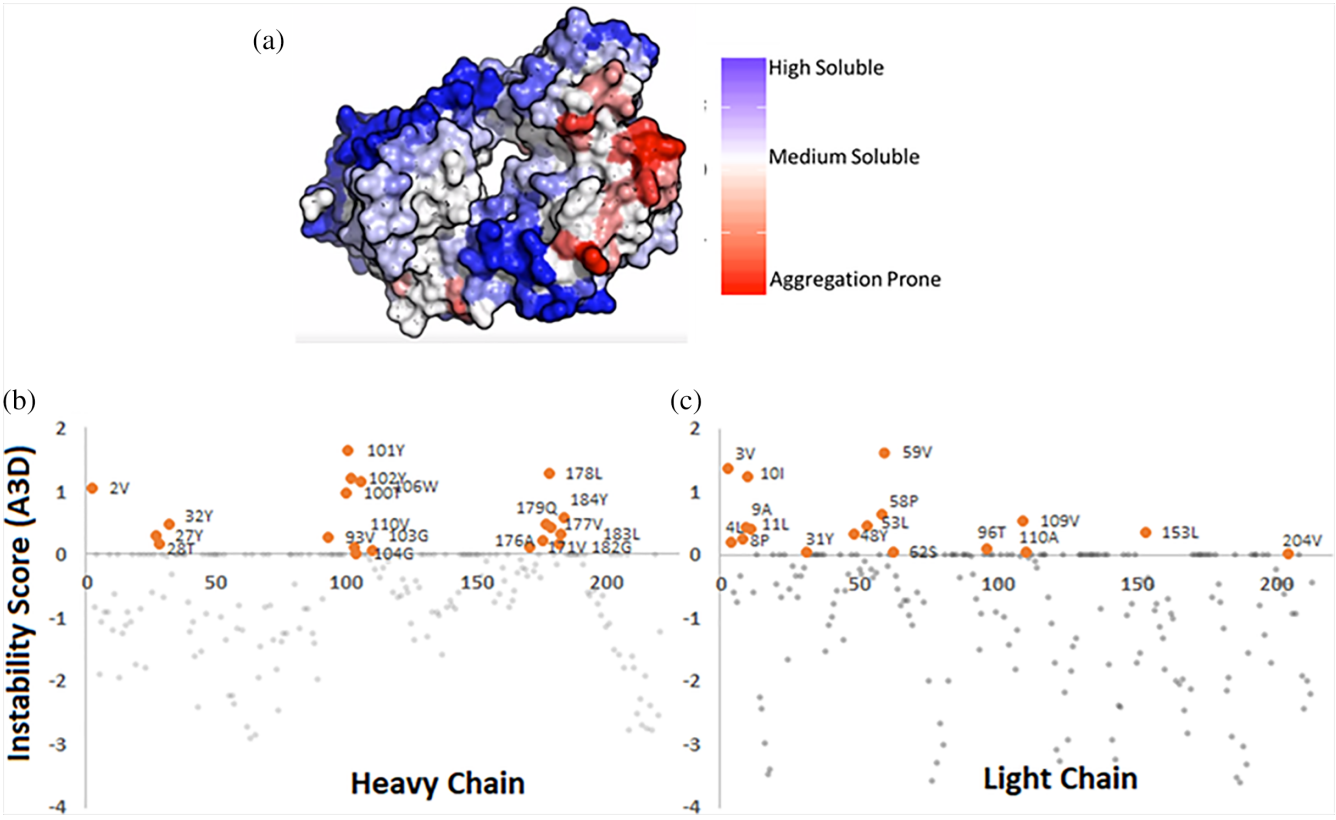

FIGURE 4 Surface analysis of mAb protein. (a) Red color gradient shows the instability or aggregation prone patches while blue color shows the soluble patches on the surface. (b and c) A3D scores of heavy and light chain of mAb, it shows the aggregation/interaction propensity of these residues with other molecule

TABLE 2 Listing the quality scores (ProTsav, GalaxyWeb and 3D refine) of the homology modeled structures of the "difficult to remove" HCPs

I-Tasser model	Cathepsin D	Clusterin	Galectin-3-binding protein	G-protein coupled receptor	Insulin	Lipoprotein lipase	Metalloproteinase inhibitor 1	Nidogen-1	SPARC	Sulfated glycoprotein 1
Model	Model 4	Model 2	Model 4	Model 2	Model 1	Model 1	Model 3	Model 1	Model 5	Model 1
ProTsav score before refining	0.553	0.6391	0.6092	0.7054	0.628	0.6261	0.5878	0.5616	0.695	0.9617
3-D refined	Model 3	Model 5	Model 5	Model 3	Model 5	Model 5	Model 5	Model 5	Model 5	Model 5
Score	0.6354	0.7286	0.6991	0.6969	0.6855	0.6334	0.6688	0.7203	0.7896	0.7398
Galaxy refine	Model 3	Model 3	Model 3	Model 2	Model 5	Model 5	Model 2	Model 5	Model 2	Model 4
Score	0.5236	0.6025	0.5763	0.6134	0.5994	0.5103	0.573	0.6102	0.5843	0.6702

Abbreviation: HCP, host cell protein.

affinity of these complexes were calculated using PRODIGY server[30] and the estimated ΔG and K_D values for 10 HCP-mAb complexes are shown in Figure 5a.

Binding energies of these complexes (ΔG and K_D) indicate high affinity of HCPs toward mAb. All 10 HCPs share similar binding free energies ($\Delta G \leq -10$ kcal/mol), considered as strong association of protein–protein interaction. However, clusterin showed relatively highest affinity whereas sulfate glycoprotein has the lowest (Figure 5a). Electrostatic interactions play a major role in deciding binding affinity of the two molecules. H-bond is a type of electrostatic interaction that can be detected in the protein–protein complex to estimate its stability. H-bonds in given 10 HCPs-mAb complexes were identified. CoCoMaps servers[31] were used to study H-bonds involvement in these complexes. Figure 5b shows the number of H-bonds in all 10 complexes in heavy and light chain of mAb. Here again clusterin exhibited highest number of H-bonds (15 bonds). SPARC also showed a large number of H-bonds in its complex with mAb. In summary, all 10 complexes exhibited significant binding energy with one or more H-bonds.

After examining the H-Bonds, residues at protein–protein interface were detected. This was determined by using the change in

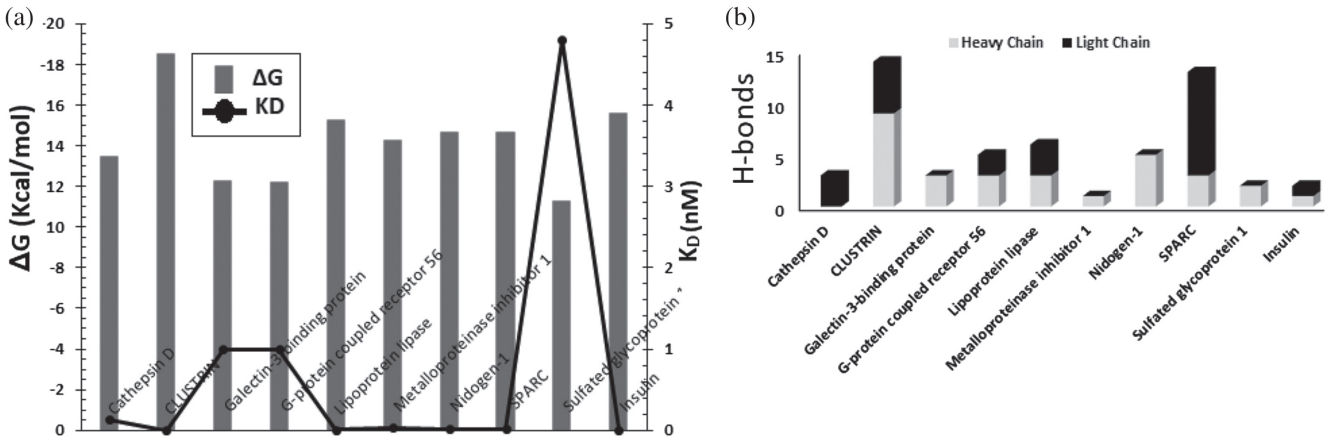

FIGURE 5 Binding affinity estimation of best poses of 10 HCP-mAb complexes. (a) Δ*G* and K_D values for 10 HCP-mAb complexes. (b) Number of H-bonds in 10 HCPs-mAb complexes in heavy and light chain of mAb. *X*-axis represent the complex of different HPCs with mAb

TABLE 3 Top five residues that showed maximum change in exposed surface area in free to bound state from heavy and light chain of mAb in complex with HCPs

HCPs	Heavy chain	Light chain
Cathepsin D	**TRP106** ASN33 **TYR101** TYR52 **GLY104**	ASN93 SER30 THR91 TYR31 SER28
Clusterin	**SER182** ARG43 **LEU178** SER181 GLY42	**VAL3** ARG24 **ALA9** GLN159 **ILE10**
Galectin-3-binding protein	**TRP106 TYR101** TYR52 ASP57 SER31	TRP90 ASN93 THR91 SER92
G-protein coupled receptor 56	**TYR101 TRP106 TYR32 TYR102** ASN33	THR91 ASN93 SER55 ASN52 **LEU53**
Lipoprotein lipase	**TYR101 TRP106** ASP57 TYR52 **THR28**	ASN93 THR91 **TYR31** SER30 SER92
Metalloproteinase inhibitor 1	**TYR101 THR28 TYR32** TYR52 SER31	SER30 THR91 **TYR48** TRP90 SER55
Nidogen-1	**TYR102 TRP106 TYR101 TYR32** TYR52	**VAL59 LEU53** ASN93 ASN52 SER51
SPARC	**TYR101 TRP106** TYR52 ASP57 **GLY104**	ARG24 SER28 SER51 THR91 LYS18
Sulfated glycoprotein 1	**TYR101 TYR32 TRP106** TYR52 ASN55	**TYR31** TRP90
Insulin	**TYR101 TRP106 TYR52** ASN55 **TYR102**	ASN93 **TYR31** TRP90 THR91 PRO94

Note: Residues detected as unstable in surface study (Figure 4a) of mAbs are in bold.
Abbreviation: HCP, host cell protein.

solvent exposed area in free to complexed state. Table 3 shows the top five residues from mAb that showed maximum change in surface area from free to bound state from heavy and light chain. Residues that are predicted unstable or prone to interaction from surface study using A3D server (list shown in Figure 4) are represented in bold in Table 3. It is seen that each complex has minimum two and maximum six residues from mAb that are detected unstable and sit at the interface of the complex. It indicates that mAb interaction with HCPs is driven by the process of burying these unstable residues to attain higher stability in complex state. A closer observation of residues shown in Table 3 confirmed that TYR101 and TRP106 are common in all the complex except clusterin complex. This suggest that binding region of these nine HCPs on heavy chain of mAb is similar while clusterin binds to a different position. TYR101 and TRP106 also showed high A3D score ≥ 1 (Figure 4) in surface study of mAb, implying a higher degree of instability and increased susceptibility to interactions with other molecules.

3.5 | Structural integrity and functional analysis

Structural integrity of the biosimilars at the secondary and tertiary levels of structural organization were assessed using CD and fluorescence spectroscopy. As is evident from Figure 6a, the far-UV spectrum of all the three biosimilars overlapped with each other indicating lack of significant changes in the secondary structure. As a general structural characteristic of any mAb, antiparallel β-pleated sheet was dominant, as evidenced by a dip at 216–218 nm. Data from the fluorescence experiments also showed overlap of the tertiary structure as evidenced from the common emission maxima at 350 nm and lack of red/blue wavelength shift for all the three biosimilars (as shown in Figure 6b).

The functional activity of the biosimilars was assessed via its binding affinity to the FcγIIIa receptor. Association and dissociation profiles for all the three biosimilars appear to be quite similar (Figure 6c). Also the binding affinity constants obtained for all the

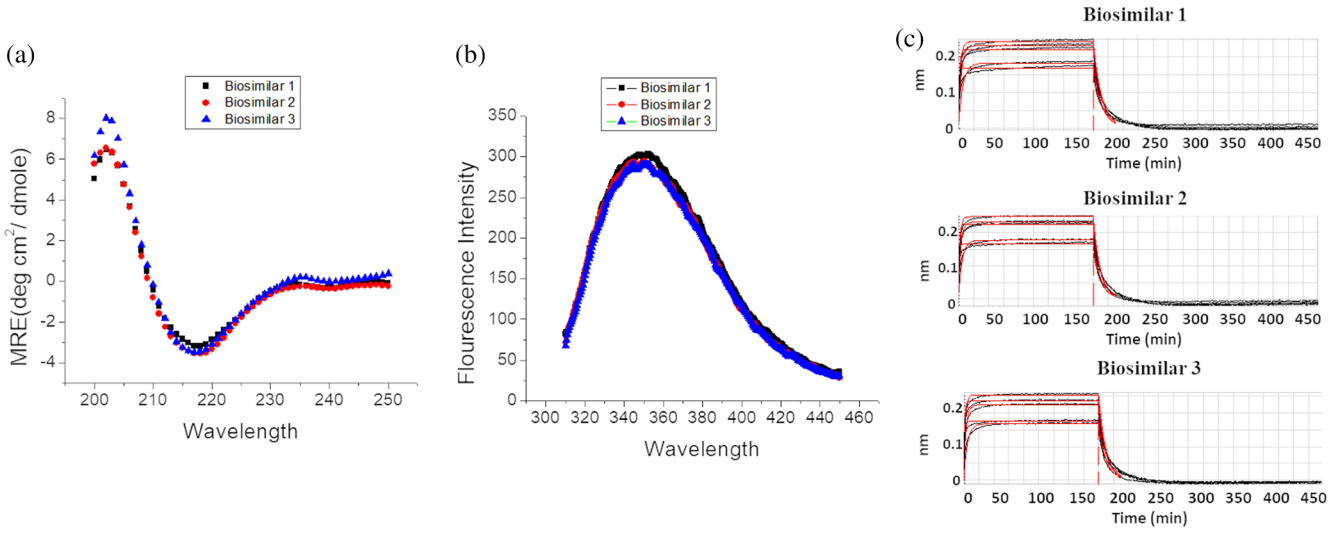

(d)

Sample	KD (μM)	Reference Range
Biosimilar1	9.7±0.28	
Biosimilar 2	8.76±0.33	7.4μM-10.9μM
Biosimilar 3	7.01±0.23	

FIGURE 6 Higher order structure and function analyzed using: (a) far-UV CD spectroscopy; (b) fluorescence spectroscopy; and (c) receptor binding using biolayer interferometry profiles overlaid for the three biosimilars. (d) Kinetic binding affinities obtained for the three biosimilars. No considerable changes in structure or function is observed for the three biosimilars in the presence of the coeluting HCPs

TABLE 4 Listing the probable mechanism by which the "difficult to remove" HCPs copurify with the target mAb product

HCP	Predicted binding strength with mAb	Probable mechanism of retention
Cathepsin D	Low	Coelution/variable cell line aging
Clusterin	Higher moderate	Product association
SPARC	Lower moderate	Product association
Lipoprotein lipase	Higher moderate	Product association
Galectin-3-binding protein	Low	Coelution/variable cell line aging
G-protein coupled receptor 56	Low	Coelution/variable cell line aging
Metalloproteinase inhibitor 1	Lower moderate	Product association
Insulin-like growth factor-binding protein 3	Higher moderate	Product association
Nidogen-1	Lower moderate	Product association
Sulfated glycoprotein	Low	Coelution/variable cell line aging

Abbreviation: HCP, host cell protein.

three biosimilars were also estimated to be statistically similar and well within the specified range for the investigated mAb (Figure 6d), except for Biosimilar 3, which showed slightly higher affinity (7.01 ± 0.23 μm) than the reference value (7.4–10.9 μm) of binding affinity of rituximab interaction with FcϪIIIa receptors. The small change (improvement) in observed affinity value could be explained based on three basic observations made for Biosimilar 3: (a) The levels of HCPs in Biosimilar 3 were least among the three biosimilars investigated; (b) clusterin, cathepsin D and G-protein coupled receptor 56 are the three "difficult to remove" HCPs that were found in all the three biosimilars; and (c) galectin-3-binding protein is the only problematic HCP that was uniquely found in Biosimilar 3, but not in Biosimilars 1 and 2. The computational docking study showed that galectin-3 binding protein binding affinity in terms of ΔG and K_D is not relatively higher than other difficult to remove HCPs. Similar conclusion is also be made using the H-bond numbers for this HCP. Taken together, it is expected that the difficult to remove HCPs present in Biosimilar 3 exhibit low-binding affinities with mAb and their relatively lower levels as compared to the Biosimilars 1 and 2. This perhaps translates into slightly better experimental K_D for Biosimilar 3.

4 | DISCUSSION

In this work, we have identified 10 HCPs expressed in CHO cells as "difficult to remove" using information from literature.[7,10-12] The ICH Q6B guideline lays down the product specifications for biotherapeutics, but does not address the exact composition and concentration of acceptable HCPs in biotherapeutics.[32] Historical industry practices required the HCPs to be kept under 100 ppm.[2,4,33] With the rise of biosimilars across the globe, process changes are inevitable as biosimilar manufacturers do

not have access to the process used by the manufacturer of the innovator product.[34] Researchers have shown that these process changes or manufacturing drifts could influence both the levels of HCPs as well the HCP species finally end up in the biotherapeutic product.[10,35,36] Thus, while the criterion of 100 ppm target limit may be satisfied, manufacturers need a deeper understanding of the HCPs present in the product and their impact on the product's safety and efficacy. In this article, we focused on the 10 HCPs that exhibited all the three established features that allowed them to be categorized as difficult to remove: (a) propensity to associate with the mAb, (b) tendency to copurify with the products on with the resins during downstream processing, and (c) exhibiting significant changes in the expression as a function of cell age.[7]

Even though, not all 10 HCPs were found in each of the three biosimilars, their presence in these products reinforce the findings on challenges and risks posed by them. The common HCPs in all the three biosimilars, cathepsin D, clusterin, and G-protein coupled receptor represent lysosomal, secretory and membrane expressed CHO host cell impurities, respectively. Clusterin has been reported to retain in both protein A elutes as well as final formulated product in as many as 29 mAbs spanning through all the four IgG subtypes.[37] It exhibits multivalent interaction with Fc as well as Fab region of the mAb.[38] Cathepsin D, on the other hand, is generally found in the final drug substance/product, exhibits proteolytic activity[39] and is known to cause fragmentation of the mAb products.[40] G-protein coupled receptor has been characterized to have attractive association with the mAb product even under moderately high salt conditions during product elution.[11] Lipoprotein Lipase and metalloproteinase inhibitor-1 were found in two of the three mAbs that were investigated. Lipoprotein lipase has recently been attributed to cause degradation of polysorbates, commonly used as excipients for preventing aggregate formation in mAb formulations.[8] Nidogen-1, SPARC, insulin-like growth factor binding protein, sulfated glycoprotein 1, and galectin-3-binding protein were found only in one of the three biosimilars. In addition, as evident from Table 1, it is seen that apart from these "difficult to remove" HCPs, indeed other HCPs were also present across the biosimilar product that were investigated.

One factor that could be attributed for the widely different distribution of these HCPs in various biosimilars of the same mAb is perhaps the divergence in process conditions employed by the respective manufacturers of these biosimilars. This is particularly true of both upstream as well as downstream process conditions. In upstream processing, the cell culture platform is increasingly adopting high cell densities and perfusion cell culture modes for biotherapeutic production.[10,12,14,41] These newer modes impact a particular subset of HCPs, as evidenced from a cell cultivation operated in batch and fed-batch mode that resulted in expression of common HCPs in both modes on Day 3 (equivalent cell densities), but subsequently led to higher expression of few select HCPs in fed-batch mode.[41] In addition, it is seen that the difficult to remove HCPs exhibited near equivalent affinities to the biosimilar, except for the sulfated glycoprotein. These could trigger competitive binding from among the HCPs and thereby depending upon the existing process conditions, certain HCPs get favored vis-à-vis others and end up coeluting with the product.

As seen from this study, the relatively lower levels of the HCPs in the final product (<100 ppm) does not cause any structural perturbations or functional changes (except for slight changes in binding affinity for Biosimilar 3) to the target therapeutic activity. Thus, at any instant only a small ensemble of the mAb is associated with these HCPs while a large majority remains intact and un-complexed. Based on the experimental and computational data in this study, we propose the following schemes/mechanisms by which the 10 "difficult to remove" HCPs persist/copurify with the main product (Table 4).

A direct application of the findings from this study would be to design a targeted purification scheme for selective clearance of HCPs that are deemed to be problematic due to their persistence in the final mAb product. For example, insulin-like growth factor-binding protein 3 is shown to copurify with the mAb via product association (Table 4). Therefore, the associative characteristics of this HCP could be countered by reversing the interaction using high salt concentration during product elution. In contrast, for sulfated glycoprotein such an approach is unlikely to work as the mechanism of its copurification is via coelution/variable cell line aging. Thus, with the limited mechanistic understanding developed in this study, well-designed process conditions could be chosen for effective and targeted removal of HCPs, that are otherwise "difficult to remove." More elaborate studies employing docking analysis with sufficiently well resolved full mAb structures (resolution >2 Å) with HCPs, along with experimental validation using biolayer interferometry/surface plasmon resonance spectroscopy would be required to further build up on the understanding gained in this study.

5 | CONCLUSIONS

Our aim in this article was to identify the "difficult to remove" HCPs that are present in the three marketed biosimilar mAbs and further shed light into the underlying interactions between the mAb molecule and the HCPs that result in this behavior. Some of the HCPs observed here were common to the 10 HCPs that have been previously established as difficult to remove with the existing mAb purification platform. The identified HCPs were modeled owing to lack of their solved structures and docked with the mAb molecule. It was shown that these HCPs have near equivalent affinity to a discontinuous patch of aminoacids on the mAb surface that are unstable owing to their tendency to bury themselves and strong attractive interaction of mAb-HCP causes coeluting of these impurities with the target product. This study also helped in identifying the crucial residues responsible for mAb-HCPs interaction. Careful mutation or biochemical modification of these residues may weaken the interaction that results in purified mAb free from HCPs. Similarly, residues that are involved in surface instability of mAb can also be targeted to address the purification process. A probable mechanism via which the "difficult to remove" HCPs copurify with the mAb product is proposed.

ACKNOWLEDGMENTS

This work was funded by the Department of Biotechnology, Ministry of Science and Technology (BT/COE/34/SP15097/2015). The

authors would also like to acknowledge Prof. B. Jayaram and Dr. Ashutosh Shandilya, IIT Delhi for their useful inputs in designing and performing homology modeling of the HCPs in this study.

CONFLICT OF INTEREST

The authors declare that they have no conflict of interest.

ORCID

Anurag S. Rathore https://orcid.org/0000-0002-5913-4244

REFERENCES

1. Tsuruta LR, Lopes dos Santos M, Moro AM. Biosimilars advancements: moving on to the future. *Biotechnol Prog*. 2015;31(5):1139-1149.
2. Hogwood CE, Bracewell DG, Smales CM. Measurement and control of host cell proteins (HCPs) in CHO cell bioprocesses. *Curr Opin Biotechnol*. 2014;30C(7):153-160.
3. Shukla AA, Hubbard B, Tressel T, Guhan S, Low D. Downstream processing of monoclonal antibodies—application of platform approaches. *J Chromatogr B*. 2007;848(1):28-39.
4. Bracewell DG, Francis R, Smales CM. The future of host cell protein (HCP) identification during process development and manufacturing linked to a risk-based management for their control. *Biotechnol Bioeng*. 2015;112(9):1727-1737.
5. Schwertner D, Kirchner M. Are generic HCP assays outdated. *Bioprocess Int*. 2010;3(1):56-61.
6. Thalmer J, Freund J. Use of a cascade immunization protocol to elicit antibodies to multiple antigen mixtures. *J Immunol Methods*. 1984; 100:245.
7. Valente KN, Levy NE, Lee KH, Lenhoff AM. Applications of proteomic methods for CHO host cell protein characterization in biopharmaceutical manufacturing. *Curr Opin Biotechnol*. 2018;53(10):144-150.
8. Chiu J, Valente KN, Levy NE, Min L, Lenhoff AM, Lee KH. Knockout of a difficult-to-remove CHO host cell protein, lipoprotein lipase, for improved polysorbate stability in monoclonal antibody formulations. *Biotechnol Bioeng*. 2017;114(5):1006-1015.
9. Shukla AA, Hinckley P. Host cell protein clearance during protein A chromatography: development of an improved column wash step. *Biotechnol Prog*. 2008;24(5):1115-1121.
10. Valente KN, Lenhoff AM, Lee KH. Expression of difficult-to-remove host cell protein impurities during extended Chinese hamster ovary cell culture and their impact on continuous bioprocessing. *Biotechnol Bioeng*. 2015;112(6):1232-1242.
11. Levy NE, Valente KN, Choe LH, Lee KH, Lenhoff AM. Identification and characterization of host cell protein product-associated impurities in monoclonal antibody bioprocessing. *Biotechnol Bioeng*. 2014; 111(5):904-912.
12. Valente KN, Schaefer AK, Kempton HR, Lenhoff AM, Lee KH. Recovery of Chinese hamster ovary host cell proteins for proteomic analysis. *Biotechnol J*. 2014;9(1):87-99.
13. Kateja N, Agarwal H, Saraswat A, Bhat M, Rathore AS. Continuous precipitation of process related impurities from clarified cell culture supernatant using a novel coiled flow inversion reactor (CFIR). *Biotechnol J*. 2016;11(10):1320-1331.
14. Madsen JA, Farutin V, Carbeau T, et al. Toward the complete characterization of host cell proteins in biotherapeutics via affinity depletions, LC–MS/MS, and multivariate analysis. *MAbs*. 2015;7(6): 1128-1137.
15. Zhang Y. I-TASSER server for protein 3D structure prediction. *BMC Bioinform*. 2008;9(1):40.
16. Jayaram B, Dhingra P, Lakhani B, Shekhar S. Bhageerath—targeting the near impossible: pushing the frontiers of atomic models for protein tertiary structure prediction. *J Chem Sci*. 2012;124(1):83-91.
17. Kelley LA, Mezulis S, Yates CM, Wass MN, Sternberg MJE. The Phyre2 web portal for protein modeling, prediction and analysis. *Nat Protoc*. 2015;10(6):845-858.
18. Kim DE, Chivian D, Baker D. Protein structure prediction and analysis using the Robetta server. *Nucleic Acids Res*. 2004;32(suppl_2):W526-W531.
19. Källberg M, Wang H, Wang S, et al. Template-based protein structure modeling using the RaptorX web server. *Nat Protoc*. 2012;7(8):1511-1522.
20. Singh A, Kaushik R, Mishra A, Shanker A, Jayaram B. ProTSAV: a protein tertiary structure analysis and validation server. *Biochim Biophys Acta Proteins Proteom*. 2016;1864(1):11-19.
21. Ko J, Park H, Heo L, Seok C. GalaxyWEB server for protein structure prediction and refinement. *Nucleic Acids Res*. 2012;40(W1):W294-W297.
22. Bhattacharya D, Nowotny J, Cao R, Cheng J. 3Drefine: an interactive web server for efficient protein structure refinement. *Nucleic Acids Res*. 2016;44(W1):W406-W409.
23. Berman HM, Westbrook J, Feng Z, et al. The protein data bank. *Nucleic Acids Res*. 2000;28(1):235-242.
24. Kozakov D, Hall DR, Xia B, et al. The ClusPro web server for protein–protein docking. *Nat Protoc*. 2017;12(2):255-278.
25. Chakravorty D, Singh S, Saravanan P, Patra S. Design of lead peptide drugs from mushroom targeting cysteine proteases. *Med Chem Res*. 2013;22(4):2038-2049.
26. Nupur N, Chhabra N, Dash R, Rathore AS. Assessment of structural and functional similarity of biosimilar products: rituximab as a case study. *MAbs*. 2018;10(1):143-158.
27. Ly L, Wasinger VC. Protein and peptide fractionation, enrichment and depletion: tools for the complex proteome. *Proteomics*. 2011;11(4): 513-534.
28. Zambrano R, Jamroz M, Szczasiuk A, Pujols J, Kmiecik S, Ventura S. AGGRESCAN3D (A3D): server for prediction of aggregation properties of protein structures. *Nucleic Acids Res*. 2015;43(W1):W306-W313.
29. Comeau SR, Gatchell DW, Vajda S, Camacho CJ. ClusPro: a fully automated algorithm for protein–protein docking. *Nucleic Acids Res*. 2004; 32(suppl_2):W96-W99.
30. Xue LC, Rodrigues JP, Kastritis PL, Bonvin AMJJ, Vangone A. PRODIGY: a web server for predicting the binding affinity of protein–protein complexes. *Bioinformatics*. 2016;32(23):3676-3678.
31. Vangone A, Spinelli R, Scarano V, Cavallo L, Oliva R. COCOMAPS: a web application to analyze and visualize contacts at the interface of biomolecular complexes. *Bioinformatics*. 2011;27(20):2915-2916.
32. Rudge SR, Nims RW. ICH Guideline Q6B Specifications: Test Procedures and Acceptance Criteria for Biotechnological/Biological Products. *ICH Qual Guidel An Implement Guid*. ICH Steering Committee. 1999;1-16.
33. Shukla AA, Thömmes J. Recent advances in large-scale production of monoclonal antibodies and related proteins. *Trends Biotechnol*. 2010; 28(5):253-261.
34. Rathore AS. Follow-on protein products: scientific issues, developments and challenges. *Trends Biotechnol*. 2009;27(12):698-705.
35. Gronemeyer P, Ditz R, Strube J. DoE based integration approach of upstream and downstream processing regarding HCP and ATPE as harvest operation. *Biochem Eng J*. 2016;113(9):158-166.
36. Goey CH, Tsang JMH, Bell D, Kontoravdi C. Cascading effect in bioprocessing—the impact of mild hypothermia on CHO cell behavior and host cell protein composition. *Biotechnol Bioeng*. 2017;114(12): 2771-2781.
37. Zhang Q, Goetze AM, Cui H, et al. Characterization of the co-elution of host cell proteins with monoclonal antibodies during protein a purification. *Biotechnol Prog*. 2016;32(3):708-717.
38. Wilson MR, Easterbrook-Smith SB. Clusterin binds by a multivalent mechanism to the fc and fab regions of IgG. *Biochim Biophys Acta Protein Struct Mol Enzymol*. 1992;1159(3):319-326.

39. Bee JS, Tie L, Johnson D, Dimitrova MN, Jusino KC, Afdahl CD. Trace levels of the CHO host cell protease cathepsin D caused particle formation in a monoclonal antibody product. *Biotechnol Prog*. 2015;31(5):1360-1369.
40. Robert F, Bierau H, Rossi M, et al. Degradation of an fc-fusion recombinant protein by host cell proteases: identification of a CHO cathepsin D protease. *Biotechnol Bioeng*. 2009;104(6):1132-1141.
41. Park JH, Jin JH, Ji IJ, An HJ, Kim JW, Lee GM. Proteomic analysis of host cell protein dynamics in the supernatant of fc-fusion protein-producing CHO DG44 and DUKX-B11 cell lines in batch and fed-batch cultures. *Biotechnol Bioeng*. 2017;114(10):2267-2278.

SUPPORTING INFORMATION

Additional supporting information may be found online in the Supporting Information section at the end of this article.

Received: 15 January 2021 Revised: 13 April 2021 Accepted article published: 17 April 2021 Published online in Wiley Online Library:

(wileyonlinelibrary.com) DOI 10.1002/jctb.6765

Recent advances in integrated process analytical techniques, modeling, and control strategies to enable continuous biomanufacturing of monoclonal antibodies

Viki Chopda,[a] Aron Gyorgypal,[a] Ou Yang,[b] Ravendra Singh, PhD, Assistant Research Professor,[a] Rohit Ramachandran,[a] Haoran Zhang,[a] George Tsilomelekis,[a] Shishir P S Chundawat[a]* and Marianthi G Ierapetritou[b]

Abstract

Continuous bioprocessing is significantly changing the biological drugs (or biologics) manufacturing landscape by potentially improving product quality, process stability, and overall profitability, as was similarly seen during the adoption of advanced manufacturing processes for small molecule drugs in the past decade. However, the implementation of continuous manufacturing for biological processes producing protein-based drug molecules, such as monoclonal antibodies (mAbs), is facing several new hurdles. The barriers to continuous bioprocessing can be overcome through improved process understanding via better predictive capabilities enabled by hybrid modeling that can also lead to robust process control. This review article summarizes the recent advances and ongoing obstacles faced during the use of advanced process analytical technologies (PAT), process modeling, and control strategies to enable continuous manufacturing of mAbs. In addition, this review also discusses the process strategies and future directions of advanced continuous manufacturing approaches that have been adapted by other industries and that could be implemented for mAbs production soon.

Keywords: biotechnology; industrial biotechnology; mathematical modelling; pharmaceuticals; process control; proteins

INTRODUCTION

The U.S. Food and Drug Administration (FDA) approved the first recombinantly produced insulin biological drug product (or biologics) back in 1982, and this opened a new horizon for complex biomolecule based drug manufacturing using living systems.[1] Since then, several biologics, including monoclonal antibodies (mAbs), have been approved to treat many autoimmune diseases, cancers, and genetic disorders in patients. Biologics have also proven to be effective in the treatment of bacterial and viral infections. For example, several mAbs (e.g., Itolizumab from Biocon) are being used in ongoing clinical trials for treatment of SARS-CoV-2 virus infections.[2] The reason why mAbs are a popular choice for the treatment of a myriad of diseases is often their specificity and safety. Furthermore, the availability of well-established platform technologies for upstream production and downstream purification processes has also enabled mass production of protein-based biologics. However, the production of a biological drug product with consistent quality and low cost remains a challenge. Consequently, it is critical to improve product quality and optimize the biologics production process through the implementation of innovative manufacturing strategies, such as the integrated in/on/at-line process monitoring, modeling, and control that are being adopted by other industries.[3] The FDA released critical guidance for the application of process analytical technology (PAT) in the pharmaceutical manufacturing industries.[4] The application of PAT systems, also called process monitoring and analysis systems, in manufacturing has paved the way for continuous process/product improvements through strengthened process supervision, knowledge-based data analysis, integration of quality-by-design (QdB) concepts, and real-time feedback control.[5] Figure 1 outlines how process modeling, PAT, and control systems can work synergistically together for a continuous mAbs production line to meet both industrial and regulatory requirements.

* *Correspondence to: SPS Chundawat, Department of Chemical and Biochemical Engineering, Rutgers, The State University of New Jersey, 98 Brett Road, Piscataway, NJ 08854, USA. E-mail: shishir.chundawat@rutgers.edu*

a *Department of Chemical and Biochemical Engineering, Rutgers, The State University of New Jersey, Piscataway, NJ, USA*

b *Department of Chemical and Biomolecular Engineering, University of Delaware, Newark, DE, USA*

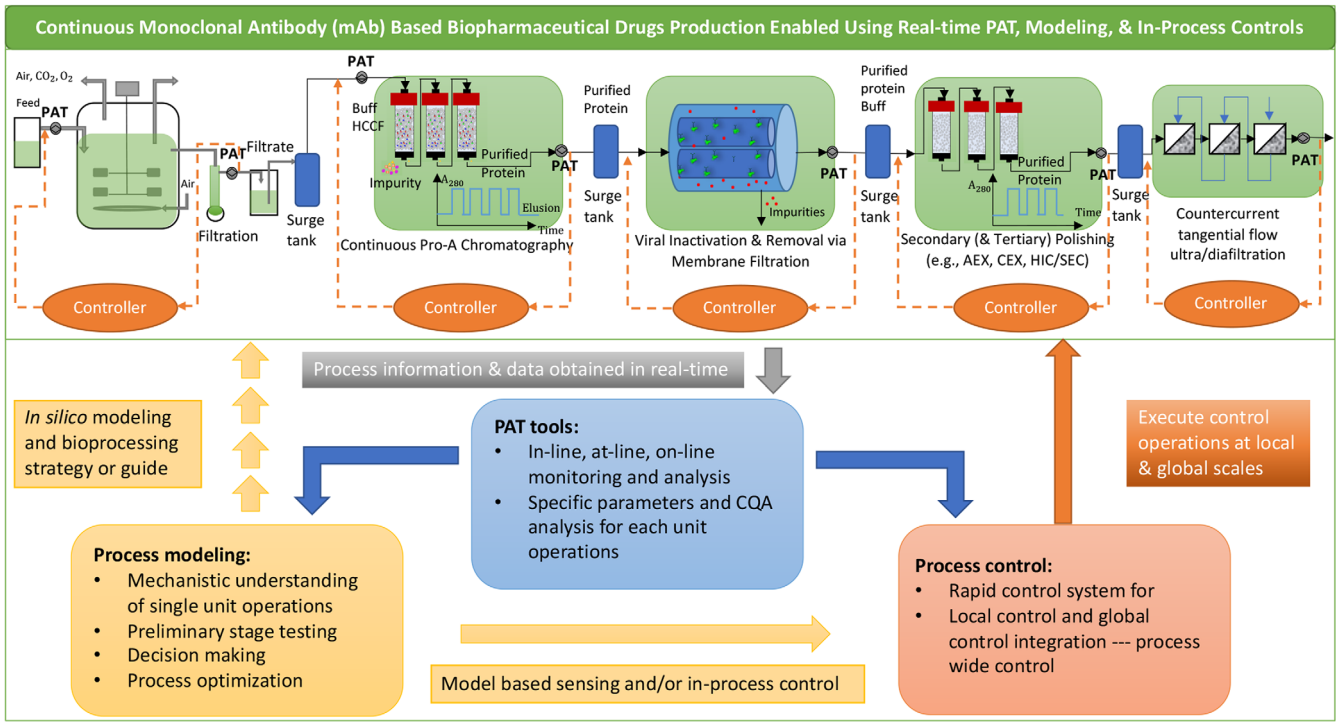

Figure 1. Schematic outline of continuous mAb based biopharmaceuticals production line and how advanced PAT, modeling, and in-process control strategies would enable mAb production with desired quality and yield.

In the last decade, the paradigm of continuous manufacturing (CM) has gained traction due to demonstrated benefits in small-molecule pharmaceutical based drug manufacturing, and it is now being evaluated for biologics production.[6] However, the implementation of principles of continuous manufacturing for biologics production is not trivial and has, therefore, not seen rapid industry-wide commercial adoption.[7, 8] Recent advances in using CM techniques are mostly limited to individual unit operations with limited integration into the overall process. Currently, there are no commercial products being manufactured by end-to-end continuous bioprocessing; however, a few research case studies have been reported from the collaboration of academia and industry.[9, 10] In particular, a 2021 guideline on integrated continuous biomanufacturing proposed an implementation strategy for biopharmaceutical companies and contract manufacturers, and provided a roadmap for vendors equipment design.[10] Overall, the slow adoption of CM can be primarily attributed to the fact that the continuous upstream portion is not being utilized to its maximum potential via PAT and control strategies, and that the continuous downstream equipment and sensing technology are not yet fully mature. Furthermore, the current industrial mindset is batch process oriented and, even with simple batch setups, many companies fail to comply with regulatory standards. Hence, there is much hesitation in to the adoption of comparatively more complex continuous processes for commercial applications.[8] Besides, for reliable end-to-end continuous processes to be operated, reliable predictive tools are needed in addition to the regular PAT tools strategically placed along the entire CM line. For example, decision of loading sample onto the chromatographic column after continuous upstream operation is challenging due to the dynamic nature of upstream processes. This demands quicker analysis (within seconds or even minutes) of culture media for mAb concentrations to make faster decisions for downstream operations. Some authors have reported case studies where using at-line high performance liquid chromatography (HPLC) or near infra-red (NIR) spectroscopy has enabled real-time decision making.[11] However, in most scenarios, off-line drawn samples are tested from the culture broth rather than in/at-line for perfusion bioreactors. Another important process task in continuous manufacturing is implementable control of surge tanks between unit operations. Surge tanks are critical and play an important role as intermediary step in a continuous series of process steps. Control of surge tanks necessitates the use of layered control strategies to ensure robust control.[12] As continuous processing involves a series of steps with diverse reaction kinetics and principles, application of PAT and/or control alone will not ensure robust in-process control. Hence, hybrid modeling and data analytics based tools must be used to make prompt decisions using real-time data and past learnings from previous design space results.[13, 14] Therefore, there is significant motivation to develop a clear scientific, technological, and regulatory infrastructure to enable broader industry-wide adoption of continuous biomanufacturing in the future.

Here, we summarize the progress and hurdles in the implementation of CM for biologics like mAbs. We highlight the key issues related to the integration of PAT, modeling, and in-process control strategies for continuous biomanufacturing. Lastly, we discuss future directions and leveraging CM strategies that have been successfully adopted by various other industries in recent years.

CURRENT STATUS OF CONTINUOUS MANUFACTURING OF BIOLOGICS

A typical biomanufacturing process is comprised of an upstream cell culture step, where a recombinant cell line harboring a gene of interest is used to produce the desired bioproduct, followed

by a series of downstream purification steps. To maximize process throughput and improve process economics, there has been an increasing emphasis on replacing traditional batch unit operations with continuous processes. Recent technological innovations that have empowered this transition for mAbs production are briefly discussed below.

Upstream cell culture step

Compared to downstream unit operations, continuous upstream cell culture is now well established. More than twenty commercially-relevant biologics have been produced using cell perfusion bioreactor technology.[7] Cell separation devices, such as alternating tangential flow (ATF) and tangential flow filtration (TFF), are used not only during perfusion (for achieving high cell density) but also for the initial clarification of cell culture broth.[15] Table 1 highlights the advances in equipment and PAT technology that have enabled the transition from batch to continuous upstream operations. ATF or TFF can be used in various ways (like at the N-1 perfusion seed culture stage) to enable high seed density process, concentrated fed-batch operations, or continuous perfusion operations that offer various advantages. For example, if the product is stable and longer operational duration is not an issue for manufacturing, then concentrated fed-batch can be used. If the product is stable, but manufacturing does not have the facilities to incorporate full-scale perfusion technology, then it can opt for high density processes and implement perfusion at the N-1 stage to lower the scale of continuous operation. In cases where the product is not stable in the culture medium (e.g., hormones), then perfusion might be the preferred approach. The reasoning is that, during perfusion, steady states can be maintained, and they are reported to yield consistent product quality over time. However, process integration is still a major challenge given that continuous operations need to be compatible with several other stages of biomanufacturing to meet regulatory requirements. For example, while implementing perfusion technology, integration with immediate downstream capture step is challenging due to the difficulty in establishing a balance between the different optimal mass flow rates for these distinct unit operations. To tackle this issue, surge tanks can be introduced, where the ATF filtrate can be kept on hold for a limited time; however, the impact of surge tank hold time on product quality is needed to support such operations.[12] Another hurdle is the limited process optimization for continuous perfusion operations due to time and resource constraints.[16] To this end, there is a critical need for the development of scale-down equipment[17] and associated process models to better enable exploration of the design space of perfusion technology and to enable more efficient integration with downstream steps.

Downstream purification steps

The biologic product produced from a cell culture often needs to undergo multiple steps of purification and characterization. For example, a typical mAb product needs to be processed by 2–3 batch modes of protein chromatography, such as: initial capture step (e.g., ProA affinity chromatography) followed one or two ion-exchange or multimodal chromatography based polishing steps, prior to product formulation. Besides these, there are several intermittent protein concentration and buffer exchange, viral inactivation, and filtration based operations. Overall, these diverse unit operations make it challenging to establish a truly integrated continuous process. To this end, important advances have been made, which are summarized in Table 1. Two major options being investigated include periodic counter-current chromatography (PCC) and simulated moving bed chromatography (SMB).[18] However, these processes generally involve multiple separation columns that require precise synchronization of all chromatographic events and prompt decisions for desired protein fraction collection. Hence, rapid modification of downstream protocols is needed to enable real-time response to changes in intermediate product quality attributes as influenced by upstream operations. Lastly, there is a critical need for the development of scale-down equipment (with integrated software and PAT) that would enable more efficient integration with continuous microscale based perfusion systems to explore the downstream protein purification/concentration design space more efficiently and cost-effectively.[17]

Process analytics

The Food and Drug Administration (FDA) and other regulatory authorities have advocated for an increased role of Process Analytical Technology (PAT) and Quality by Design (QbD) for drug substance/product manufacturing since 2004. Hence, it has become important to closely monitor the critical process parameters (CPPs) and critical material attributes (CMAs) for deviations that can impact final product critical quality attributes (CQAs, such as mAb glycosylation, charge, or aggregate states); it is also important to incorporate in-process control measures in real-time to address failure-modes.[19] This has resulted in significant advances in monitoring tools that have been developed over the last two decades. Some examples include on-line cell biomass and cell culture monitoring via capacitance sensing[20] and spectroscopic techniques (e.g., Raman spectroscopy[21] and NIR spectroscopy,[22] Fourier Transform InfraRed spectroscopy[23] or FTIR, and Attenuated Total Reflectance based FTIR or ATR-FTIR[24] spectroscopy). Although major advances have been achieved for the integration of PAT in the upstream cell culture step, downstream processes still lag in advanced PAT implementation. Currently, there is a growing trend towards the incorporation of automated sample preparation devices, such as flow injection analysis (FIA) systems integrated with dedicated at-line HPLCs, for monitoring several biologic drug CQAs.[25] However, these techniques have not been widely adopted due to a lack of dedicated hardware and software customization, as well as a lack of associated protocol development for fully autonomous drug CQA analysis using FIA-based PAT. Nonetheless, real-time monitoring of CQAs using PAT is undoubtedly a major direction for future research.

Process integration

Various levels of process integration have been reported in the literature, including: (i) partial integration of a continuous upstream process with an immediate product capture step, (ii) complete end-to-end integration wherein a continuous upstream unit operation is linked to a continuous capture step followed by batch downstream purification steps, and (iii) end-to-end closed system wherein process fluids are not exposed to the manufacturing environment.[7] A desirable continuous manufacturing process must have all process unit operations fully integrated with appropriate PAT tools and process model based 'soft' sensors to enable real-time decisions to be undertaken autonomously based on process deviations or disturbances. To the best of our knowledge, while there is no reported case study in the open literature that demonstrates the successful implementation of a fully integrated upstream and downstream process for the scalable production of biotherapeutics (like mAbs), this is now likely being implemented at least at pilot-scale by some leading pharmaceutical companies.[10]

Table 1. Enabling technology and advances for continuous biomanufacturing. Table highlights recent advances made in different aspects of a typical mAb production process and efforts on integrating these solutions to deliver an end-to-end solution for continuous biomanufacturing

Operation	Operation Technology Type	Specific Technology Advances	Examples of Some Technology Vendors	Limitations and/or Recommendations for Areas of Improvement
Upstream	*Raw materials*: Cell culture media and feed, Amino acid mixtures, Other cell culture additives, Anti-clumping agents	• Serum free and chemically defined media compositions for cell line screening • Customized media formulations for optimizing cell culture performance as per process requirements (e.g., for high cell density, perfusion, or batch feed) • Customized media, feed, additives, and specific formulations for manipulating drug product quality (e.g., Glutamax)	• ThermoFisher • MilliporeSigma • Bio-concept • Gibco • Irvine Scientific • Lonza	• Relationships between media composition and final mAb drug product CQAs (e.g., glycosylation) is still not well understood • Media composition is either not well defined or proprietary, making it challenging to rationally optimize media composition for process • Extensive media screening is often required for specific cell lines and clone types or as per actual process (batch *vs.* continuous) requirements • Operating costs are high due to significantly increased media/reagent requirements for continuous processes (*versus* classical batch processes)
Upstream	*Process Equipment*: Cell retention devices to enable cell banking, initial harvesting, N-1 cell culture, and/or perfusion	• Acoustic separators • Gravitational settlers • Centrifuge settlers • Tangential flow filtration (TFF) • Alternating tangential flow (ATF) • Spin filters • Rotating cylindrical (Vortex flow or external spin filters) • Rotating disc (controlled shear filters)	• Repligen • Cytiva • Sartorius • Pall Sciences	• *For gravity, acoustics, and centrifuge-based*: Not suitable for animal cell culture due to low settling velocities, as well as high capital and maintenance costs. Detailed investigation still needed to study impact of geometric designs on cell culture performance. • *For membrane filtration-based*: Membrane fouling & high viscosity impacts performance. Cell bleeding along with methods that can reduce in host cell lysis and ultimately cause release of host cell proteins and genomic materials, can prolong membrane life & reduce fouling.
Upstream & Downstream	*Process Equipment and Analytical Instrumentation*: Single-use technology for higher throughput process development and scale-up	• *Single-use bioreactors*: Wave bioreactor, Biostat Cultibag, CELLtainer, XRS-20, Appliflex, Hyclone, XDR, Mobius Cellready • *High-throughput single use bioreactors*: Ambr-15, Ambr-250, Dasbox, Dasgip • *Single-use microperfusion bioreactors*: Breeze • *Single-use chromatographic devices*: Single-use, single-pass TFF	• Pall Sciences • Sartorius • Cytiva • Infors • Applikon • ERBI • Eppendorf	• Specialized construction materials required to prevent release of leachable/extractable components into actual process streams • Unique PAT sensor designs required (e.g., for Wave & Breeze) • Scale-up dependent on vendor supplied data due to limited in-house R&D data availability for single-use process equipment • Mixing and computational fluid dynamics (CFD) studies still required for single-use equipment with unique geometry • Suitable scale-down models must also be developed for validation at process-scale (e.g., Breeze)
Downstream	*Process Consumables*: Chromatography-bed resins	• High binding capacity & specificity • Resistance to fouling	• Cytiva • Pall Sciences	• Resin leaching and fouling can hamper operations. Continuous monitoring of resin performance and life is highly recommended.
Downstream	*Process Equipment*:	• Simulated moving bed with 6-columns	• Cytiva	

Table 1. Continued

Operation	Operation Technology Type	Specific Technology Advances	Examples of Some Technology Vendors	Limitations and/or Recommendations for Areas of Improvement
	Continuous DSP operations for initial capture, polishing, viral inactivation/filtration, buffer exchange, and/or concentration.	• Sequential multi-column chromatography (MCC) with 4-columns • Periodic countercurrent chromatography (PCC) with 3 columns • Twin-column chromatography • Continuous countercurrent tangential chromatography	• Biorad	• High cost for operation and maintenance of multiple columns. Challenges associated with in-process validation and ensuring real-time product quality • Issues with pooling protein fractions with undesired CQAs • Real-time monitoring of individual columns with feedback control • Integrated control of intermediate surge tanks for all DSP steps
Downstream	*Process Equipment*: Non-chromatographic methods for initial capture and viral clearance	• Continuous aqueous two-phase protein extraction • Continuous protein precipitation	-	• Issues with poor recovery and resolution compared to classical chromatographic separation • Issues with scale-up is still a major issue
PAT sensors	*Process Analytical Instrumentation*: Real-time process monitoring in-line, on-line, and/or at-line of material & quality attributes	• Viable cell density – In-line capacitance probe • CQAs – In-line spectroscopic methods (Raman, NIR), At-line U/HPLC-UV/Fluorescence/Mass Spectrometry	• Aber • Kaiser • Agilent • Waters • ThermoFisher	• Specific parameters such as amino acid and metal ion concentrations that play a critical role in glycosylation need to be monitored in real-time • CQAs, such as glycosylation, charge variants, and protein aggregation is still being done in offline mode. These CQAs need to be analyzed in/at/on-line mode to enable real-time control of CQAs using advanced process models/control
Process integration	*Process Mode*: Continuous upstream with continuous capture, Continuous upstream with continuous downstream (capture plus polishing), End-to-end closed system	• Modular integrated process building approach is being now implemented • Custom designed integration as per process requirement to enable fully continuous (or hybrid semi-continuous) approach is now possible	• Pall Sciences • Sartorius	• Bioburden control is still an issue • Process synchronization is an issue despite inclusions of surge tanks due to lack of advanced PAT, model, and control options • Local control should be assisted with global and advanced supervisory controls • Reliable scale-down models needed for process validation
Predictive tools	Soft sensors based PAT, hybrid modeling, & process control	• Advanced integrated software packages that enable automated bioprocess management via data collection, data storage, data analysis, process data modeling, and overall process control	• DataHow • Spectrahow • Insilico Biotechnology • Lucullus • SIMCA Online	• There is currently lack of availability of suitable process data to enable more effective process management • Need for improved data flow and analysis across multiple unit operations to enable fully continuous biomanufacturing

Table 2. Critical quality attributes associated with final drug product and examples of real-time PAT implementation to enable continuous biomanufacturing

Quality Attribute	Influence	Process Location/s	Measurement or Process Analytical Technique (PAT)	CQA Monitoring Style using PAT
Protein Titer	Cell productivity	Upstream Downstream	• Affinity chromatography • Capillary electrophoresis • Raman spectroscopy • Infrared spectroscopy (IR)	On-line[27] At-line[28,29] Offline
Osmolality	Cell Viability & growth	Upstream	• Osmometry • Raman spectroscopy • Near-infrared (NIR) spectroscopy	On-line[30,31] At-line[32] Offline
pH	Protein stability	Upstream Downstream	• Potentiometry • Infrared spectroscopy (IR)	On-line[30]
Host Cell Proteins (HCP)	Contaminant decrease in drug efficacy, Adverse immunogenic reaction	Upstream Downstream	• Infrared spectroscopy (IR) • Liquid chromatography with UV based detection	On-line[29] At-line[33] Offline
Host Cell DNA (HCD)	Contaminant decrease in drug efficacy, Adverse immunogenic reaction	Upstream, Downstream	• Reverse phase high performance liquid chromatography (RP-HPLC) with UV • Enzyme-linked immunosorbent assays (ELISA)	At-line[34] Offline
Protein Aggregation	Decreased production, Lower drug activity & safety	Upstream, Downstream (Protein A Capture, Viral Inactivation, Ultra/dia-filtration or UF/DF)	• Size exclusion chromatography (SEC) • Infrared spectroscopy (IR) • Dynamic light scattering (DLS) • Analytical ultra-centrifugation (AUC)	In-line[35] Off-line[29]
Charge Variants	Drug safety, immunogenicity, and efficacy	Upstream Downstream	• Ion exchange chromatography (IEC) • Capillary electrophoresis (CE) • Iso-electric focusing (IEF)	Online[36] Offline[37]
Size Variants	Drug safety, immunogenicity, and efficacy	Upstream Downstream	• Size exclusion chromatography (SEC)	On-line[38] Offline
Glycosylation	Drug Efficacy, immunogenicity, stability	Upstream Downstream	• Hydrophilic interaction liquid chromatography (HILIC) • Capillary electrophoresis (CE)	On-line[25,39] At-line[40] Offline

INTEGRATED PROCESS ANALYTICAL TECHNOLOGY (IPAT)

With the adoption of the Guidance for Industry as outlined in ICH Q8, there has been an increasing demand for improved process understanding with the goal of delivering a quality product with consistent performance.[26] This can be achieved by understanding the effect of process inputs, such as raw material attributes and process parameters on the CQAs; this process envelope is known as the design space. For a process to work in a designated design space, it is important to have real-time information (i.e., using PAT sensors) on process parameters that can have a significant impact on product attributes and to be able to control the process via feedback and/or feedforward control strategies. Hence, this section focuses primarily on advances in the integrated PAT tools and sensors used in both upstream cell culture cultivation and downstream purification. Table 2 depicts the important quality attributes and the current state of process monitoring. Figure 2 depicts the general use of common PAT tools and automation during a continuous bioprocess and how process control can be conducted using these tools. The recent trends of PAT toolkit development and implementation are discussed below.

To a significant extent, PAT has enabled process automation and real-time control of a few process parameters for upstream operation. For example, pH, dissolved oxygen, temperature, and glucose concentrations are a few of the upstream parameters that have been reported to be well controlled. However, monitoring and control of product quality attributes (such as biological activity, aggregate states, charge variants, and glycosylation levels) is not possible in real-time and there are only a few cases where these CQAs were monitored via at-line PAT. There are two main reasons for this lag in advanced PAT adoption. One is the availability of robust and inexpensive sensors that can detect these small variations in a complex bioreactor environment. The other reason is a lack of complete understanding of the impact of process parameters on product CQAs, which further limits application of suitable control strategies. Some recent advanced PAT implementation case studies are further highlighted here. Raman spectroscopy has gained significant attention for implementation in both upstream and downstream processes. A key advantage in use of Raman spectroscopy in CM as PAT is the ability to simultaneously allow in-line monitoring and prediction of key culture parameters (such as concentrations of glutamine, glutamate, glucose, lactate, and ammonium), in addition to predicting viable cell density and

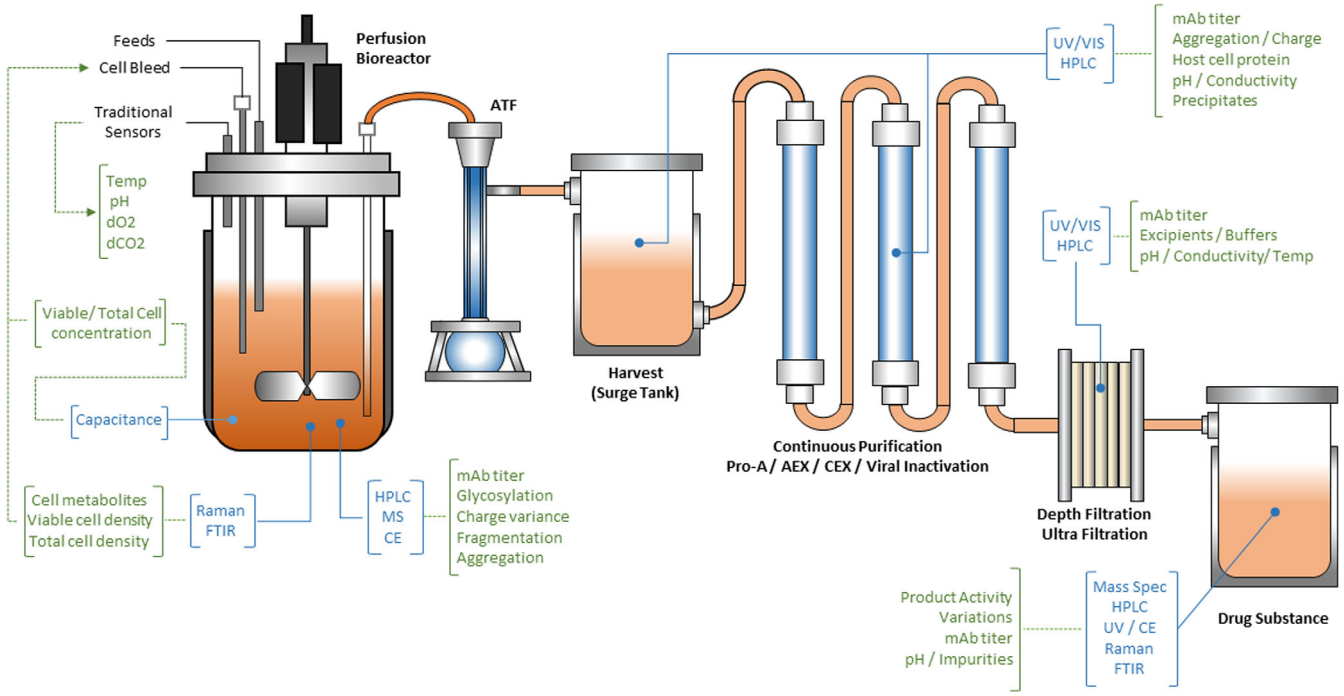

Figure 2. Example of specific PAT tools implemented during mAb manufacturing to monitor CQAs. Blue denotes the process analytical techniques that feeds information from the process and green denotes specific CQAs that are measured during each step of the bioprocess.

total cell density.[41] The use of a single PAT probe to characterize multiple culture parameters simplifies the task of sample analysis by replacing multiple sensors with a single sensor that can gather multiple sets of information at once. In addition, Raman spectroscopy has been used for controlling lactate concentration which has led to improvements in cell density, viability, and protein production in mammalian cell culture[42] as well as with controlling glucose levels in the bioreactor.[43, 44] Using Raman spectroscopy to predict different mAb isotypes and glycosylation species with low prediction errors and through a permeate stream (without sample removal) has also been reported.[45, 46] A recent study also successfully implemented Raman spectroscopy for fine-tuning mAb galactosylation levels in real-time by controlling lactic acid feeding rate.[47] However, this technique has certain limitations, such as giving highly overlapping spectral signatures that require deconvolution and having poor sensitivity to lower concentration species (which makes it difficult to continually observe all desired products). Moreover, the requirement of robust calibration models for process validation and the need for raw data preprocessing using complex chemometric approaches are some of the other technical drawbacks that come along with the application of Raman spectroscopy as a PAT tool. However, based on technological advances that are continuing to be made, Raman based PAT will find applications in monitoring of a wide range of process parameters and quality attributes to suit the on-line monitoring needs of continuous biomanufacturing processes.

Spectroscopic monitoring tools implemented in upstream and downstream processing unit operations have become versatile due to fast acquisition times and the ability to gather a multitude of data with each acquisition. The use of in-line FTIR and Raman spectroscopy probes has also been studied as a substitute approach for at/off-line HPLC analysis during protein chromatography to measure protein concentration and detect trace contaminants.[23] A recent study utilized FTIR to monitor the purity and quantity of fibroblast growth factor 2 in real-time.[48] Other uses of FTIR for quality evaluation have been applied for protein detection in aqueous two phase extraction[49] and for in-line measurements of protein concentration during ultrafiltration.[50] Overall, spectroscopic techniques are now showing an increasing trend as PAT tools being used towards real-time decision making.[51]

Another classical but realistic PAT approach is aseptic sampling and rapid at-line analysis for desired portfolio of quality tests. For example, UHPLC was used to enable continuous real-time monitoring of multiple mAb CQAs, namely: amino acid composition,[52] charge states,[53, 54] and glycosylation.[25, 55] Another example is Zipchip technology, which is based on the principle of Capillary Electrophoresis (CE); this principle has gained popularity as an alternative technique to UHPLC for elucidation of product attributes, such as glycosylation and charge heterogeneity.[25, 26, 41, 42] The increasing popularity of CE can be attributed to the rapid analysis times, which are usually within 1 min of sample processing *versus* HPLC, where analysis may take around 10–60 min. Notably, both HPLC and CE based PAT techniques suffer from low-efficiency and the longer time needed for sample preparation (or derivatization), which further delays the total time needed for analysis and hinders their utility as on-line monitoring systems. However, implementing these techniques at-line is still a real challenge because the hardware integration and software development that are often needed also require multi-disciplinary expertise and collaboration between multiple stakeholders (e.g., FIA and HPLC equipment vendors). Furthermore, enabling feedback control for controlling CQAs in-process requires more work that can better link the impact of varying CPPs and CMAs to achieve desired CQAs.[56–59]

There has been a trend towards use of in-line spectroscopic PAT to acquire process data over traditional off-line methods (such as HPLC). The main advantage of such PAT is the easier integration of in-line spectroscopic probes to rapidly acquire process data via

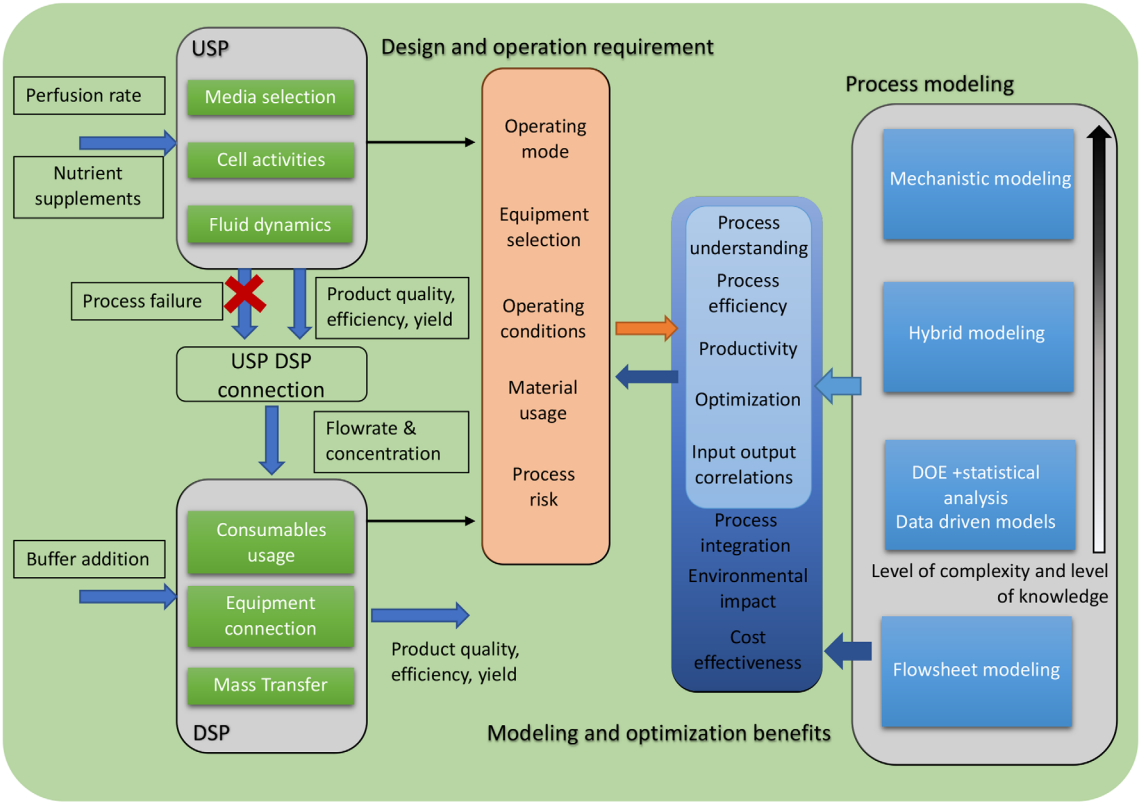

Figure 3. Challenges associated with the implementation of advanced process models for upstream and downstream operations for continuous mAbs manufacturing. Boxes on the left highlight the critical components that are needed to better understand both USP and DSP. Orange box highlights the challenges of continuous manufacturing in process design and operations. Blue box, adjacent to the orange box, lists capabilities of process modeling strategies. Process modeling box also catalogs the various modeling methods in order of increasing computational complexity.

non-invasive means compared to off-line HPLC. However, the complex and highly overlapping spectral spectroscopic signatures of background organic molecules, in conjunction with the low concentration of target species to be analyzed, require access to appropriate statistical tools that can accurately deconvolute, analyze, and apply suitable control strategy. Multivariable data analysis (MVDA) approaches hold considerable promise due to their ability to correlate one or multiple events in a bioreactor and in subsequent unit operations.[60] Chemometric tools (such as MVDA) and other techniques, such as principal component analysis (PCA), partial least squares (PLS), and orthogonal partial least square techniques,[61] have been used to analyze spectrometric signatures. Raman PAT based dynamic feeding strategies have been implemented for CHO cell cultivation based off robust PLS calibration models for shake flask and bioreactor cultures,[62] as well as chemometric based models for predicting key cell culture metabolites.[63] As we begin to exploit the potential of various spectroscopic (and non-spectroscopic) techniques for use along with soft sensors, this will shape how advanced PAT tools allow faster data acquisition and provide better control of both upstream and downstream unit operations.

INTEGRATED PROCESS MODELING

To overcome the challenges associated with the implementation of PAT technologies, model-based methods are often developed to assist in estimating the process parameters and product-related attributes for making real-time control decisions.[64] With longer operating times for continuous operations, building a predictive model for process analysis is critical to achieving in-time operational adjustments and decision making. By working towards QdB and 'digital twin', process modeling can also be used for regulatory decision-making.[65] The current modeling work has focused on improvement of both single unit operations and integrated processes with multiple operations. Figure 3 summarizes the critical inputs, outputs, and challenges for continuous biopharmaceutical operations and possible modeling approaches to overcome such challenges. In the following section, we review the capabilities of different modeling methods for facilitating continuous biomanufacturing for mAbs production and address possible approaches to the current challenges in the field of CM of biologics.

Improvement of single unit operation

For each unit operation, predicting productivity, product quality attributes, and the possibility of process deviations or failures is critical to achieving stable continuous production for longer durations. Mechanistic, data-driven, and hybrid modeling based approaches are currently being explored in continuous operations at all stages of process operations. In general, mechanistic models mainly focus on the improvement of process understanding and performance based on first principles and tracking the dynamic changes for upstream and downstream operations. Data-driven models investigate the statistical relations between input and output data and demonstrate the predictive correlations between process parameters and product qualities. Hybrid models are built under the mechanistic model framework with unknown parts of equations represented by data driven models.

Table 3. Summary of how process modeling and in-process controls have been used in recent times to facilitate unit operations selection and design unit connections, as well as maximizing mAb production efficiency and enabling continuous biomanufacturing

Mechanistic models: Apply cell metabolism/biochemical reactions, cell culture, and fluid dynamic theories to mathematically capture upstream (USP) and downstream (DSP) processes. For USP, flux balance/metabolic flux analysis, reaction kinetics modeling, and CFD simulations are often used. Sometimes to simplify kinetic models, empirical relations are used. These methods are combined to improve model prediction capabilities. For DSP, various fluid dynamics, diffusion, and thermodynamic theories are applied, such as general rate model, plate model, and Darcy's law.

Modeling approach	Modeling platform	Model details or representative examples	Reference
Dynamic flux balance analysis (DFBA)	MATLAB	Gassing and dilution rates modeled in ambr15 bioreactor. DFB model could predict metabolic changes, such as glucose consumption, and lactate consumption/ production shift.	Kelly *et al.*[68]
Comparing response surface modeling *versus* kinetic modeling	MATLAB	Continuous USP (1.5-L bioreactor and ATF) modeled to simulate cell culture and glycosylation process under different viable cell density and media supplement concentrations.	Karst *et al.*[66]
GFA (glycosylation flux analysis) + random forest modeling analysis	MATLAB	Modeled cell growth/culture in 1.5-L bioreactor to capture IgG galactosylation flux activity and predicted mAb protein glycosylation state during the cell culture	Hutter *et al.*[69]
Flux balance analysis (FBA)	Insilico Inspector (Insilico Biotechnology)	Improved process understanding of the role of reactive oxygen species in metabolic pathways and further assist with bioprocess intensification for high seed density USP cell culture cultivations	Brunner *et al.*[71]
^{13}C metabolic flux analysis (MFA)	INCA software package	Compared fed-batch *versus* perfusion by capturing CHO metabolic phenotypes to understand the metabolic effects on cell biomass and protein production	Templeton *et al.*[70]
Basis flux models	MATLAB	Basis flux model reduces the flux modes compared to the elementary flux model and can be used to identify the metabolic states with its corresponding reaction rates in perfusion bioreactors	Rodrigues *et al.*[72]
Data-driven approach + EFM + kinetic modeling	MATLAB	Modeled a 2-L stirred bioreactor to simulate process metabolic network under different initial values and feed stream compositions (e.g., glucose, glutamine, alanine)	Abbate *et al.*[73]
CFD	Ansys Fluent	Simulated the ATF system and predicted pressure and local fluid dynamic profiles for water and supernatant solutions to understand fluid dynamics changes under different feed/permeate fluxes	Radoniqi *et al.*[74]
Kinetic	-	Simulated cells and micelles blocking the ATF membrane to estimate transmembrane pressure	Kelly *et al.*[67]
General rate models	MATLAB	Applied mechanistic models to simulate the PCC protein-A capture step and used multi-objective optimization to maximize mAb productivity and resin utilization. Authors also integrated PCC operations with other downstream unit operations.	Gomis-Fons *et al.*[75]
Transport dispersive model	C++	Designed and optimized sequential multi-column chromatography and maximize productivity. Understand adsorbent properties (e.g., size, mass transfer) effect on chromatography performance.	Ng *et al.*[76]
General rate models	MATLAB	Evaluated interconnected feeding rate, breakthrough percentage, and disconnected feeding time effect on twin-column chromatography system operation. Applied process optimization to achieve high productivity and DSP capacity utilization.	Shi *et al.*[77,78] Sun *et al.*[79]
Lumped kinetic models	MATLAB	Simulated twin-column CaptureSMB process. Optimize productivity and capacity by considering the effect of loading flowrate and column size.	Baur *et al.*[80]
General rate models	-	Compare and optimize design of single column batch and multicolumn continuous protein A chromatography. Evaluated performances under different upstream scenarios.	Guo *et al.*[81]

Table 3. Continued

General rate model + Reinforcement learning	CADET, MATLAB	Simulated 2 column continuous CEX for separation of charged variants using mechanistic models. Optimized flowrates to obtain maximum yield and productivity by machine learning method.	Nikita *et al.*[82]
CFD	OpenFOAM, SALOME, ParaView	Simulated fluid dynamics and pH distribution inside coiled flow inverter under different feed inputs for viral inactivation DSP step	David *et al.*[83]
CFD	ANSYS Fluent Workbench, with importing SOLIDWORKS CAD geometry	Investigated mixing inside tubular reactors by capturing velocity profiles during viral inactivation step. RTD were obtained here.	Parker *et al.*[84]
Stagnant Film Model (SFM) + Osmotic Pressure Model (OPM) + Boundary Layer Model (BLM) for	-	Simulated concentration polarization and mass transfer in Single-Pass-Tangential-Flow-Filtration (SPTFF). Understand membrane resistance, fluid properties, feed pressure, and flow effect on output flux and protein/ excipient concentrations.	Huter and Strube[85]

Data-driven Models: Design of experiment[86] are implemented to choose different statistical designs and plan sets of experiments. Supported by data-driven model/regression to statistically evaluate interactions between inputs and outputs of the process, identify major effects, and reduce the number of experiments to characterize the system. Popular DOE methods include full factorial, fractional factorial, Plackett-Burman, central composite, and Box–Behnken designs. Data-driven models include linear regression, response surface models, multivariate analysis, and machine learning methods.

Hybrid Models: Combine data-driven and mechanistic models. Usually, apply a data-driven model to capture complex nonlinear relations and use mechanistic models to capture critical physical and chemical interactions. Hybrid models have been widely used in both upstream and downstream batch processes.

Modeling approach	Modeling platform	Model details or representative examples	Reference
DOE + linear regression	MODDE, JMP	Used batch data to predict and correlate combinations of culture media and feed composition to cell growth, productivity, and titer. Further predicted media and feed effect in perfusion bioreactor.	Kuiper *et al.*[87]
DOE + response surface model	GraphPad Prism 6 Software, MODDE	Media screening using batch culture and applied response surface model to quantify impact of feed supplements on culture performance (e.g., productivity, cell growth, metabolism, morphology) to finally obtain desired perfusion media composition.	Mayrhofer *et al.*[88]
ANN + mechanistic model	MATLAB	Build a hybrid model to capture the flux duration of the cross-flow ultrafiltration processes. The performance of the model has been tested in batch, fed-batch continuous UF mode.	Krippl *et al.*[89]
DOE+ stepwise model fitting	JMP	Using DOE test different type of continuous chromatography (2 column, 4 column) and investigate feed titers, loading flow rates, and target breakthrough effects. Using the model to optimize capacity utilization and productivity	Baur *et al.*[90]
PCA and PLS regression. Data-driven + lumped kinetic model	MATLAB	Using statistical model to understand the relations between yield, purity, and dynamic binding capacities with chromatography operating data. Using hybrid modeling to understand the effect of the aging parameters, including binding capacity deterioration and mass transfer rate decrease, and to further optimize and forecast the online process information at different operating states.	Feidl, *et al.*[91]

In bioreactor modeling, to capture the relationship between operating conditions (temperature, pH, dissolve oxygen, agitation, perfusion rate, media supplements, etc.), productivity, and product quality, mechanistic modeling methods (such as kinetic modeling[66, 67] and flux balance analysis)[68–70] have been widely used. As shown in Table 3, in recent years, dynamic flux balance models have been found to be a promising method for continuous bioreactor modeling to capture the intracellular metabolite flux changes based on extracellular process conditions. Furthermore, a basis flux model has been developed that reduces the stoichiometric numbers comparing to traditional elementary flux models while identifying the metabolic states.[72] The effect of operating conditions, such as perfusion rate, aeration rate, and media supplements concentrations, are captured by simulating cell metabolism pathways.[68] With a better understanding of cell metabolism, batch and continuous processing have been compared to investigate the cell metabolic differences.[70] The dynamic process models can simulate substrate consumption and metabolite production rates, which can be used to build a high-throughput screening platform to assist in media development and clone screening.[92] However, most mechanistic models usually focus on limited media supplements and operating conditions.[93] In order to deal with media screening for a large number of nutrients, data-driven and hybrid models can be used instead. By augmenting Design of Experiments (DoE) with statistical models, such as multiple linear regression and response

surface models, the optimum media formulation can be obtained by quantifying the impact of different feed nutrients on cell growth, metabolites, and productivity.[87, 94, 95] Such methods can also be applied to build correlations between operating conditions with CQAs and to obtain optimum design space for temperature, pH, and time of production shift.[93, 96] Compared to mechanistic models, data-driven models have the ability to capture more variations in process conditions and product properties at the same time, but they are usually poorly extrapolated. Statistical analysis, such as principle component analysis (PCA) and multivariate analysis, can be used to understand the effect of culture variations on productivity and product heterogeneity.[97] Such multivariate analyses can also assist in process understanding by investigating cell metabolic profiles and shifts in physiological states during perfusion cultures over different process scales.[98] Other machine learning methods (such as support vector machines, neural networks, and Bayesian networks) have also been adopted for metabolic pathway analysis,[99] but have not been widely used in analysis of perfusion systems.

In general, perfusion cultivation failure often results from contamination and/or filter clogging of cell retention devices. These uncertainties in the upstream process impacts downstream operations and results in overall process shutdown. Mechanistic modeling can be used to predict process deviations or failure during continuous bioreactor operation. Computational fluid dynamics (CFD) simulations have been used to better understand localized fluid behavior and filter fouling to predict the lifetime and working efficiency of these filters.[74] Similarly, kinetic modeling has also been used to capture pore blockage by cells and micelles, which could also be used to predict upstream/downstream filter fouling.[67]

Multi-column chromatography (MCC) and continuous flow-through chromatography are used in primary capture and polishing steps. Multiple process parameters exist (including interconnected loading time, flow rate, feed titer, and bed height) that impacts buffer consumption, productivity, product quality, and yield. Compared to batch operations, continuous chromatography has even more operating parameters. Thus, the design and control of chromatography operations, as well as predicting the efficiency and yield of each column, are important for the development of continuous chromatography and its integration with upstream processes.[100] Mechanistic models, such as transport-dispersive models and general rate models, have been widely used to simulate fluid diffusion and binding kinetics in chromatography processing.[75, 76, 82, 101–103] To simulate MCC, recent studies have integrated mechanistic models with column scheduling and interconnection nodes. Optimization methods have been applied to investigate the interconnection feeding rate, feed concentration, yield, and resin capacities to improve productivity and resin utilization.[75, 76, 82, 101, 102] DoE with statistical models have been used to assist with high-throughput screening of downstream process operation parameters.[104, 105] Such methods also been applied to continuous downstream unit operations to identify the design space for different operations.[106] In addition, DoE can be used for parameter testing and support process optimization while reducing the experimental burden.[106] Parameter correlations can be also captured by multivariate analysis. Hybrid model has been used to capture the effect of the aging parameters (such as binding capacity deterioration and mass transfer rate decreases) on continuous chromatography performance and to further optimize and forecast the online process information at different operating states.[107] Continuous cation exchange chromatography (CEX) and anion exchange chromatography (AEX) membrane adsorbers have also been simulated to capture the efficiency of charged variant removal.[82, 108] First-principles based models for continuous chromatography and current chromatography technologies have been reviewed by Behere and Yoon,[100] Kumar and Lenhoff,[109] as well as Lin *et al*.[110] Methods have also been proposed to capture aggregate formation,[111] especially in batch process.[112, 113] However, limited modeling work has focused on aggregates and host cell proteins for simulation of downstream processes during continuous operations.

Other downstream unit operations, such as virus inactivation, can be simulated by CFD to capture pH effects[83] and residence time distribution (RTD) variance.[84] Mass transfer through the single-pass tangential flow filtration (SPTFF) can be obtained by a physicochemical model, such as stagnant film model, osmotic pressure model, or boundary layer model. Product concentration, filtration flux, and operation pressure can also be predicted and optimized using these process models to facilitate production performance improvement.[85]

In recent years, hybrid models have been used in both upstream and downstream batch operations modeling.[13, 114, 115] These models capture the missing nonlinear relationships and interaction variables, all of which improve the models' predictive ability.[116] In addition, a hybrid model has been used to capture resin aging in chromatography and to improve the resin lifetime.[107] Integrating with on-line monitoring tools, a hybrid model can be applied for real-time optimization of downstream processes.[116] Other modeling methods, such as surrogate models, can also be used for dynamic process modeling, process scheduling, and sensitivity or feasibility analysis at a lower computational cost.[117] However, there are still limited reports that have incorporated hybrid modeling during continuous biopharmaceutical production for process development.

Improvement of integrated process

Building an integrated continuous process requires a consistency of upstream/downstream flow rates, and the operation of different units will be compromised based on the capacities of other operations in the CM process train. In addition, different types of products will be suitable for different types of operating modes. Thus, a preliminary design and scheduling of the integrated process is critical in the decision of continuous operations. Based on both upstream and downstream operations, *in silico* integrated process models that capture each unit operation can be built.[118, 118, 119] The size and locations of surge tanks can also be designed by coupling mechanistic models with control systems that are critical to dealing with equipment failures and unexpected deviations during continuous operations.[12] However, due to the high computational costs of mechanistic models, which can cause difficulty with process analysis and optimization, the final integrated process models are usually simplified by using empirical equations,[118] hybrid models, and regression models or developed based on process simulators that use inbuilt input–output relations.[120–126] With the reduced computational costs, these simplified models can be integrated with PAT and a control system to achieve dynamic process control.[127] In addition, simulators are widely used in process development and design to capture mass balances and optimize process scheduling. Sensitivity analysis and optimization methods can be used with integrated models for early-stage process development and decision making. With support from the economic analysis, environmental impact analysis, and productivity/quality prediction, the operating modes

(including batch, continuous, and hybrid) can be compared and selected.[121, 124, 128] A recent publication covered the evaluation of continuous, batch, hybrid models with single-use and stainless steel equipment, and it studied the effects of process parameters, media costs, market success, product lifetime, and manufacturing scales on the cost effectiveness of different operating modes.[129] Alternative operating platforms can also be evaluated using such integrated models. For example, it has been shown that continuous non-protein A based purification/capture platforms (e.g., precipitation) provide a significant cost savings over protein A based downstream platforms.[130] Obtaining residence time distribution for each unit operation will support and guide process parameter adjustments and facilitate improvement of individual unit operations. Process failure caused by product contamination, equipment failure, or operation errors exist along the entire train of continuous operations. Monte Carlo analysis can be used to investigate the impact of failure rate on integrated continuous processes in terms of economics, such as cost of good values, flexibility of scheduling, and lot sizing decision.[131–133] For manufacturing platforms that contain multiple products, dynamic scheduling can also be used to support the operational decisions for multi-product operations and to provide optimal control policy.[133]

INTEGRATED ADVANCED PROCESS CONTROL

The control of mAb and other protein production processes has been studied and emphasized for several decades.[134] However, the production methods for the biopharmaceutical industry have evolved considerably in the past decade. Growing emphasis has been given to real-time adjustment of process operations through implementation of advanced feedback/feedforward control strategies in order to consistently produce therapeutic products with predefined CQAs.[3] The control system must ideally optimize the resources involved in manufacturing, reduce offline QC-lab based testing, and facilitate real time release (RTR) of biopharmaceutical products.[135] In feedback control systems, the process parameters and/or quality attributes are measured in real time, but corrective actions are taken automatically only after the disturbances affect product quality. A feed-forward control strategy (which is complementary to feedback control strategy) takes proactive actions before process disturbances impact product quality.[136] Thus, a control algorithm is needed to generate the control actions (i.e., manipulated variable signal). Depending on the need, either proportional integral derivative (PID) controller or model predictive controller (MPC) can be used for feedback control. PID is relatively straightforward to implement, whereas MPC represents a family of more advanced controllers that utilize a process model and optimization tools to predict the signal of manipulating variables. MPC performs better in many scenarios, such as when the process is dead time (or lag) dominant and exhibits a strong interaction amongst control variables. However, MPC is more expensive in terms of computational time because optimization steps must be performed for every control action taken.

On the other hand, the digital or 'smart' revolution in manufacturing has begun with an explosion in process monitoring, control, automation, and high-performance computing capabilities. Combined with the development of data analytics, advanced manufacturing concepts are transforming product and process designs. However, most of these advancements and new directions have taken place in non-pharmaceutical sectors, such as oil and gas, that traditionally have been several decades ahead in terms of technology adoption. Within the pharmaceutical sector, biomanufacturing processes (in particular) have seen the least amount of technological breakthrough and, therefore, represent a niche area for further scientific advancements and commercial implementation of advanced in-process control strategies.

Design and implementation of the control system

The design and implementation of an effective control system for mAb production process analogous to the multi-level control strategy proposed by the FDA is highly desired.[137] Here, Level 1 (also known as adaptive Engineering controls) is essentially the local level control where process variables (e.g., pH, temperature, output flow rate, and dissolved oxygen) are robustly measured in real-time using sensors that are already commercially available and controlled using classical control systems. These process parameters (controlled variables) are known to directly influence cell-culture properties and mAb product quality. This is the most basic type of closed-loop control but will nevertheless mitigate the risk of producing out-of-specification product, provided that the identified correlations are accurate. In the past, significant attention was paid to developing Level 1 control systems. For example, Ashoori *et al.* have investigated the control of pH and temperature on bioproceses.[138] Khan *et al.* were concerned with controlling dissolved oxygen in a fermenter using a PID (Proportional-Integral-Derivative) Controller.[139] The structure and functional activity of a monoclonal IgG1 antibody produced at the outer limits of numerical ranges of fed-batch culture control parameters (such as pH and temperature) were examined with the aim of providing assurance that an antibody produced under varying culture conditions was of consistent quality based on a carefully defined set of specifications.[140] It has also been shown that accurate control of flow rates, media composition, and cell density of a CHO cell perfusion bioreactor allowed the production of a constant glycosylation profile for over 20 days.[93]

The second level (Level 2) of control strategy, which is called model-based Pharmaceutical controls and is relatively less developed, is based on direct measurement of the cell culture output properties that directly correlate with mAb product yield for the biomanufacturing process. These properties include viable cell density and extracellular metabolites (e.g., lactate). In the third level (Level 3) control strategy, in-process material attributes (such as varying media batch/lot) and quality attributes (mAb glycosylation and charge states) can be measured and appropriate control actions can be taken correspondingly. Both mAb glycosylated (or charge state intermediates) and the concentration of cell metabolites are important early indicators of mAb product quality. Therefore, this control layer can allow faster regulation of the key CQAs. Much less attention, however, has been paid to implementing Levels 2 and 3 control strategies in continuous mAb manufacturing and, therefore, this is still an underexplored area of research.

A growing interest has been seen towards the utilization of advanced process control (APC) strategies, such as model predictive control (MPC) and integrated feedforward control, both of which can be built upon the control structures described in the Levels 1–3 strategies.[141, 142] A significant number of studies have focused on MPC of fermentation processes.[138, 143, 144] However, most work in this area is patented and this signifies the importance of applying MPC for continuous biomanufacturing.[145, 146]

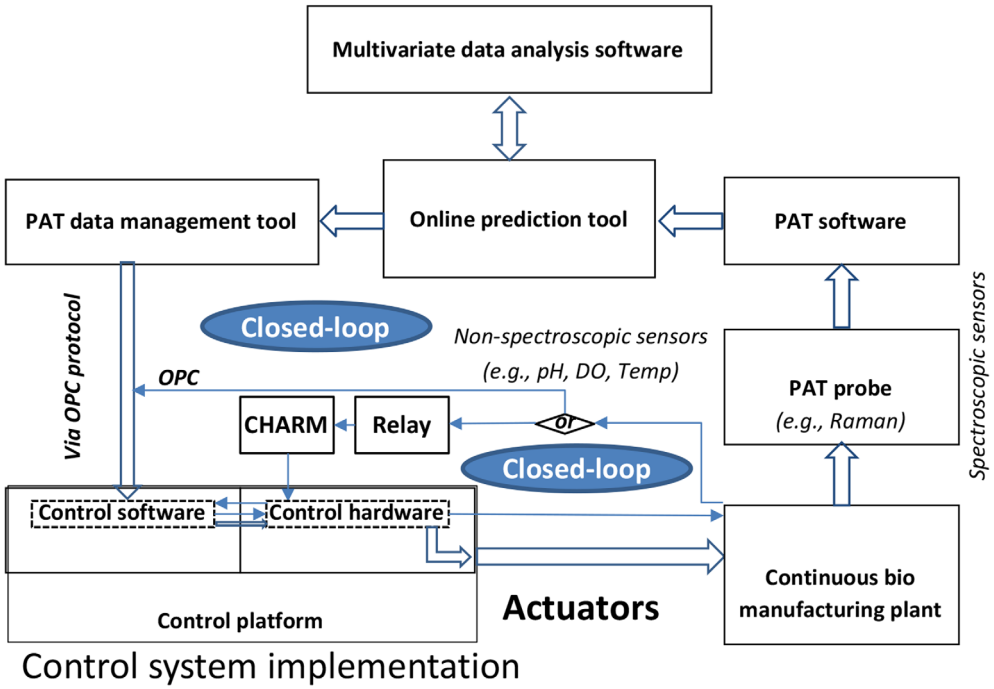

Figure 4. General outline of control system implementation for a continuous biopharmaceutical manufacturing plant using suitable PAT and process models.

High cell density and high titers of mAb production via cell medium design and rational control of the bioreactor were first proposed back in the mid-1990s.[147] In recent years, significant advances have been made in the area of control of upstream processes for achieving desired mAb product CQAs. O'Callaghan *et al.* (2010) compared the cellular control of recombinant human IgG4 monoclonal antibody synthesis in different CHO cell lines.[148] CHO cell line specific prediction and control of recombinant mAb N-linked glycosylation has also been investigated.[149] Metabolic control of recombinant mAb N-glycosylation in GS-NS0 cells was proposed.[150] Sha *et al.* (2016) studied N-Glycosylation design and control of mAb production.[151] However, to date and to the best of our knowledge, MPC has not yet been fully deployed for the control of continuous mAb production processes in the open literature. Feedforward control is useful in cases where there are large disturbances that can be measured, characterized, and controlled to proactively mitigate the undesired effect on product quality. Therefore, a significant amount of work has focused on feedforward and combined feedforward/feedback control of fermentation processes in general.[152–154] Feedforward control has also been applied for chromatographic separation.[155] However, feedforward control strategy has not been used yet for mAb production.

The essential steps for the implementation of control systems in continuous biomanufacturing processes are shown in Fig. 4. The monitoring tools (sensors),[156] control hardware, and software required for implementation of the control system need to be identified as the first step.[157] In the second step, the sensors need to be integrated within the physical plant to facilitate real-time on/in/at-line monitoring. This step integrates sensors with the equipment in the plant through a suitable sampling interface, software, and hardware. The measured signals are then sent to the control platform in step 3. For spectroscopic sensors, the development of suitable calibration models,[158] online prediction tools, and their integration with PAT data management tool and the control platform via the OPC (OLE process control) communication protocol are additional steps to be considered. Through these steps, the measured signal, along with any other signals (e.g., alarms), can be sent to the control platform to be recorded in the historian, and any data from the control platform can be sent back to the PAT data management tool for data storage, inspection, and auditing purposes. The plant can then be integrated with the control platform in step 4. In this step, the plant hardware/unit operations are connected with the control platform so that they can be operated through the control interface. Standard industrial communication protocols (such as Fieldbus, EtherNet/IP, or OLE process control) can be used to establish such communications. Subsequently, the control loops need to be implemented into the control platform, and the plant can be run under a closed-loop scenario.

Several studies related to the application of control systems in manufacturing industries, including the pharmaceutical industry, have been published over the last few decades. In these studies, emphasis has been given mainly to the development of cutting-edge on-line measurement and monitoring tools. Several spectroscopic techniques have, for example, been successfully implemented in pharmaceutical manufacturing processes,[159–163] and in food manufacturing processes.[164–167] A few attempts have been made to demonstrate the integration of control hardware/software and sensors with the plant and, therefore, to implement the control system into an actual pilot-plant process.[168] Ladner *et al.*[169] developed an at-line microreactor for automation of enzymatic reactions that enables the real-time quality control necessary for mAb production. This methodology, called D-PES (which stands for Diffusion-mediated Proteolysis combined with an Electrophoretic Separation), can subsequently perform mAb tryptic digestion and electrophoresis separation of proteolysis products in an automated manner. This approach presents a fast and easy

way for the quality control of mAbs.[169] Steinebach *et al.*[170] proposed a model-based adaptive control of a continuous capture process for mAbs production. The proposed adaptive procedure maintains a specified yield at optimal operating conditions in the presence of process disturbances, such as changes in the upstream titer and aging of the resin. Hogiri *et al*. proposed a pH-shift control strategy for producing mAbs in CHO cell cultures using a pH-dependent dynamic model.[171] Karst *et al*. implemented several control loops to enable the stable operation of a fully integrated mAb production process.[66] The liquid flow across the integrated process was regulated using three direct feedback control loops. In particular, the flow rate in the ProA capture unit was set by a volumetric feed pump. Its effective value, including valve switch times, was checked periodically by collecting the flow through at the unit outlet. In two separate control loops, the harvest rate from and the feed flow rate to the reactor were adjusted to keep the weight of the surge tank and the reactor volume constant. In addition, the volumetric fraction between the base and the enriched media in the feed stream was adjusted according to the viable cell density set point. The latter was controlled online through direct feedback of the biocapacitance probe measurement to the bleed pump.

PAT has been found to be useful for Level 2 process control and is an emerging control strategy. Most of the efforts here have been focused on real time monitoring and control of the glucose concentration. Berry *et al*. proposed a Raman spectroscopy based in-process glucose control system.[172] A nonlinear model predictive controller has also been proposed to control the glucose concentration.[43] Matthews *et al*. proposed glucose monitoring and adaptive feeding of mammalian cell culture in the presence of strong autofluorescence using near Infrared Raman Spectroscopy.[173] Closed loop control of lactate concentration in mammalian cell culture by Raman spectroscopy has been proposed as well.[42]

Over the last few years, various methods and tools for downstream biomanufacturing process control have been developed. Patel *et al*. proposed a multi-angle light scattering PAT tool for real-time monitoring of mAb molecular weight that is useful for downstream process control.[174] Real-time monitoring and control of the column loading phase of a protein A capture step has been also proposed.[175] A PAT approach based on ultraviolet/visible light (UV/VIS) spectroscopy for the inline protein concentration measurements needed for quality control and automation of downstream separations has been developed.[176] Papathanasiou *et al*. proposed a model-based control strategy for intensification of downstream processes.[177] A significant amount of work has been particularly done in the area of chromatographic separation process control. A model-based adaptive control of a continuous capture process for mAbs production has been presented by Steinebach *et al.*[170] The model-based control presented in this work guarantees not only operation of the process at fixed specifications in terms of yield and purity, but also maintenance of optimal performance with respect to resin utilization and buffer consumption.[170] Mendhe *et al*. compared PAT based approaches for making real-time pooling decisions for process chromatography by using the incorporation of feedforward control.[155] A dynamic control strategy of a continuous chromatography process independent of cell culture titer and impurities has also been developed.[178] In addition, online control of the twin-column countercurrent solvent gradient process for biochromatography has been implemented.[179] Advanced control strategies for the multicolumn countercurrent solvent gradient purification process have been also developed.[180] NIR has been applied for the real-time control of loading in Protein A chromatography in continuous manufacturing of monoclonal antibodies.[11]

These recent advances lay a solid foundation for the implementation of a robust process control strategy in continuous biopharmaceuticals manufacturing. The risk of product or process deviations in a continuous setup necessitates the use of robust and intelligent controllers that are capable of handling deviations in a fully automated manner.[181] Developing such integrated controllers has several challenges with respect to developing model predictive control strategies, control hardware, and software integration, and interfacing between the unit operation equipment and control system. However, a fully integrated closed-loop continuous mAb manufacturing process has not yet been reported in the open literature and, therefore, this is an active and open area of research.

CONCLUSIONS

Based on ongoing scientific and technological advances in various research fields, significant opportunities have surfaced in recent years for improving the efficiency of manufacturing processes and quality assurance systems in the biopharmaceutical drug manufacturing sector. Continuous biomanufacturing approaches are being continually pursued by academia/industry via the introduction of novel and innovative analytical techniques/methods for rapid/robust PAT, predictive product and process model development, and finally, the integrated implementation of PAT-models with advanced process control strategies to produce biologics with the desired quality attributes in an economically viable manner.

ACKNOWLEDGEMENTS

The authors acknowledge support from the U. S. Food and Drug Administration (FDA) through FDA-CBER Award Number 1R01FD006588.

REFERENCES

1 Kinch MS, An overview of FDA-approved biologics medicines. *Drug Discov Today* **20**:393–398 (2015).
2 Ahmed, A; India's biocon secures approval to use drug on coronavirus patients, 2020. https://www.reuters.com/article/india-biocon-idINKCN24C0JU
3 Singh R, Gernaey KV and Gani R, Model-based computer-aided framework for design of process monitoring and analysis systems. *Comput Chem Eng* **33**:22–42 (2009). http://doi.org/10.1016/j.compchemeng.2008.06.002.
4 FDA Center for Drug Evaluation and Research. Guidance for industry PAT - a framework for innovative pharmaceutical development, manufacturing, and quality assurance (Docket No. FDA-2003-D-0032). Available: https://www.fda.gov/regulatory-information/search-fda-guidance-documents/pat-framework-innovative-pharmaceutical-development-manufacturing-and-quality-assurance (2004).
5 Gnoth S, Jenzsch M, Simutis R and Lübbert A, Process analytical technology (PAT): batch-to-batch reproducibility of fermentation processes by robust process operational design and control. *J Biotechnol* **132**:180–186 (2007).
6 Farid SS, Thompson B and Davidson A, Continuous bioprocessing: The real thing this time?. *mAbs* **6**:1357–1361 (2014). http://doi.org/10.4161/mabs.36151.
7 Fisher AC, Kamga MH, Agarabi C, Brorson K, Lee SL and Yoon S, The current scientific and regulatory landscape in advancing integrated

continuous biopharmaceutical manufacturing. *Trends Biotechnol* **37**: 253–267 (2019).
8 Konstantinov KB and Cooney CL, White paper on continuous bioprocessing may 20–21 2014 continuous manufacturing symposium. *J Pharm Sci* **104**:813–820 (2015).
9 Feidl F, Vogg S, Wolf M, Podobnik M, Ruggeri C, Ulmer N *et al*., Process-wide control and automation of an integrated continuous manufacturing platform for antibodies. *Biotechnol Bioeng* **117**: 1367–1380 (2020).
10 Coffman J, Brower M, Connell-Crowley L, Deldari S, Farid SS, Horowski B *et al*., A common framework for integrated and continuous biomanufacturing. *Biotechnol Bioeng* **118**:1721–1735 (2021).
11 Thakur G, Hebbi V and Rathore AS, An NIR-based PAT approach for real-time control of loading in protein A chromatography in continuous manufacturing of monoclonal antibodies. *Biotechnol Bioeng* **117**:673–686 (2020).
12 Thakur G, Saxena N, Tiwari A and Rathore AS, Control of surge tanks for continuous manufacturing of monoclonal antibodies. *Biotechnol Bioeng* **118**:1913–1931 (2021). https://doi.org/10.1002/bit.27706.
13 Narayanan H, Sokolov M, Morbidelli M and Butté A, A new generation of predictive models: the added value of hybrid models for manufacturing processes of therapeutic proteins. *Biotechnol Bioeng* **116**:2540–2549 (2019).
14 Narayanan H, Luna MF, von Stosch M, Cruz Bournazou MN, Polotti G, Morbidelli M *et al*., Bioprocessing in the digital age: the role of process models. *Biotechnol J* **15**:1–10 (2020).
15 Karst DJ, Serra E, Villiger TK, Soos M and Morbidelli M, Characterization and comparison of ATF and TFF in stirred bioreactors for continuous mammalian cell culture processes. *Biochem Eng J* **110**:17–26 (2016).
16 Xu S, Gavin J, Jiang R and Chen H, Bioreactor productivity and media cost comparison for different intensified cell culture processes. *Biotechnol Prog* **33**:867–878 (2017).
17 Mozdzierz NJ, Love KR, Lee KS, Lee HL, Shah KA, Ram RJ *et al*., A perfusion-capable microfluidic bioreactor for assessing microbial heterologous protein production. *Lab Chip* **15**:2918–2922 (2015).
18 Vogg S, Müller-Späth T and Morbidelli M, Current status and future challenges in continuous biochromatography. *Curr Opin Chem Eng* **22**:138–144 (2018).
19 Gomes J, Chopda VR and Rathore AS, Integrating systems analysis and control for implementing process analytical technology in bioprocess development. *J Chem Technol Biotechnol* **90**:583–589 (2015).
20 O'Regan, T. Development of Dielectric Spectroscopic monitoring methods for the prediction of viable cell density and volume in mammalian cell culture. MSc Thesis. Dublin City Univ. (2012). http://doras.dcu.ie/16790/
21 Santos RM, Kaiser P, Menezes JC and Peinado A, Improving reliability of Raman spectroscopy for mAb production by upstream processes during bioprocess development stages. *Talanta* **199**:396–406 (2019).
22 Cervera AE, Petersen N, Lantz AE, Larsen A and Gernaey KV, Application of near-infrared spectroscopy for monitoring and control of cell culture and fermentation. *Biotechnol Prog* **25**:1561–1581 (2009).
23 Großhans S, Rüdt M, Sanden A, Brestrich N, Morgenstern J, Heissler S *et al*., In-line Fourier-transform infrared spectroscopy as a versatile process analytical technology for preparative protein chromatography. *J Chromatogr A* **1547**:37–44 (2018).
24 Boulet-Audet M, Kazarian SG and Byrne B, In-column ATR-FTIR spectroscopy to monitor affinity chromatography purification of monoclonal antibodies. *Sci Rep* **6**:1–13 (2016).
25 Tharmalingam T, Wu C-H, Callahan S and Goudar T, A framework for real-time glycosylation monitoring (RT-GM) in mammalian cell culture. *Biotechnol Bioeng* **112**:1146–1154 (2015).
26 Center for Drug Evaluation and Research, Center for Biologics Evaluation and Research. ICH Q8(R2) pharmaceutical development, Docket Number: FDA-2005-D-0154. (2009). https://www.fda.gov/regulatory-information/search-fda-guidance-documents/q8r2-pharmaceutical-development.
27 Chemmalil L, Prabhakar T, Kuang J, West J, Tan Z, Ehamparanathan V *et al*., Online/at-line measurement, analysis and control of product titer and critical product quality attributes (CQAs) during process development. *Biotechnol Bioeng*. **117**:3757–3765 (2020). https://doi.org/10.1002/bit.27531.
28 Wang Y, Feng P, Sosic Z and Zang L, Monitoring glycosylation profile and protein titer in cell culture samples using ZipChip CE-MS. *J Anal Bioanal Tech*. **8**:359 (2017). https://doi.org/10.4172/2155-9872.1000359.
29 Capito F, Skudas R, Kolmar H and Hunzinger C, At-line mid infrared spectroscopy for monitoring downstream processing unit operations. *Process Biochem*. **50**:997–1005 (2015). https://doi.org/10.1016/j.procbio.2015.03.005.
30 Mattes R, Root D, Sugui MA, Chen F, Shi X, Liu J *et al*., Real-time bioreactor monitoring of osmolality and pH using near-infrared spectroscopy. *Bioprocess Int*. **7**:44–50 (2009).https://bioprocessintl.com/analytical/upstream-development/real-time-bioreactor-monitoring-of-osmolality-and-ph-using-near-infrared-spectroscopy-183756/.
31 Webster TA, Hadley BC, Hilliard W, Jaques C and Mason C, Development of generic raman models for a GS-KOTM CHO platform process. *Biotechnol Prog*. **34**:730–737 (2018). https://doi.org/10.1002/btpr.2633.
32 Hakemeyer C, Strauss U, Werz S, Jose GE, Folque F and Menezes JC, At-line NIR spectroscopy as effective PAT monitoring technique in Mab cultivations during process development and manufacturing. *Talanta*. **90**:12–21 (2012). https://doi.org/10.1016/j.talanta.2011.12.042.
33 Doneanu CE, Xenopoulos A, Fadgen K, Murphy J, Skilton SJ, Prentice H *et al*., Analysis of host-cell proteins in biotherapeutic proteins by comprehensive online two-dimensional liquid chromatography/mass spectrometry. *MAbs*. **4**:24–44 (2012). https://doi.org/10.4161/mabs.4.1.18748.
34 Pinto IF, Soares RRG, Mäkinen ME-L, Chotteau V and Russom A, Multiplexed microfluidic cartridge for at-line protein monitoring in mammalian cell culture processes for biopharmaceutical production. *ACS Sens* **6**:842–851 (2021). https://doi.org/10.1021/acssensors.0c01884.
35 Williams A, Read EK, Agarabi CD, Lute S and Brorson KA, Automated 2D-HPLC method for characterization of protein aggregation with in-line fraction collection device. *J Chromatogr B Anal Technol Biomed Life Sci*. **1046**:122–130 (2017). https://doi.org/10.1016/j.jchromb.2017.01.021.
36 Dai J, Lamp J, Xia Q and Zhang Y, Capillary isoelectric focusing-mass spectrometry method for the separation and online characterization of intact monoclonal antibody charge variants. *Anal Chem*. **90**:2246–2254 (2018). https://doi.org/10.1021/acs.analchem.7b04608.
37 Füssl F, Cook K, Scheffler K, Farrell A, Mittermayr S and Bones J, Charge variant analysis of monoclonal antibodies using direct coupled pH gradient cation exchange chromatography to high-resolution native mass spectrometry. *Anal Chem*. **90**:4669–4676 (2018). https://doi.org/10.1021/acs.analchem.7b05241.
38 Ehkirch A, Goyon A, Hernandez-Alba O, Rouviere F, D'Atri V, Dreyfus C *et al*., A novel online four-dimensional SEC×SEC-IM×MS methodology for characterization of monoclonal antibody size variants. *Anal Chem* **90**:13929–13937 (2018). https://doi.org/10.1021/acs.analchem.8b03333.
39 Camperi J, Dai L, Guillarme D and Stella C, Fast and automated characterization of monoclonal antibody minor variants from cell cultures by combined protein-A and multidimensional LC/MS methodologies. *Anal Chem*. **92**:8506–8513 (2020). https://doi.org/10.1021/acs.analchem.0c01250.
40 Chi B, Veyssier C, Kasali T, Uddin F and Sellick CA, At-line high throughput site-specific glycan profiling using targeted mass spectrometry. *Biotechnol Rep* **25**:e00424 (2020). https://doi.org/10.1016/j.btre.2020.e00424.
41 Abu-Absi NR, Kenty BM, Cuellar ME, Borys MC, Sakhamuri S, Strachan DJ *et al*., Real time monitoring of multiple parameters in mammalian cell culture bioreactors using an in-line Raman spectroscopy probe. *Biotechnol Bioeng* **108**:1215–1221 (2011).
42 Matthews TE, Berry BN, Smelko J, Moretto J, Moore B and Wiltberger K, Closed loop control of lactate concentration in mammalian cell culture by Raman spectroscopy leads to improved cell density, viability, and biopharmaceutical protein production. *Biotechnol Bioeng* **113**:2416–2424 (2016).
43 Craven S, Whelan J and Glennon B, Glucose concentration control of a fed-batch mammalian cell bioprocess using a nonlinear model predictive controller. *J Process Control* **24**:344–357 (2014). http://doi.org/10.1016/j.jprocont.2014.02.007.
44 Rowland-Jones RC and Jaques C, At-line raman spectroscopy and design of experiments for robust monitoring and control of miniature bioreactor cultures. *Biotechnol Prog* **35**:e2740 (2019).

45 Yilmaz D, Mehdizadeh H, Navarro D, Shehzad A, O'Connor M and McCormick P, Application of Raman spectroscopy in monoclonal antibody producing continuous systems for downstream process intensification. *Biotechnol Prog* **36**:e2947 (2020). https://doi.org/10.1002/btpr.2947.
46 Patil U, Crum M, Vu B, Wasden K, Kourentzi K and Willson RC, Continuous Fc detection for protein a capture process control. *Biosens Bioelectron* **165**:112327 (2020). https://doi.org/10.1016/j.bios.2020.112327.
47 Eyster T, Talwar S, Fernandez J, Foster S, Hayes J, Allen R *et al.*, Tuning monoclonal antibody galactosylation using Raman spectroscopy-controlled lactic acid feeding. *Biotechnol Prog* **37**:e3085 (2021).
48 Sauer DG, Melcher M, Mosor M, Walch N, Berkemeyer M, Scharl-Hirsch T *et al.*, Real-time monitoring and model-based prediction of purity and quantity during a chromatographic capture of fibroblast growth factor 2. *Biotechnol Bioeng* **116**:1999–2009 (2019).
49 Pei Y, Wang J, Wu K, Xuan X and Lu X, Ionic liquid-based aqueous two-phase extraction of selected proteins. *Sep Purif Technol* **64**:288–295 (2009).
50 Thakur G, Thori S and Rathore AS, Implementing PAT for single-pass tangential flow ultrafiltration for continuous manufacturing of monoclonal antibodies. *J Membr Sci* **613**:118492 (2020).
51 Tiernan H, Byrne B and Kazarian SG, ATR-FTIR spectroscopy and spectroscopic imaging for the analysis of biopharmaceuticals. *Spectrochim Acta A Mol Biomol Spectrosc* **241**:118636 (2020).
52 Powers DN, Wang Y, Fratz-Berilla EJ, Velugula-Yellela SR, Chavez B, Angart P *et al.*, Real-time quantification and supplementation of bioreactor amino acids to prolong culture time and maintain antibody product quality. *Biotechnol Prog* **35**:1–11 (2019).
53 Tiwari A, Kateja N, Chanana S and Rathore AS, Use of HPLC as an enabler of process analytical technology in process chromatography. *Anal Chem* **90**:7824–7829 (2018).
54 Patel BA, Pinto NDS, Gospodarek A, Kilgore B, Goswami K, Napoli WN *et al.*, On-line ion exchange liquid chromatography as a process analytical technology for monoclonal antibody characterization in continuous bioprocessing. *Anal Chem* **89**:11357–11365 (2017).
55 Li MY, Ebel B, Paris C, Chauchard F, Guedon E and Marc A, Real-time monitoring of antibody glycosylation site occupancy by in situ Raman spectroscopy during bioreactor CHO cell cultures. *Biotechnol Prog* **34**:486–493 (2018).
56 Ma S and Nashabeh W, Analysis of protein therapeutics by capillary electrophoresis. *CE in Biotechnology: Practical Applications for Protein and Peptide Analyses*. Vieweg+Teubner Verlag; **5**:55–89 (2001). https://doi.org/10.1007/978-3-322-83021-0_9.
57 Szabo Z, Guttman A, Bones J and Karger BL, Rapid high-resolution characterization of functionally important monoclonal antibody N-glycans by capillary electrophoresis. *Anal Chem* **83**:5329–5336 (2011).
58 Wang L, Bo T, Zhang Z, Wang G, Tong W and Da Yong Chen D, High resolution capillary isoelectric focusing mass spectrometry analysis of peptides, proteins, and monoclonal antibodies with a flow-through microvial interface. *Anal Chem* **90**:9495–9503 (2018). http://doi.org/10.1021/acs.analchem.8b02175.
59 Guerra A, von Stosch M and Glassey J, Toward biotherapeutic product real-time quality monitoring. *Crit Rev Biotechnol* **39**:289–305 (2019).
60 Jenzsch M, Bell C, Buziol S, Kepert F, Wegele H and Hakemeyer C, Trends in process analytical technology: present state in bioprocessing. *Adv Biochem Eng Biotechnol* **123**:211–252 (2017).
61 Flury B, Murtagh F and Heck A, Multivariate data analysis. *Math Comput* **50**:352 (1988).
62 Domján J, Fricska A, Madarász L, Gyürkés M, Köte Á, Farkas A *et al.*, Raman-based dynamic feeding strategies using real-time glucose concentration monitoring system during adalimumab producing CHO cell cultivation. *Biotechnol Prog* **36**:1–12 (2020).
63 Rafferty C, Johnson K, O'Mahony J, Burgoyne B, Rea R and Balss KM, Analysis of chemometric models applied to Raman spectroscopy for monitoring key metabolites of cell culture. *Biotechnol Prog* **36**:1–16 (2020).
64 Smiatek J, Jung A and Bluhmki E, Towards a digital bioprocess replica: computational approaches in biopharmaceutical development and manufacturing. *Trends Biotechnol* **38**:1141–1153 (2020). http://doi.org/10.1016/j.tibtech.2020.05.008.
65 Kumar A, Udugama IA, Gargalo CL and Gernaey KV, Why is batch processing still dominating the biologics landscape? towards an integrated continuous bioprocessing alternative. *Processes* **8**:1641 (2020). http://doi.org/10.3390/pr8121641.
66 Karst DJ, Steinebach F, Soos M and Morbidelli M, Process performance and product quality in an integrated continuous antibody production process. *Biotechnol Bioeng* **114**:298–307 (2017).
67 Kelly W, Scully J, Zhang D, Feng G, Lavengood M, Condon J *et al.*, Understanding and modeling alternating tangential flow filtration for perfusion cell culture. *Biotechnol Prog* **30**:1291–1300 (2014).
68 Kelly W, Veigne S, Li X, Subramanian SS, Huang Z and Schaefer E, Optimizing performance of semi-continuous cell culture in an ambr15™ microbioreactor using dynamic flux balance modeling. *Biotechnol Prog* **34**:420–431 (2018).
69 Hutter S, Wolf M, Papili Gao N, Lepori D, Schweigler T, Morbidelli M *et al.*, Glycosylation flux analysis of immunoglobulin G in chinese hamster ovary perfusion cell culture. *Processes* **6**:176 (2018). http://doi.org/10.3390/pr6100176.
70 Templeton N, Xu S, Roush DJ and Chen H, 13C metabolic flux analysis identifies limitations to increasing specific productivity in fed-batch and perfusion. *Metab Eng* **44**:126–133 (2017).
71 Brunner M, Kolb K, Keitel A, Stiefel F, Wucherpfennig T, Bechmann J *et al.*, Application of metabolic modeling for targeted optimization of high seeding density processes. *Biotechnol Bioeng* **118**:1793–1804 (2021). http://doi.org/10.1002/bit.27693.
72 Rodrigues D, Abdalmoaty MR, Jacobsen EW, Chotteau V and Hjalmarsson H, An integrated approach for modeling and identification of perfusion bioreactors via basis flux modes. *Comput Chem Eng* **149**:107238 (2021). http://doi.org/10.1016/j.compchemeng.2021.107238.
73 Abbate T, Fernandes de Sousa S, Dewasme L, Bastin G and Vande Wouwer A, Inference of dynamic macroscopic models of cell metabolism based on elementary flux modes analysis. *Biochem Eng J* **151**:107325 (2019). http://doi.org/10.1016/j.bej.2019.107325.
74 Radoniqi F, Zhang H, Bardliving CL, Shamlou P and Coffman J, Computational fluid dynamic modeling of alternating tangential flow filtration for perfusion cell culture. *Biotechnol Bioeng* **115**:2751–2759 (2018).
75 Gomis-Fons J, Andersson N and Nilsson B, Optimization study on periodic counter-current chromatography integrated in a monoclonal antibody downstream process. *J Chromatogr A* **1621**:461055 (2020). https://doi.org/10.1016/j.chroma.2020.461055.
76 Ng CKS, Rousset F, Valery E, Bracewell DG and Sorensen E, Design of high productivity sequential multi-column chromatography for antibody capture. *Food Bioprod Process* **92**:233–241 (2014).
77 Shi C, Gao ZY, Zhang QL, Yao SJ, Slater NK and Lin DQ, Model-based process development of continuous chromatography for antibody capture: a case study with twin-column system. *J Chromatogr A* **1619**:936 (2020).
78 Shi C, Zhang QL, Jiao B, Chen XJ, Chen R, Gong W *et al.*, Process development and optimization of continuous capture with three-column periodic counter-current chromatography. *Biotechnol Bioeng* **1996**:1–10 (2021). http://doi.org/10.1002/bit.27689.
79 Sun Y-N, Shi C, Zhang QL, Yao SJ, Slater NK and Lin DQ, Model-based process development and evaluation of twin-column continuous capture processes with protein A affinity resin. *J Chromatogr A* **1625**:300 (2020).
80 Baur D, Angarita M, Müller-Späth T and Morbidelli M, Optimal model-based design of the twin-column CaptureSMB process improves capacity utilization and productivity in protein A affinity capture. *Biotechnol J* **11**:135–145 (2016).
81 Guo J, Jin M and Kanani D, Optimization of single-column batch and multicolumn continuous protein A chromatography and performance comparison based on mechanistic model. *Biotechnol J* **15**:2000192 (2020).
82 Nikita S, Tiwari A, Sonawat D, Kodamana H and Rathore AS, Reinforcement learning based optimization of process chromatography for continuous processing of biopharmaceuticals. *Chem Eng Sci* **230**:116171 (2021).
83 David L, Waldschmidt LM, Lobedann M and Schembecker G, Simulation of pH level distribution inside a coiled flow inverter for continuous low pH viral inactivation. *Biotechnol Bioeng* **117**:429–437 (2020).
84 Parker SA, Amarikwa L, Vehar K, Orozco R, Godfrey S, Coffman J *et al.*, Design of a novel continuous flow reactor for low pH viral inactivation. *Biotechnol Bioeng* **115**:606–616 (2018).

85 Huter MJ and Strube J, Model-based design and process optimization of continuous single pass tangential flow filtration focusing on continuous bioprocessing. *Processes* **7**:317 (2019). http://doi.org/10.3390/pr7060317

86 Ritacco FV, Wu Y and Khetan A, Cell culture media for recombinant protein expression in Chinese hamster ovary (CHO) cells: history, key components, and optimization strategies. *Biotechnol Prog* **34**: 1407–1426 (2018).

87 Kuiper M, Spencer C, Fäldt E, Vuillemez A, Holmes W, Samuelsson T *et al*., Repurposing fed-batch media and feeds for highly productive CHO perfusion processes. *Biotechnol Prog* **35**:e2821 (2019).

88 Mayrhofer P, Reinhart D, Castan A and Kunert R, Rapid development of clone-specific, high-performing perfusion media from established feed supplements. *Biotechnol Prog* **36**:1–14 (2020). http://doi.org/10.1002/btpr.2933.

89 Krippl M, Dürauer A and Duerkop M, Hybrid modeling of cross-flow filtration: Predicting the flux evolution and duration of ultrafiltration processes. *Sep Purif Technol* **248**:64 (2020).

90 Baur D, Angelo JM, Chollangi S, Xu X, Müller-Späth T, Zhang N *et al*., Model assisted comparison of protein A resins and multi-column chromatography for capture processes. *J Biotechnol* **285**:64–73 (2018).

91 Feidl F, Luna MF, Podobnik M, Vogg S, Angelo J, Potter K *et al*., Model based strategies towards protein A resin lifetime optimization and supervision. *J Chromatogr A* **1625**:261 (2020).

92 Gagliardi TM, Chelikani R, Yang Y, Tuozzolo G and Yuan H, Development of a novel, high-throughput screening tool for efficient perfusion-based cell culture process development. *Biotechnol Prog* **35**:1–12 (2019).

93 Karst DJ, Scibona E, Serra E, Bielser JM, Souquet J, Stettler M *et al*., Modulation and modeling of monoclonal antibody N-linked glycosylation in mammalian cell perfusion reactors. *Biotechnol Bioeng* **114**:1978–1990 (2017).

94 Mayrhofer P and Kunert R, in Screening of Media Supplements for High-Performance Perfusion Cultures by Design of Experiment BT - Animal Cell Biotechnology: Methods and Protocols. *Animal Cell Biotechnology*, ed. by Pörtner R. Methods in Molecular Biology (MIMB, volume 2095), Humana, New York, NY: Springer US, pp. 27–39 (2020). https://doi.org/10.1007/978-1-0716-0191-4_3.

95 Dhanasekharan K, Berdugo-Davis C, Liu X, Richey C, Segu Z, Vinci V *et al*., Rapid development and scale-up of biosimilar trastuzumab: a case study of integrated cell line and process development. *Bioprocess Int* **13** (2015).

96 Kim YJ, Paik SH, Han SK, Lee S, Jeong Y, Kim JY *et al*., Quality by design characterization of the perfusion culture process for recombinant FVIII. *Biologicals* **59**:37–46 (2019).

97 Walther J, Lu J, Hollenbach M, Yu M, Hwang C, McLarty J *et al*., Perfusion cell culture decreases process and product heterogeneity in a head-to-head comparison with fed-batch. *Biotechnol J* **14**:1–10 (2019).

98 Vernardis SI, Goudar CT and Klapa MI, Metabolic profiling reveals that time related physiological changes in mammalian cell perfusion cultures are bioreactor scale independent. *Metab Eng* **19**:1–9 (2013).

99 Cuperlovic-Culf M, Machine learning methods for analysis of metabolic data and metabolic pathway modeling. *Metabolites* **8**:4 (2018). http://doi.org/10.3390/metabo8010004.

100 Behere K and Yoon S, Chromatography bioseparation technologies and in-silico modelings for continuous production of biotherapeutics. *J Chromatogr A* **2020**:461376 (1627).

101 Shi C, Gao ZY, Zhang QL, Yao SJ, Slater NK and Lin DQ, Model-based process development of continuous chromatography for antibody capture: a case study with twin-column system. *J Chromatogr A* **2020**:460936 (1619).

102 Noriko Y, Optimization of flow-through chromatography of proteins. *J Chem Eng Jpn* **53**:1–8 (2020).

103 Vetter FL, Zobel-Roos S and Strube J, PAT for continuous chromatography integrated into continuous manufacturing of biologics towards autonomous operation. *Processes* **9**:472 (2021). http://doi.org/10.3390/pr9030472.

104 Cramer SM and Holstein MA, Downstream bioprocessing: recent advances and future promise. *Curr Opin Chem Eng* **1**:27–37 (2011).

105 Nfor BK, Verhaert PDEM, van der Wielen LAM, Hubbuch J and Ottens M, Rational and systematic protein purification process development: the next generation. *Trends Biotechnol* **27**:673–679 (2009).

106 Baur D, Angelo J, Chollangi S, Müller-Späth T, Xu X, Ghose S *et al*., Model-assisted process characterization and validation for a continuous two-column protein A capture process. *Biotechnol Bioeng* **116**: 87–98 (2019).

107 Feidl F, Luna MF, Podobnik M, Vogg S, Angelo J, Potter K *et al*., Model based strategies towards protein A resin lifetime optimization and supervision. *J Chromatogr A* **2020**:461261 (1625).

108 Khanal O, Kumar V, Westerberg K, Schlegel F and Lenhoff AM, Multicolumn displacement chromatography for separation of charge variants of monoclonal antibodies. *J Chromatogr A* **1586**:40–51 (2019).

109 Kumar V and Lenhoff AM, Mechanistic modeling of preparative column chromatography for biotherapeutics. *Annu Rev Chem Biomol Eng* **11**:235–255 (2020). http://doi.org/10.1146/annurev-chembioeng-102419-125430.

110 Lin D-Q, Zhang Q-L and Yao S-J, Model-assisted approaches for continuous chromatography: current situation and challenges. *J Chromatogr A* **2021**:461855 (1637).

111 Trnovec H, Doles T, Hribar G, Furlan N and Podgornik A, Characterization of membrane adsorbers used for impurity removal during the continuous purification of monoclonal antibodies. *J Chromatogr A* **2020**:460518 (1609).

112 Kluters S, Wittkopp F, Jöhnck M and Frech C, Application of linear pH gradients for the modeling of ion exchange chromatography: separation of monoclonal antibody monomer from aggregates. *J Sep Sci* **39**:663–675 (2016).

113 Lee YF, Jöhnck M and Frech C, Evaluation of differences between dual salt-pH gradient elution and mono gradient elution using a thermodynamic model: simultaneous separation of six monoclonal antibody charge and size variants on preparative-scale ion exchange chromatographic resin. *Biotechnol Prog* **34**:973–986 (2018).

114 Zalai D, Koczka K, Párta L, Wechselberger P, Klein T and Herwig C, Combining mechanistic and data-driven approaches to gain process knowledge on the control of the metabolic shift to lactate uptake in a fed-batch CHO process. *Biotechnol Prog* **31**:1657–1668 (2015).

115 Wang G, Briskot T, Hahn T, Baumann P and Hubbuch J, Estimation of adsorption isotherm and mass transfer parameters in protein chromatography using artificial neural networks. *J Chromatogr A* **1487**: 211–217 (2017).

116 Herwig, C. *Hybrid Modelling and Multi- Parametric Control of Bioprocesses*. MDPI Special Issue in Bioengineering, MDPI, Basel, Switzerland pp. 1–125 (2018). https://doi.org/10.3390/books978-3-03842-746-9.

117 Gargalo CL, de Las Heras SC, Jones MN, Udugama I, Mansouri SS, Krühne U *et al*., *Towards the Development of Digital Twins for the Bio-Manufacturing Industry*. Springer, Berlin, Heidelberg, pp. 1–34 (2020). https://doi.org/10.1007/10_2020_142.

118 Sencar J, Hammerschmidt N and Jungbauer A, Modeling the residence time distribution of integrated continuous bioprocesses. *Biotechnol J* **15**:1–12 (2020). http://doi.org/10.1002/biot.202000008.

119 Gomis-Fons J, Schwarz H, Zhang L, Andersson N, Nilsson B, Castan A *et al*., Model-based design and control of a small-scale integrated continuous end-to-end mAb platform. *Biotechnol Prog* **36**:e2995 (2020). http://doi.org/10.1002/btpr.2995.

120 Walther J, Godawat R, Hwang C, Abe Y and Sinclair A, The business impact of an integrated continuous biomanufacturing platform for recombinant protein production. *J Biotechnol* **213**:3–12 (2015).

121 Yang O, Prabhu S and Ierapetritou M, Comparison between batch and continuous monoclonal antibody production and economic analysis. *Ind Eng Chem Res* **58**:5851–5863 (2019). https://doi.org/10.1021/acs.iecr.8b04717.

122 Gupta P, Kateja N, Mishra S, Kaur H and Rathore AS, Economic assessment of continuous processing for manufacturing of biotherapeutics. *Biotechnol Prog* **37**:e3108 (2021). http://doi.org/10.1002/btpr.3108.

123 Xenopoulos A, A new, integrated, continuous purification process template for monoclonal antibodies: process modeling and cost of goods studies. *J Biotechnol* **213**:42–53 (2015).

124 Pleitt K, Somasundaram B, Johnson B, Shave E and Lua LHL, Evaluation of process simulation as a decisional tool for biopharmaceutical contract development and manufacturing organizations. *Biochem Eng J* **150**:107252 (2019).

125 Cataldo AL, Burgstaller D, Hribar G, Jungbauer A and Satzer P, Economics and ecology: modelling of continuous primary recovery

and capture scenarios for recombinant antibody production. *J Biotechnol* **308**:87–95 (2020).
126 Arnold L, Lee K, Rucker-Pezzini J and Lee JH, Implementation of fully integrated continuous antibody processing: effects on productivity and COGm. *Biotechnol J* **14**:1800061 (2019).
127 Helgers H, Schmidt A, Lohmann LJ, Vetter FL, Juckers A, Jensch C *et al.*, Towards autonomous operation by advanced process control—process analytical technology for continuous biologics antibody manufacturing. *Processes* **9**:1–31 (2021).
128 Pollock J, Coffman J, Ho SV and Farid SS, Integrated continuous bioprocessing: economic, operational, and environmental feasibility for clinical and commercial antibody manufacture. *Biotechnol Prog* **33**:854–866 (2017).
129 Mahal H, Branton H and Farid SS, End-to-end continuous bioprocessing: impact on facility design, cost of goods and cost of development for monoclonal antibodies. *Biotechnol Bioeng* (2021). http://doi.org/10.1002/bit.27774.
130 Bansode V, Gupta P, Kateja N and Rathore AS, Contribution of protein A step towards cost of goods for continuous production of monoclonal antibody therapeutics. *J Chem Technol Biotechnol* (2021). https://doi.org/10.1002/jctb.6686.
131 Satzer P, Komuczki D, Pappenreiter M, Cataldo AL, Sissolak B and Jungbauer A, Impact of failure rates, lot definitions and scheduling of upstream processes on the productivity of continuous integrated bioprocesses. *J Chem Technol Biotechnol* (2021). http://doi.org/10.1002/jctb.6648.
132 Pollock J, Ho SV and Farid SS, Fed-batch and perfusion culture processes: economic, environmental, and operational feasibility under uncertainty. *Biotechnol Bioeng* **110**:206–219 (2013).
133 Oyebolu FB, Allmendinger R, Farid SS and Branke J, Dynamic scheduling of multi-product continuous biopharmaceutical facilities: a hyper-heuristic framework. *Comput Chem Eng* **125**:71–88 (2019).
134 Handa-Corrigan A, Nikolay S, Fletcher D, Mistry S, Young A and Ferguson C, Monoclonal antibody production in hollow-fiber bioreactors: process control and validation strategies for manufacturing industry. *Enzyme Microb Technol* **17**:225–230 (1995).
135 Hamlin MD, Process systems engineering for pharmaceutical manufacturing. *Johnson Matthey Technol Rev* **63**:292–298 (2019).
136 Singh R, Muzzio JF, Ierapetritou M and Ramachandran R, A combined feed-forward/feed-back control system for a QbD-based continuous tablet manufacturing process. *Processes* **3**:339–356 (2015). http://doi.org/10.3390/pr3020339.
137 Lee SL, O'Connor TF, Yang X, Cruz CN, Chatterjee S, Madurawe RD *et al.*, Modernizing pharmaceutical manufacturing: from batch to continuous production. *J Pharm Innov* **10**:191–199 (2015).
138 Ashoori A, Moshiri B, Khaki-Sedigh A and Bakhtiari MR, Optimal control of a nonlinear fed-batch fermentation process using model predictive approach. *J Process Control* **19**:1162–1173 (2009).
139 Khan O, Madhuranthakam CMR, Douglas P, Lau H, Sun J and Farrell P, Optimized PID controller for an industrial biological fermentation process. *J Process Control* **71**:75–89 (2018).
140 Moran EB, McGowan ST, McGuire JM, Frankland JE, Oyebade IA, Waller W *et al.*, A systematic approach to the validation of process control parameters for monoclonal antibody production in fed-batch culture of a murine myeloma. *Biotechnol Bioeng* **69**:242–255 (2000).
141 Bhaskar A, Barros FN and Singh R, Development and implementation of an advanced model predictive control system into continuous pharmaceutical tablet compaction process. *Int J Pharm* **534**:159–178 (2017).
142 Singh R, Ierapetritou M and Ramachandran R, System-wide hybrid MPC–PID control of a continuous pharmaceutical tablet manufacturing process via direct compaction. *Eur J Pharm Biopharm* **85**:1164–1182 (2013).
143 Mjalli FS and Al-Asheh S, Neural-networks-based feedback linearization versus model predictive control of continuous alcoholic fermentation process. *Chem Eng Technol* **28**:1191–1200 (2005).
144 Chang L, Liu X and Henson MA, Nonlinear model predictive control of fed-batch fermentations using dynamic flux balance models. *J Process Control* **42**:137–149 (2016).
145 Maina A. Macharia; Michael E. Tay; Patrick D. Noll. Model predictive control of a fermentation feed in biofuel production. (2007). Patent WO2008055200A3. https://patents.google.com/patent/WO2008055200A3/en
146 James F. Bartee; Maina A. Macharia; Patrick D. Noll; Michael E. Tay. Nonlinear model predictive control of a biofuel fermentation process. (2013). Patent WO2008141317A1. https://patents.google.com/patent/WO2008141317A1/en
147 Xie L and Wang DI, High cell density and high monoclonal antibody production through medium design and rational control in a bioreactor. *Biotechnol Bioeng* **51**:725–729 (1996).
148 O'Callaghan PM, McLeod J, Pybus LP, Lovelady CS, Wilkinson SJ, Racher AJ *et al.*, Cell line-specific control of recombinant monoclonal antibody production by CHO cells. *Biotechnol Bioeng* **106**:938–951 (2010).
149 Grainger RK and James DC, CHO cell line specific prediction and control of recombinant monoclonal antibody n-glycosylation. *Biotechnol Bioeng* **110**:2970–2983 (2013).
150 Hills AE, Patel A, Boyd P and James DC, Metabolic control of recombinant monoclonal antibody N-glycosylation in GS-NS0 cells. *Biotechnol Bioeng* **75**:239–251 (2001).
151 Sha S, Agarabi C, Brorson K, Lee DY and Yoon S, N-glycosylation design and control of therapeutic monoclonal antibodies. *Trends Biotechnol* **34**:835–846 (2016).
152 Warnes MR, Glassey J, Montague GA and Kara B, Application of radial basis function and feedforward artificial neural networks to the *Escherichia coli* fermentation process. *Neurocomputing* **20**:67–82 (1998).
153 Arndt M and Hitzmann B, Feed forward/feedback control of glucose concentration during cultivation of *Escherichia coli*. *IFAC Proc* **34**:403–407 (2001).
154 Choi M, Al-Zahrani SM and Lee SY, Kinetic model-based feed-forward controlled fed-batch fermentation of lactobacillus rhamnosus for the production of lactic acid from Arabic date juice. *Bioprocess Biosyst Eng* **37**:1007–1015 (2014).
155 Mendhe R, Thukkaram M, Patil N and Rathore AS, Comparison of PAT based approaches for making real-time pooling decisions for process chromatography - use of feed forward control. *J Chem Technol Biotechnol* **90**:341–348 (2015).
156 Singh R, Gernaey KV and Gani R, An ontological knowledge-based system for the selection of process monitoring and analysis tools. *Comput Chem Eng* **34**:1137–1154 (2010).
157 Singh R, Sahay A, Muzzio F, Ierapetritou M and Ramachandran R, A systematic framework for onsite design and implementation of a control system in a continuous tablet manufacturing process. *Comput Chem Eng* **66**:186–200 (2014).
158 Vanarase AU, Alcalà M, Jerez Rozo JI, Muzzio FJ and Romañach RJ, Real-time monitoring of drug concentration in a continuous powder mixing process using NIR spectroscopy. *Chem Eng Sci* **65**:5728–5733 (2010).
159 Fountain W, Dumstorf K, Lowell AE, Lodder RA and Mumper RJ, Near-infrared spectroscopy for the determination of testosterone in thin-film composites. *J Pharm Biomed Anal* **33**:181–189 (2003).
160 Roggo Y, Jent N, Edmond A, Chalus P and Ulmschneider M, Characterizing process effects on pharmaceutical solid forms using near-infrared spectroscopy and infrared imaging. *Eur J Pharm Biopharm* **61**:100–110 (2005).
161 De Beer TRM, Bodson C, Dejaegher B, Walczak B, Vercruysse P, Burggraeve A *et al.*, Raman spectroscopy as a process analytical technology (PAT) tool for the in-line monitoring and understanding of a powder blending process. *J Pharm Biomed Anal* **48**:772–779 (2008).
162 Rodionova OY, Sokovikov YV and Pomerantsev AL, Quality control of packed raw materials in pharmaceutical industry. *Anal Chim Acta* **642**:222–227 (2009).
163 Eliasson C, Macleod NA, Jayes LC, Clarke FC, Hammond SV, Smith MR *et al.*, Non-invasive quantitative assessment of the content of pharmaceutical capsules using transmission Raman spectroscopy. *J Pharm Biomed Anal* **47**:221–229 (2008).
164 Scotter C, Use of near infrared spectroscopy in the food industry with particular reference to its applications to on/in-line food processes. *Food Control* **1**:142–149 (1990).
165 Wählby U and Skjöldebrand C, NIR-measurements of moisture changes in foods. *J Food Eng* **47**:303–312 (2001).
166 Vlachos N, Skopelitis Y, Psaroudaki M, Konstantinidou V, Chatzilazarou A and Tegou E, Applications of Fourier transform-infrared spectroscopy to edible oils. *Anal Chim Acta* **573–574**:459–465 (2006).

167 Huang H, Yu H, Xu H and Ying Y, Near infrared spectroscopy for on/in-line monitoring of quality in foods and beverages: a review. *J Food Eng* **87**:303–313 (2008).
168 Singh R, Sahay A, Karry KM, Muzzio F, Ierapetritou M and Ramachandran R, Implementation of an advanced hybrid MPC–PID control system using PAT tools into a direct compaction continuous pharmaceutical tablet manufacturing pilot plant. *Int J Pharm* **473**: 38–54 (2014).
169 Ladner Y, Mas S, Coussot G, Bartley K, Montels J, Morel J *et al*., Integrated microreactor for enzymatic reaction automation: an easy step toward the quality control of monoclonal antibodies. *J Chromatogr A* **1528**:83–90 (2017).
170 Steinebach F, Angarita M, Karst DJ, Müller-Späth T and Morbidelli M, Model based adaptive control of a continuous capture process for monoclonal antibodies production. *J Chromatogr A* **1444**:50–56 (2016).
171 Hogiri T, Tamashima H, Nishizawa A and Okamoto M, Optimization of a pH-shift control strategy for producing monoclonal antibodies in Chinese hamster ovary cell cultures using a pH-dependent dynamic model. *J Biosci Bioeng* **125**:245–250 (2018).
172 Berry BN, Dobrowsky TM, Timson RC, Kshirsagar R, Ryll T and Wiltberger K, Quick generation of Raman spectroscopy based in-process glucose control to influence biopharmaceutical protein product quality during mammalian cell culture. *Biotechnol Prog* **32**: 224–234 (2016).
173 Matthews TE, Smelko JP, Berry B, Romero-Torres S, Hill D, Kshirsagar R *et al*., Glucose monitoring and adaptive feeding of mammalian cell culture in the presence of strong autofluorescence by near infrared Raman spectroscopy. *Biotechnol Prog* **34**:1574–1580 (2018).
174 Patel BA, Gospodarek A, Larkin M, Kenrick SA, Haverick MA, Tugcu N *et al*., Multi-angle light scattering as a process analytical technology measuring real-time molecular weight for downstream process control. *MAbs* **10**:945–950 (2018). https://doi.org/10.1080/19420862.2018.1505178.
175 Rüdt M, Brestrich N, Rolinger L and Hubbuch J, Real-time monitoring and control of the load phase of a protein A capture step. *Biotechnol Bioeng* **114**:368–373 (2017).
176 Zobel-Roos S, Mouellef M, Siemers C and Strube J, Process analytical approach towards quality controlled process automation for the downstream of protein mixtures by inline concentration measurements based on ultraviolet/visible light (UV/VIS) spectral analysis. *Antibodies* **6**:24 (2017).
177 Papathanasiou MM, Steinebach F, Morbidelli M, Mantalaris A and Pistikopoulos EN, Intelligent, model-based control towards the intensification of downstream processes. *Comput Chem Eng* **105**:173–184 (2017).
178 Chmielowski RA, Mathiasson L, Blom H, Go D, Ehring H, Khan H *et al*., Definition and dynamic control of a continuous chromatography process independent of cell culture titer and impurities. *J Chromatogr A* **1526**:58–69 (2017).
179 Krättli M, Steinebach F and Morbidelli M, Online control of the twin-column countercurrent solvent gradient process for biochromatography. *J Chromatogr A* **1293**:51–59 (2013).
180 Papathanasiou MM, Avraamidou S, Oberdieck R, Mantalaris A, Steinebach F, Morbidelli M *et al*., Advanced control strategies for the multicolumn countercurrent solvent gradient purification process. *AIChE J* **62**:2341–2357 (2016).
181 Rathore AS, Nikita S, Thakur G and Deore N, Challenges in process control for continuous processing for production of monoclonal antibody products. *Curr Opin Chem Eng* **31**:100671 (2021).

ARTICLE

BIOTECHNOLOGY & BIOENGINEERING WILEY

Side-by-side comparability of batch and continuous downstream for the production of monoclonal antibodies

Laura David[1] | Peter Schwan[2] | Martin Lobedann[2] | Sven-Oliver Borchert[2] | Bastian Budde[2] | Maike Temming[2] | Mike Kuerschner[2] | Francisca Maria Alberti Aguilo[2] | Kerstin Baumarth[2] | Tobias Thüte[2] | Benjamin Maiser[2] | Andreas Blank[2] | Viktorija Kistler[2] | Nils Weber[2] | Heiko Brandt[2] | Martin Poggel[2] | Klaus Kaiser[2] | Karl Geisen[2] | Felix Oehme[2] | Gerhard Schembecker[3]

[1]Invite GmbH, Leverkusen, Germany

[2]Bayer AG, Leverkusen, Germany

[3]BCI, Plant and Process Design, TU Dortmund University, Dortmund, Germany

Correspondence
Laura David, Invite GmbH, Chempark, Geb. W32, 51368 Leverkusen, Germany.
Email: david@invite-research.com

Funding information
German Federal State North Rhine-Westphalia, Grant/Award Number: 005-1010-0009; European Regional Development Fund, Grant/Award Number: 005-1010-0009; Bundesministerium für Bildung und Forschung, Grant/Award Number: 031A616M

Abstract

Continuous processing is the future production method for monoclonal antibodies (mAbs). A fully continuous, fully automated downstream process based on disposable equipment was developed and implemented inside the MoBiDiK pilot plant. However, a study evaluating the comparability between batch and continuous processing based on product quality attributes was not conducted before. The work presented fills this gap comparing both process modes experimentally by purifying the same harvest material (side-by-side comparability). Samples were drawn at different time points and positions in the process for batch and continuous mode. Product quality attributes, product-related impurities, as well as process-related impurities were determined. The resulting polished material was processed to drug substance and further evaluated regarding storage stability and degradation behavior. The in-process control data from the continuous process showed the high degree of accuracy in providing relevant process parameters such as pH, conductivity, and protein concentration during the entire process duration. Minor differences between batch and continuous samples are expected as different processing conditions are unavoidable due to the different nature of batch and continuous processing. All tests

Abbreviations: A280, absorbance at 280 nm wavelength; AEX, anion exchange chromatography; AF, asymmetry factor; B/E, bind and elute; CEX, cation exchange chromatography; Cfu, colony forming units; CGE-nr, capillary gel electrophoresis at nonreducing conditions; CGE-r, capillary gel electrophoresis at reducing conditions; CHO, Chinese hamster ovary; cIEF, capillary isoelectric focusing; col, column; DNA, deoxyribonucleic acid; DSP, downstream process; ELISA, enzyme-linked immunosorbent assay; EO, ethylene oxide; FT, flow through; HC, heavy chain; HCP, host cell proteins; HETP, height equivalent to theoretical plates; HFI, helical flow inverter; HILIC, hydrophilic interaction liquid chromatography; HMW, high molecular weight; HPLC, high performance liquid chromatography; ID, identification; IgG, immunoglobulin G; JP, Japanese Pharmacopoeia; L, length; LC, light chain; LDPE, low density polyethylene; LMW, low molecular weight; LOQ, limit of quantification; mAb, monoclonal antibody; max, maximum value; mean, mean value; min, minimum value; MoBiDiK, modular bioproduction, disposable and continuous; MS, mass spectrometry; MV, membrane volume; NOR, normal operating range; OD, optical density; Ph. Eur., European pharmacopoeia; ProtA, protein A; qPCR, quantitative polymerase chain reaction; RP, reversed phase; SEC, size exclusion chromatography; TAMC, total aerobic microbial count; TGA, Therapeutic Goods Administration, Australia; TYMC, total yeast/mold count; UF/DF, ultrafiltration/diafiltration; uHPLC, ultra-high performance liquid chromatography; UO, unit operation; UPLC, ultra performance liquid chromatography; USP, upstream process; USP, United States Pharmacopeia; VF, viral filtration; VI, viral inactivation.

Symbols: H, height; σ, standard deviation.

Laura David, Peter Schwan, Martin Lobedann, Sven-Oliver Borchert, and Bastian Budde contributed equally to this study.

revealed no significant differences in the intermediates and comparability in the drug substance between the samples of both process modes. The stability study of the final product also showed no differences in the stability profile during storage and forced degradation. Finally, online data analysis is presented as a powerful tool for online-monitoring of chromatography columns during continuous processing.

KEYWORDS
continuous processing, DSP, mAb, side-by-side comparability

1 | INTRODUCTION

The development of the MoBiDiK pilot plant focuses on "Modular Bioproduction, Disposable and Continuous" suitable for the purification of any monoclonal antibody (mAb). By applying modular design principles (Bramsiepe et al., 2014), the engineering effort for the design of disposables, backbone structure, and automation is minimized. The utilization of disposable equipment in all product-contact areas eliminates the need for cleaning and enables fully closed manufacturing. Consequently, low-bioburden production in controlled, non-classified environment becomes possible. As published before, the initial project focused on a fully continuous process by linking perfusion culture in the upstream process (USP) with a fully continuous downstream process (DSP; Klutz, Magnus, et al., 2015). The current pilot plant consists of a fed-batch USP and a continuous DSP. This process mode is known as a so-called hybrid process as defined by Konstantinov and Cooney or a semi-continuous process as defined by the BioPhorum (BioPhorum, 2019; Konstantinov & Cooney, 2015). A pilot plant of the continuous DSP was built in a 110-m^2 laboratory in Leverkusen, Germany. The continuous production mode is primarily enabled by the use of BioSMB chromatography units (Bisschops, Frick, Fulton, & Ransohoff, 2009). Several other unit operations (UOs) of the continuous DSP have been evaluated in detail during the project, for example, continuous viral inactivation (David, Maiser, et al., 2019; David, Waldschmidt, Lobedann, & Schembecker, 2019; Klutz, Kurt, Lobedann, & Kockmann, 2015; Klutz, Lobedann, Bramsiepe, & Schembecker, 2016) and continuous viral filtration (David, Niklas, Budde, Lobedann, & Schembecker, 2019). Therefore, these two viral safety steps are not further discussed in this study. A high degree of inline process analytics enables a fully automated continuous process. In the past, the DSP of the process was successfully operated for 4 weeks without interruptions, demonstrating the process robustness and ability to run the process under closed conditions (data not shown).

However, the influence of the process mode on the product quality has not been investigated yet in full detail, which is an essential prerequisite for successful implementation of the technology at every stage of the product life cycle. Therefore, a comparability study was conducted where the same harvest material was purified side-by-side by a batch and a continuous DSP with similar process parameters. In-process samples were analyzed regarding product concentration, product quality attributes, product-related impurities, and process-related impurities. Regarding the continuous DSP, samples were also taken at different time points to evaluate the influence of the process duration as well as the start-up and shut-down phase on these parameters. The final product of both process modes (final drug substance) was further tested for product quality attributes and stability under different storage conditions.

2 | MATERIALS AND METHODS

2.1 | Materials

Harvest material was generated in a 200-L Sartorius fed-batch reactor (Sartorius Stedim Biotech, Göttingen, Germany) using a Chinese hamster ovary (CHO) cell culture. The processing time from vial thaw to harvest was 33 days. The maximum viable cell density was 18.02×10^6 cells/ml. The bioreactor was harvested using a Pall Stax depth filter (Pall GmbH, Dreieich, Germany). The 0.2 µm filtered product had an IgG titer of 2.8 g/L.

GE MabSelect Sure was used as Protein A (ProtA) capture resin (GE Healthcare Life Sciences, Little Chalfont, UK). GE Capto SP ImpRes was used in the intermediate bind & elute (B/E) chromatography process. Sartorius Sartobind Q membrane adsorber capsules were installed as final polishing step.

Citric buffers were employed for all chromatography steps. In case of continuous processing, buffers were 0.2 µm filtered into 200-L Sartorius Flexboy bags. Intermediates for batch processing were 0.2 µm filtered using Sartorius Sartopore 2 filters before storage. Sartorius Sartoguard NF filters were used as intermediate filters in continuous production to remove precipitates.

Pall BioSMB PD systems (Pall Biotech, Dreieich, Germany) were utilized for continuous chromatography, whereas Äkta process systems (GE Healthcare Life Sciences) were used for batch chromatography.

The Sartorius devices Sartoflow Advanced and Hydrosart 30 kDa cassettes were used for UF/DF and the Planova BioEx filter (Asahi Kasei Medical Ltd., Tokyo, Japan) was used for virus filtration.

2.2 | Analytics

Pre-defined product quality attributes were determined offline from samples drawn at pre-defined different positions and time points

within the batch and the continuous process (in-process control) as well as for the full characterization of the final product or drug substance. Sampling took place before and after every chromatography step in batch as well as in continuous mode. Three samples were taken during the steady-state phase of the purification process (early, middle, and late sample). At specific sampling positions, also samples during start-up and shut-down of the pilot plant were drawn (see Figure 2 further details).

Various analytical methods were utilized to determine different product-specific attributes as well as process-related impurities. These include product concentration, purity, charge variant distribution, binding activity, oxidation, molecular weight, N-glycan profile, as well as the determination of the impurities such as host cell proteins (HCPs), deoxyribonucleic acid (DNA), and leached ProtA. Regarding product purity, monomer/intact IgG, high molecular weight species or aggregates (HMW), potential fragments or low molecular weights (LMWs), as well as the percentage of sum of light chain (LC) and heavy chain (HC) were determined. An overview of the used analytical methods can be seen in Table 1.

In the continuous mode, the bioburden samples were derived from the retentate side of the 0.2-µm filters, as possible microbial contaminations would concentrate at these positions.

Stability tests were conducted at room temperature (18–26 °C) and 40°C for 4 weeks each. The final product solutions were stored in sterile low-density polyethylene bags during the study.

2.3 | Plant setup

The key principles this study follows to evaluate the side-by-side comparability between batch and continuous downstream processing are (a) purifying the same harvest material, (b) utilizing the same process steps, and (c) using similar parameters.

In this study, these steps are capture (ProtA), low pH viral inactivation, intermediate purification by cation exchange chromatography (CEX), and final polishing by anion exchange chromatography (AEX). Figure 1 shows the process overview for the continuous DSP including sampling spots and techniques. Before the first chromatography step, the harvest is pre-filtered by a 0.2-µm filter. ProtA chromatography is executed in B/E mode as in the batch process, but by using a BioSMB chromatography with five columns, a continuous feed stream is used and a continuous eluate stream is generated. After the ProtA step, pH is adjusted for the following low pH viral inactivation (VI). To generate the necessary hold time for the step, the novel helical flow inverter (HFI) is introduced into the system (Lobedann, David, Borchert, & Waldschmidt, 2018). Afterwards, pH and conductivity are adjusted for the following flow through (FT) UO and intermediate CEX. Another filtration step takes place before the intermediate chromatography step. The CEX is executed in B/E mode like the ProtA step, but due to the necessity of peak cutting to gain the required product purity in this step, an intermittent elution stream is generated. The CEX eluate is again adjusted regarding pH and conductivity and 0.2 µm filtered before the polishing AEX in FT mode. The material after the polishing AEX chromatography of both process modes was further processed through VF and ultrafiltration/diafiltration

TABLE 1 Analytical methods

Product attribute	Analytical method
Concentration	POROS-A high performance liquid chromatography (HPLC; pre ProtA samples)
Concentration	Absorbance at 280 nm wavelength (A280) with Light Scattering Compensation by A320 subtraction (post ProtA samples)
Purity (monomer, HMWs)	Size exclusion chromatography (SEC) HPLC
Purity (intact IgG, LMWs)	Capillary gel electrophoresis or under non-reduced conditions (CGE-nr)
Purity (LC, HC)	Capillary gel electrophoresis or under reduced conditions (CGE-r)
Charge variant distribution (main peak, basic & acidic variants)	Capillary isoelectric focusing (cIEF)
Binding activity	Binding enzyme-linked immunosorbent assay (ELISA)
Oxidation	RP-HPLC after iDES digestion
Molecular weight (intact, reduced, deglycosylated, reduced, and deglycosylated molecule)	RP-UPLC-MS
N-glycan profile	HILIC uHPLC using Prozyme kit Glykoprep®-plus Rapid N-Glycan sample preparation with the InstantAB labeling (GPPNG-LB; ProZyme, Hayward, CA)
HCPs	ELISA (resDNASEQ™ Quantitative CHO DNA Kit with PrepSEQ™ Residual DNA Sample Preparation Kit (Thermo Fisher Scientific, Waltham, MA)
DNA	Quantitative polymerase chain reaction (qPCR)
Leached Protein A	ELISA (Protein A ELISA Kit for MabSelect SuRe; Repligen, Waltham, MA)
Bioburden	Total aerobic microbial count (TAMC) and total yeast/mold count (TYMC)
Endotoxin level	Test kit N588 Pyrogent-5000 from Lonza (Basel, Switzerland; according to the harmonized testing method of Ph. Eur., USP, JP, and TGA)

Abbreviations: HC, heavy chain; HCP, host cell protein; HMW, high molecular weight; LC, light chain; LMW, low molecular weight

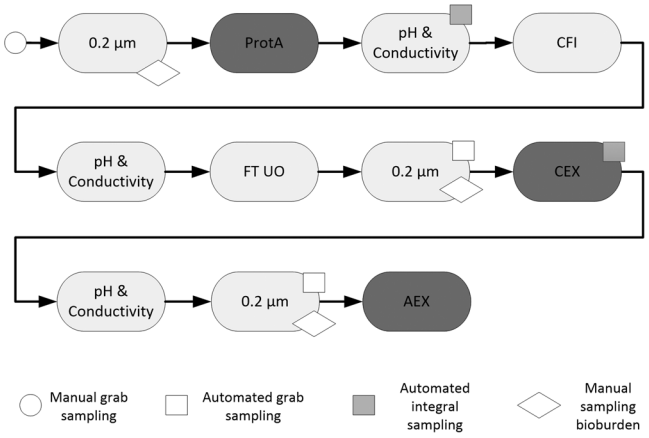

FIGURE 1 Continuous process overview including sampling points and sampling procedures

(UF/DF), all in batch mode. Therefore, the process parameters including filter areas were identical after the AEX chromatography step.

In the continuous DSP, pH and conductivity are inline-monitored and feedback-controlled if needed (Bernshausen, Lobedann, & Schwan, 2016). UV is only inline monitored. All modules are highly automated and synchronized using a SIMATIC PCS7 process control system (Siemens AG, Munich, Germany). A steady-state fluid connection exists between all modules and the entire process is a closed system. Intermediate hold times are very short due to small volumes of ~300 g in the intermediate surge tanks. The resulting average residence times can be seen in Table S1. To allow sufficient operating space, the surge tanks are dimensioned to a volume of 1 L. Sampling for bioburden and instantaneous grab samples are executed in either manual or automated mode; sampling for integral samples is achieved in the automated mode (Schwan, Kistler, & Lobedann, 2016). Grab samples are taken in a very short time and are only representative for the current status, whereas integral samples are drawn over a long period of time and are thus representative for this prolonged time. Consequently, integral sampling is applied where a constant flux exists with varying parameters, for example, the ProtA eluate stream. At sampling positions were mixing and therefore homogenization takes place, grab samples are taken. The batch DSP uses the same UO in the same process modes (B/E or FT) as the continuous DSP. Due to the different nature of both process modes, several differences exist in process control and sampling strategy. In the batch DSP, pH and conductivity adjustments are performed manually. No fluid connection exists between the different UOs. Samples are taken manually from the pooled process intermediate between the different UOs. As the purification process takes several days, process intermediates were stored at 2–8°C between UOs.

Finally, low-bioburden production plays a major role in the production of pharmaceuticals. In the batch process, all chromatography steps were sanitized with sodium hydroxide. In the continuous process, the majority of the parts were γ-irradiated with at least 25 kGy, including the chromatography columns. Where no γ irradiation was applicable, the parts were treated with ethylene oxide (EO) or autoclaved before introduction into the system.

2.4 | Experimental procedure

To preclude the impact of storage on the starting material, the harvest stored for 6 days at 2–8°C was split into two parts for the two process modes immediately before processing. 44 L of harvest material was purified in the batch process, whereas 125 L was purified in the continuous process. The harvest part for the batch purification was equilibrated to room temperature and processed on the ProtA column within approximately 2 hr. The batch production until the AEX step was carried out in 7 days comprising intermediate storage at 2–8°C. Batch chromatography processes followed standard procedures for installation and processing. This included sanitization before each step with sodium hydroxide.

During the continuous DSP, the first step was the inline calibration and adjustment of the pH and conductivity sensors inline in the conditioning modules using citrate buffers at the operating point. The entire DSP was then primed with process buffers and controlled with respect to flow, pH, and conductivity. Once steady-state conditions were reached, the harvest was connected to the first filtration module of the DSP. During the whole continuous production time (40 hr), the harvest was supplied out of a chilled vessel. The feed material was equilibrated to room temperature during the initial 0.2 µm filtration before entering the ProtA UO. The reached average flow rates during the steady-state phase can be seen in Table S2.

The shut-down phase was initialized by replacing the harvest feed with ProtA equilibration buffer. ProtA chromatography operation continued until all five columns were eluted. After stopping the ProtA module, a low pH buffer flush at the inlet of the VI module continued chasing product. CEX chromatography continued loading until the inlet protein concentration dropped below 0.15 g/L resulting in a loading density of 22 g/L of the last column load. A separate integral sample of the last two CEX elutions was taken, representing the shut-down phase of the UO. The subsequent hold-up was chased with CEX elution buffer. The AEX FT chromatography continued processing until the inlet protein concentration was below 0.15 g/L. It is important to note that the process was fully automated including start-up, shut-down, and handling of events. The established parameter control strategy ensured that only product within normal operating ranges (NORs) was further processed. To allow the comparison between both process modes, setpoints and NOR values of the batch process were established in the continuous process.

Process parameters were kept identical between batch and continuous production wherever possible. This included chromatographic buffers, resins, and membrane types. Furthermore, column load conditions with respect to conductivity and pH were the same. The AEX load density for example was comparable between both process modes at <470 mg/ml membrane. The used amount of buffers was scaled according to the column size for both process modes, meaning that the used amount of column volumes (CVs) were identical.

However, some adaptations were implemented due to the nature of the continuous process. Table 2 summarizes these adaptations and their potential impact on yield and impurities. For example, the γ

TABLE 2 Differences in batch and continuous DSP and possible impact on yield, product quality, and impurities

UO	Parameter	Batch	Continuous	Potential impact on	Potential severity
ProtA	Column	1 col x 3.4 L	5 col x 98 ml each BioSMB columns in series 1+2	–	Low
	Aseptic processing	Sanitization 0.1 M NaOH	25 kGy gamma irrad.+cyclic sanitization 0.1 M NaOH	Yield, Impurity	High
	Load density (g/L)	37	51	Yield, Impurity	Medium
	Load/wash velocity (cm/h)	300/300	150/170	Impurity	Low
	Elution	Peak cutting	No peak cutting	Yield, Impurity	Medium
	Elution velocity (cm/h)	300	50	Yield	Low
	Cycles per column	1	14	Yield, Impurity	Low
VI	pH control	Manual adjustment in hold-tank	Continuous adjustment		Low
	Time control	Manual	CFI and flow	Yield, Impurity	Low
FT UO	Load pH and conductivity	post VI neutralization – storage – dilution	Simultaneous pH & conductivity adjustment	Impurity	Low
	Load (mg/cm^2)	320	220	Impurity	Medium
	Flow rate (L·m^{-2}·h^{-1})	453	22	Impurity	Medium
	mAB feed concentration	Constant	Time-dependent	Yield, Impurity	Medium
CEX	Column	3 L (H = 20 cm)	4 col x 390 ml (H = 20 cm)	–	Low
	Linear velocity load (cm/h)	225	150–225	Yield, Impurity	Low
	Aseptic processing	1 M NaOH	25 kGy gamma irrad.+cyclic 1 M NaOH	Yield, Impurity	High
	Cycles per column	1	6	Yield, Impurity	Low
AEX	Number and size of adsorbers	200 ml	5 × 150 ml	-	Low
	Bed height (mm)	4	8	Impurity	Low
	Aseptic processing	1 M NaOH	Autoclaving		Low
	Flow rate (MV/min)	15	0.5	Impurity	High
	Load processing	Batch uniform flow rate	Staggered depending on feed bag level	Impurity	High
	mAB feed concentration	constant	Time-dependent	Yield, Impurity	Medium
	Load conductivity and pH	Manual adjustment in hold-tank	Continuous adjustment	Impurity	Medium

Abbreviations: AEX, anion exchange chromatography; CEX, cation exchange chromatography; CFI, coiled flow inverter; ProtA, Protein A; UO, unit operation

irradiation of the ProtA chromatography columns for the continuous process could impact the ligand and therefore also impact the product and impurity binding at the resin.

Finally, the aim of the process mode change was the comparability of the critical process parameters of both process modes.

2.5 | Data management

This section describes an online monitoring of column integrity for both ProtA and CEX chromatography. Asymmetry factor (AF) and height equivalent to theoretical plates (HETP) were used as indicators for column performance. As demonstrated by Bork, Holdridge, Walter, Fallon, and Pohlscheidt (2014), both indicators can be calculated directly from transition phase data.

Here, SIMATIC SIPAT (Version: 5.0.0.3; Siemens AG, Munich, Germany) was used for data management, whereas MATLAB (Version: R2016b; MathWorks, Natick, MA) was used for data analysis. With this setup, it was achieved to calculate the performance indicators as soon as a transition phase was completed and its data available in a process database. However, such time series could not be analyzed directly within the process control system without additional efforts.

To overcome this issue, merely start and endpoint of a transition phase were provided by the process control system via an OPC interface. Within SIPAT, this information was then used to collect the whole time series from a process database. MATLAB was then used to execute the data analysis. The univariate results AF and HETP were fed back to the process control system for further processing, visualization, and—in the future—use for advanced control strategies.

Moreover, data management by SIPAT includes contextualization of the data. Context information is column ID, batch ID, plant ID, and product ID. All data are stored in a SIPAT database.

3 | RESULTS & DISCUSSION

In the following sections, the results of the side-by-side comparison between batch and continuous DSP are shown with respect to process parameter control, analytical results, and online data analysis. In addition to the results presented in this study, a second identical side-by-side comparability study was performed previously

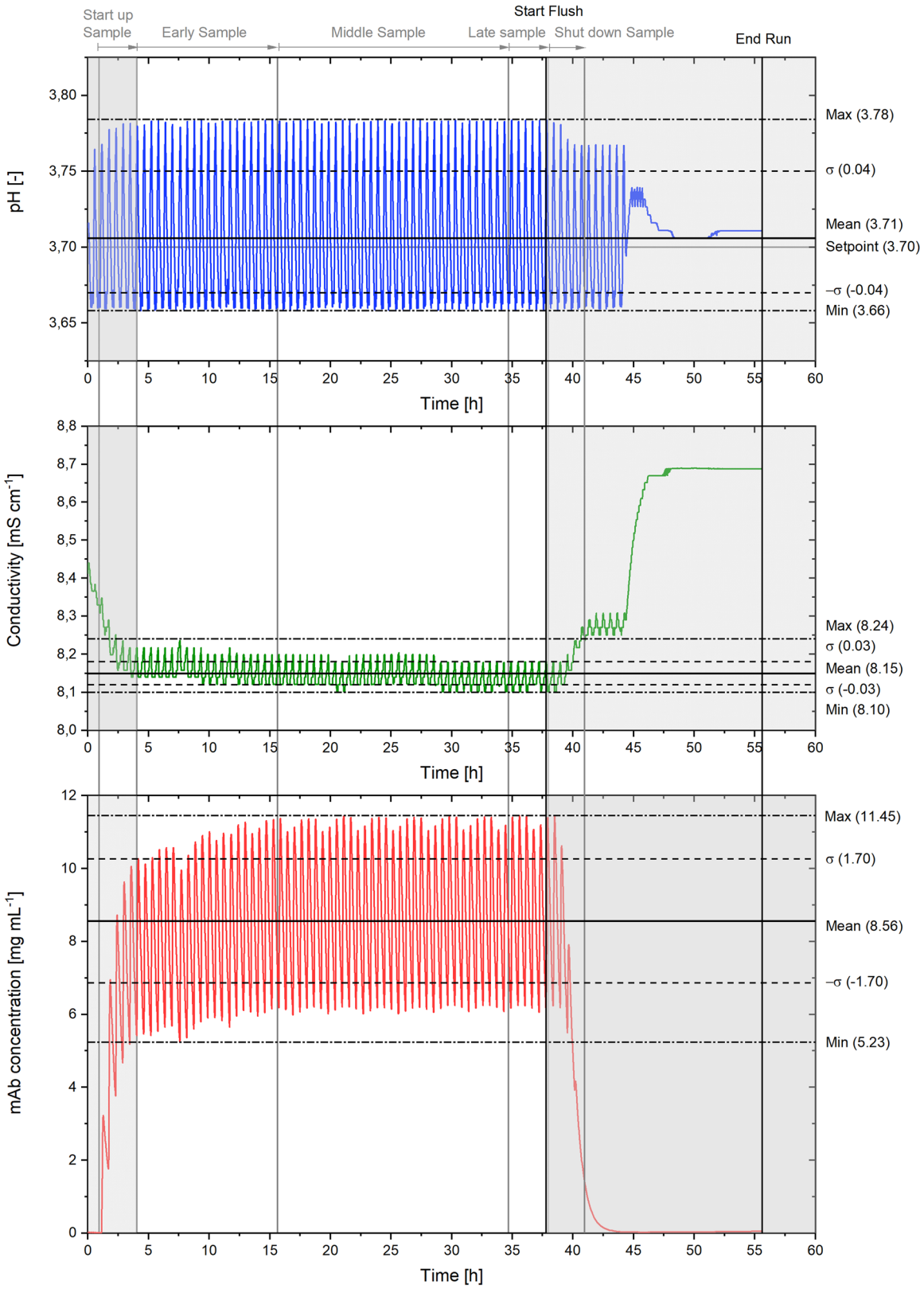

FIGURE 2 In-process control data at the conditioning module upstream to the coiled flow inverter [Color figure can be viewed at wileyonlinelibrary.com]

(data not shown). The results for this second study are comparable to the results presented in this study.

3.1 | Parameter control in the continuous process

The key to the successful application of the same process conditions in batch and continuous mode are the correct pH and conductivity values before VI, CEX, and AEX chromatography. Consequently, a rigid control strategy for these process parameters was applied throughout the entire continuous process. Two examples of the inline control results will be shown in this chapter: (a) conditioning before VI and (b) conditioning before FT UO and CEX.

Figure 2 represents inline data from the conditioning module upstream of the HFI. The startup phase lasted ~3.8 hr, after that the continuous capture chromatography was in steady state, leading to a homogenous periodic input flow into the VI UO. Figure 2 shows the pH and conductivity distribution as well as the mAb concentration based on UV measurement during the entire run. In addition, the durations of the integral sampling as well as the start of the flushing procedure are shown. The given minimum (min), maximum (max), mean, and standard deviation (±σ) values were calculated based on the time period indicated in white in Figure 2. In case of the conditioning upstream to the HFI, this time period was defined between 4.0 hr (steady state of the ProtA step reached) and 37.8 hr. Hence, this phase starts after BioSMB startup and product entering the UO. The start of the final buffer chase took place at the end of the steady state.

The upper diagram of Figure 2 shows the pH distribution. The set point for the pH feedback control was 3.70, resulting in an average reading of 3.71 with a standard deviation of 0.04 in the steady-state phase. The middle diagram in Figure 2 shows the resulting conductivity values, which were monitored during the process. Again, a tight distribution with a mean conductivity of 8.15 mS/cm and a standard deviation of 0.03 mS/cm could be observed, resulting from the pH control and the periodic change of wash and elution buffer. Finally, the mAb concentration based on UV measurement can be seen in the lower diagram of Figure 2. The mAb concentration was monitored during the process showing the results from the elution of ProtA chromatography. The start-up and shut-down phase of the plant can be clearly seen in this diagram. The mean mAb concentration slowly increased until the steady state was reached after one BioSMB cycle, as the ProtA columns were filled with harvest material instead of pure buffer. During the steady state, periodical fluctuations could be observed, which were caused by the mixture of eluate and wash buffer as well as the protein peak elution

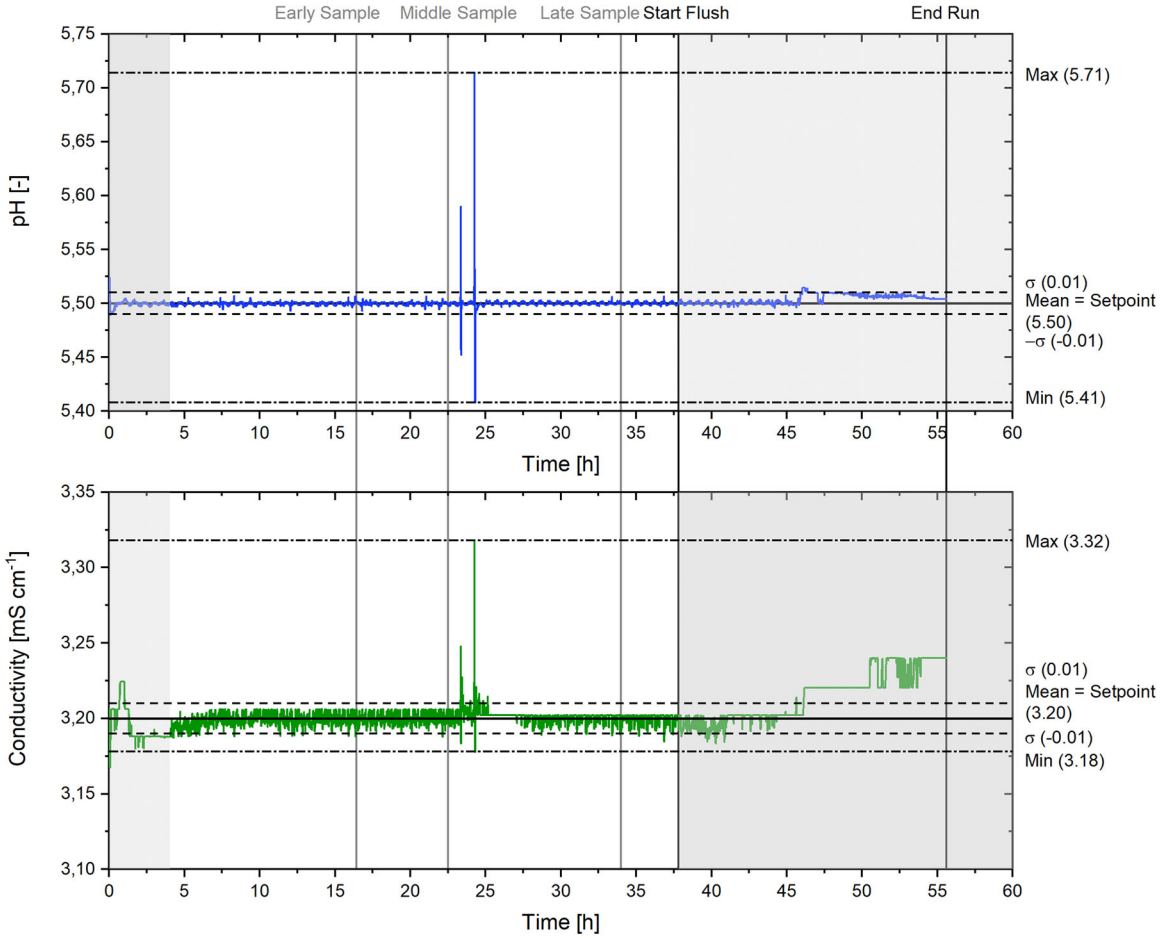

FIGURE 3 In-process control data at the conditioning module before the cation exchange chromatography (CEX) [Color figure can be viewed at wileyonlinelibrary.com]

behavior, which is characteristic for the BioSMB process (see also David, Maiser, et al., 2019). In more detail, a small fluctuation could be observed repeating every five peaks, showing minor differences in loading density between the five columns. During the first 13 hr of operation, an overall increase in mAb concentration was observed due to an adjustment of the production rate after 7 and 12 hr. At the end of the process, the shut-down phase showed typical ramp-down behavior as the plant was chased with buffer. The second example for the inline process parameter control can be seen in Figure 3. Whereas the conditioning in front of the HFI was necessary to enable sufficient VI. Here, the conditioning is needed for the successful performance of the subsequent chromatography step. pH and conductivity were adjusted simultaneously. The upper diagram of Figure 3 shows the course of pH, whereas the lower diagram shows the course of conductivity. For both pH and conductivity, high control accuracy was achieved leading to a mean value identical to the corresponding set point. The standard deviation for pH and conductivity was 0.01 pH and 0.01 mS/cm, respectively. Two events with out-of-NOR pH and conductivity values can be seen in Figure 3 at 23.3 hr and 24.2 hr, both caused by a sensor switch. All sensors relevant for process control were placed redundantly in the pilot plant, allowing sensor switches with inline flushing, cleaning, and calibration. A small dead leg allowed the flushing of cleaning buffer (sodium hydroxide) into the product line, causing an increase in pH and conductivity. As a result, the PCS software immediately paused the outflow of the conditioning module until the respective values returned into the NOR space, preventing the further processing of out-of-NOR product. Therefore, these two events are a good example of the pilot plant's capability to react to deviations and resuming the process after solving the respective issues automatically and independently.

As similar sensors were used for batch and continuous processing, the measurement precision in both process modes is comparable. For the conductivity sensors, a precision of ±5% can be assumed, whereas the precision for pH meters in general is ±0.1 pH units. During the continuous process, sensors were calibrated and adjusted before and after processing to ensure measurement accuracy and enabling the identification of the sensor drift. For pH sensors, the maximum drift was 0.07. The conductivity sensors drifted by <0.01 mS/cm at maximum. To conclude, the process control was very precise as shown by the low standard deviation. The correctness of measurement was mainly limited by the measurement probe precision. Consequently, the process control accuracy shown in this study guarantees the same process conditions for the entire DSP material based on the measurement data collected.

3.2 | Analytics

3.2.1 | Process intermediates

The results for the analytics over the course of the process can be seen in Figure 4. Product-related parameters are shown with red curves and process-related impurities with blue curves. One curve is shown for the batch results, whereas three to four curves are shown for the continuous process mode. As already described in Section 2.3, up to five different samples were taken with various methods at different time points of the continuous process.

The upper left diagram in Figure 4 shows the mAb concentration over the course of the process. As the batch and the continuous downstream were both fed with the same harvest material, the initial mAb concentration is the same with 2.8 g/L. In general, it can be observed that the mAb concentration is increased by the first and second chromatography step, whereas it decreases in between these steps. This can be explained by the stream conditioning steps and the chasing of product at the end of an AEX cycle. Comparing the three continuous samples during the steady-state phase at each sampling position to each other, only small differences in the mAb concentration and no temporal trend can be observed (maximum difference at AEX FT with 0.85 g/L). As expected, mAb concentrations are significantly lower during start-up and shut-down compared to steady state due to lower loading of the ProtA columns. The only sample where the mAb concentration is significantly higher in comparison to the other continuous samples is the start-up sample of the CEX eluate. This can be explained by start up issues of the integral sampling, resulting in a shortened sampling duration at which higher product concentrations were eluted.

Comparing batch and continuous results, differences in the mAb concentration are apparent. The batch mAb concentration is significantly higher compared to the continuous samples after ProtA and CEX chromatography. For the ProtA eluate samples, the explanation for this process behavior lies mainly in the different peak collection modes of ProtA chromatography. As already described in Table 2, peak cutting takes place in the batch process but not in the continuous process. For the continuous ProtA chromatography, fractions before and after the product peak during the elution are also part of the product stream to generate the continuous flow. This is not the case for batch chromatography where peak cutting is applied to reduce the product volume. Consequently, the mAb concentration of the batch sample is higher despite the lower loading density. In case of the CEX chromatography step, a higher loading density led to a higher product concentration in the eluate. Lower concentration in the AEX pool was attributed to a longer chase at the end of an AEX cycle.

The four small diagrams in the upper right corner of Figure 4 show the investigation of product-related impurities based on SEC-HPLC and CGE. The upper two diagrams show the HMW and monomer results measured with the SEC-HPLC. Both diagrams show no significant differences between batch and continuous as well as between different time points within the continuous process. The lower two small diagrams show the results of the CGE under reducing and non-reducing conditions. The results at non-reducing conditions show no loss or impact on intact IgG during downstream purification, for both process modes. The results of each batch sample and all corresponding continuous process samples show no major differences. The CGE-r results show a stable percentage over the entire process.

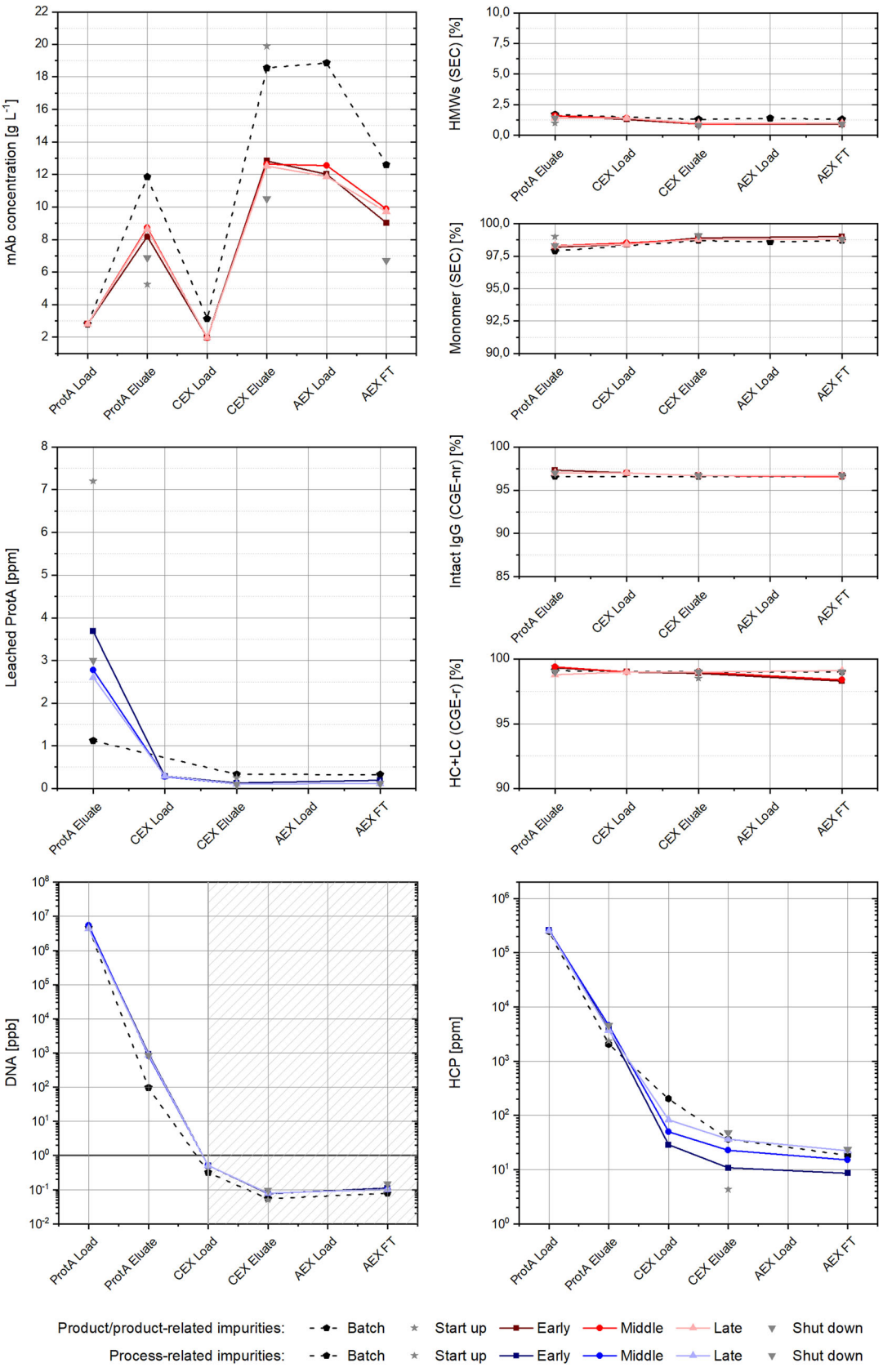

FIGURE 4 Product concentration, product- and process-related impurities over the course of the process. ppm = ng mg_{mAb}^{-1}, ppb = pg mg_{mAb}^{-1}. Gray area marks samples where the limit of detection applies [Color figure can be viewed at wileyonlinelibrary.com]

Additionally to the results for product-related impurities shown in Figure 4, the charge heterogeneity was evaluated with the help of cIEF. No differences between the different samples could be observed over the entire process of the two process modes. The charge variant distribution was stable.

In the lower part of Figure 4, the process-related impurities are shown in blue. The middle diagram on the left side shows the leached ProtA concentration over the process. In general, it can be seen that the initial ProtA to mAb ratio is higher for the continuous process than for the batch process. Mainly this effect is caused by the different eluate collection. Peak cutting results in less ProtA per mAb than without peak cutting at the same concentration of leached ProtA in the elution stream. In both process modes, the leached ProtA concentration decreased rapidly due to the FT UO before the CEX. Afterwards, the ProtA concentration was stable close to the limit of quantification (LOQ) for the assay used.

The host cell DNA concentration over the course of the process is shown in the lower left diagram in Figure 4. The gray area marks the samples where the DNA content was not quantifiable. Consequently, the data shown in this area are the respective quantification limits for each sample. Comparing the continuous and the batch samples to each other, the curves are almost identical. The major depletion of DNA takes place during the ProtA chromatography step. The remaining DNA is then removed by the FT UO afterward. Consequently, no DNA could be detected in the CEX Load samples and beyond.

The last diagram in Figure 4 on the lower right side shows the HCP concentration over the course of the process. The main reduction of HCPs takes place during ProtA chromatography, followed by FT UO and CEX. The analysis results of ProtA load and eluate are almost identical when comparing batch and continuous samples, respectively. Beginning with the CEX load samples, the results of the continuous and batch samples differ. As the specific load of mAb and the flow rate on the FT UO is higher in batch mode than in continuous mode (see Table 2), the HCP breakthrough is higher as well. During the course of the continuous process, increasing breakthrough of HCPs is detected as expected for a flow through unit operation. Nevertheless, the resulting final measurements of the AEX FT samples show similar low HCP concentrations.

Regarding yield, both process modes were able to achieve a final drug substance yield >80%. The intermediate yields between batch and continuous process can hardly be compared as a definite step yield is difficult to specify for the continuous process. Due to the nature of this process mode, the mass balance necessary for accurate yield determination is dependent on the accuracy of the equipment, for example, pumping speed and flow meter measurement. Therefore, small fluctuations in this equipment lead to equivalent yield fluctuations and finally misleading comparisons between batch and continuous process. Consequently, the authors decided to only consider the final yield.

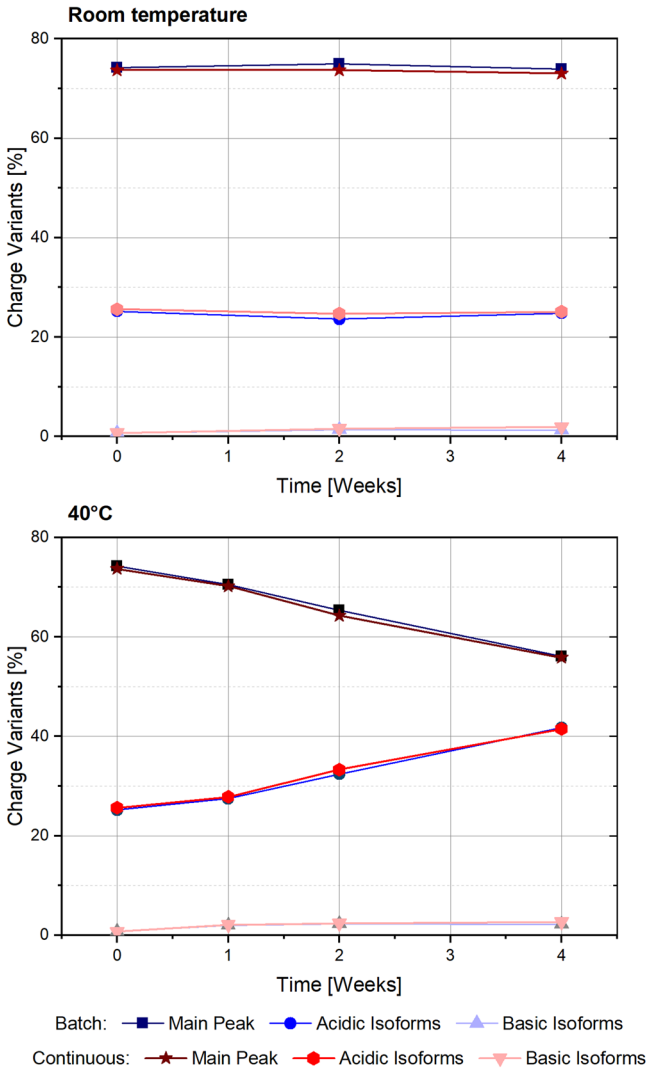

FIGURE 5 Charge variants distribution during the stability studies [Color figure can be viewed at wileyonlinelibrary.com]

3.2.2 | Final drug substance

The final drug substance results of both process modes were identical or showed no significant differences (exemplary data shown in Figure S1). All samples were within the required specifications for product and process-related impurities. Tests for host cell DNA, endotoxins, and microbial load were negative.

To conclude, the results of the final drug substance for batch and continuous processing show full comparability between both process modes. Consequently, the study design and execution can be regarded successful. In addition, the stability of the final drug substance was tested and will be discussed in the next chapter.

3.2.3 | Stability studies

The results for the charge variants distribution are given in Figure 5 (see CGE-nr and SEC results in Figures S2 and S3). The stability study

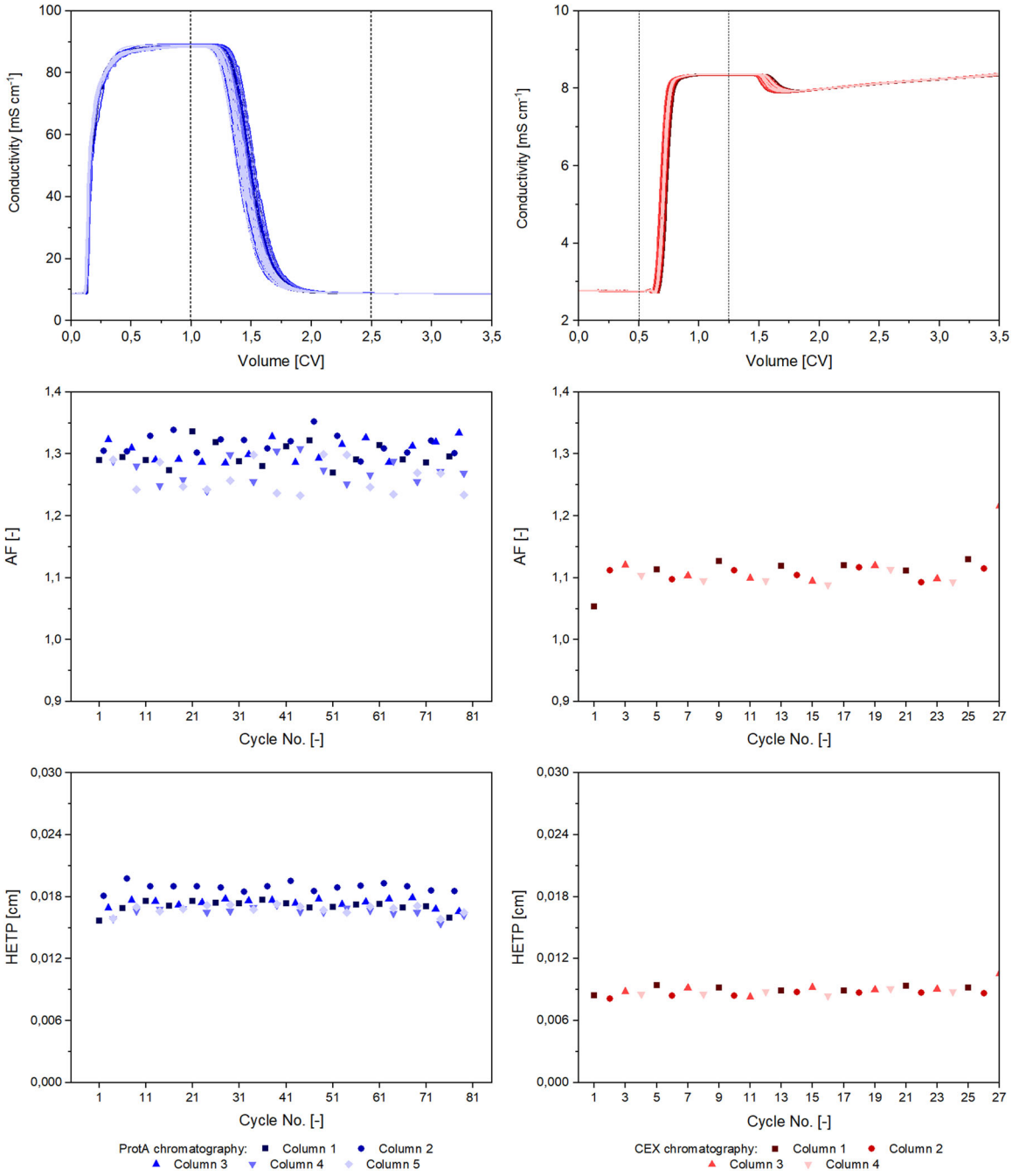

FIGURE 6 Original data and results for online data analysis In the upper left corner the conductivity time series of the transition step of Protein A chromatography is plotted over the liquid volume that passes through the column. In the upper right corner, the conductivity time series of the transition step of the CEX chromatography is plotted over the liquid volume that passes through the column. Below are the results for asymmetry factor and height equivalent to theoretical plate for the respective chromatography step. For both, each column is colored individually. CEX, cation exchange chromatography [Color figure can be viewed at wileyonlinelibrary.com]

at room temperature (upper diagram) does not show any significant impact on the charge heterogeneity. Moreover, no difference between batch and continuously produced mAb solution can be observed. At elevated temperature (40°C, lower diagram in Figure 5), a shift from the main peak to acidic isoforms as well as a slight increase of basic isoforms can be observed over the 4-week study time. Again, no significant difference between batch and continuous samples can be observed. The shift towards acidic isoforms during storage at 40°C can be explained by several effects of the chemical degradation pathway of mAbs. These include sialylation, deamidation, c-terminal lysine cleavage, and adduct formation (Khawli et al., 2010). Moreover, several effects for the formation of basic isoforms exist. Especially the oxidation of methionine, cysteine, lysine, histidine, and tryptophan was observed during the incubation of

formulated mAb at elevated temperatures (Chumsae, Gaza-Bulseco, Sun, & Liu, 2007; Lam, Yang, & Cleland, 1997; Vlasak & Ionescu, 2008).

To conclude, the stability study showed that the degradation profile of the final product is comparable between batch and continuously produced mAb considering charge heterogeneity. Moreover, the degradation profile visible at elevated temperature is explainable by already understood processes of chemical mAb degradation.

Regarding the other tested quality attributes including protein concentration, monomer concentration, HMWs, protein oxidation, and activity, no significant difference between both samples was observed at room temperature as well as at 40°C. Consequently, the comparability of batch and continuously produced final drug substance was also shown in a stability study including a wide range of relevant quality attributes.

3.3 | Microbial control

For all samples tested, the results for TAMC, TYMC, and endotoxin were below the LOQs. This leads to values <1 cfu/ml for TAMC and TYMC and <10 EE/ml for endotoxin. Consequently, the batch intermediates as well as the entire continuous process can be considered as bioburden-free during the conducted runs.

3.4 | Results of online data analysis

Figure 6 shows the original data and the respective results for AF and HETP analysis. Sixteen cycles were performed for each of the five ProtA columns, resulting in a total number of 80 cycles. For CEX chromatography, seven cycles were performed for column 1 to column 3, and six cycles for column 4, resulting in a total number of 27 cycles. Starting with ProtA (left diagrams in Figure 6), AF and HETP show a slight variation among the five columns with variation coefficients of 2.2% for AF and 5.5% for HETP, respectively. The variation coefficients regarding the different cycles for column 1 to 5 range from 1.3% to 2.0% for AF and from 2.2% to 3.3% for HETP, respectively. This indicates a high comparability in the packing quality of the column bed.

Regarding the CEX results (right diagrams in Figure 6), a similar picture presents itself. The AF and HETP show very little variation among the four columns with variation coefficients of 2.4% for AF and 5.4% for HETP, respectively. Complementary to the low variability in between the columns, the variability between column cycles of the individual columns was in a conventional range. Here, variation coefficients for column one to four range from 0.8% to 3.8% for AF and from 2.7% to 7.5% for HETP, respectively.

For both systems, ProtA and CEX, the results of the online data analysis are consistent with the results of an offline integrity tests with the more traditional pulse injection method, which has been performed by the column vendor before the process for AF estimation (ProtA columns between 1.25 and 1.37; CEX columns between 1.30 and 1.37). Overall, the method implemented has shown high capabilities to be used as a tool for online monitoring of continuous chromatography systems.

4 | CONCLUSIONS

The aim of this study was to evaluate whether batch and continuous downstream processing lead to comparable results regarding product quality attributes when performing a side-by-side comparability study. The basis was the transfer of batch process parameters to the continuous mode and the evaluation of the impact of differences on yield, product quality, and impurities. The same harvest material was purified in both process modes to ensure comparable starting positions. To ensure the same pH and conductivity levels as in batch mode, a rigid control strategy in the continuous mode was implemented, leading to small standard deviations from the respective set points. Samples were drawn at every UO in batch and continuous mode to allow comparison of product quality. In addition, during the continuous process, samples were drawn at different time points to assess product quality over the entire processing time. The intermediate samples of the batch and the continuous process showed comparability when taking inevitable differences into account. In addition, the samples of the continuous process during start-up, steady-state, and shut-down were comparable as well. Moreover, the analytics of the final drug substance showed the comparability between batch and continuous mode over various product quality attributes, product-related and process-related impurities, as well as storage and degradation behavior. Moreover, it was shown that the samples in the continuous mode led to consistent results at all time points. Finally, online data analysis was introduced as a powerful tool for online evaluation of chromatography column integrity.

To the knowledge of the authors, it was demonstrated for the first time that changing the process mode does not impact final drug substance characteristics. This opens a way to switch the process mode—independent from the product life cycle, from clinical trials to large-scale production. Finally, this study is an important milestone to implement continuous processing and thereby to speed up the availability of new, promising therapeutics through closed processing and the usage of quality by design principles.

ACKNOWLEDGMENTS

The authors would like to thank all contributing laboratories and quality units at Leverkusen and Wuppertal site of Bayer AG for their valuable contribution. Part of this study was funded by the German federal ministry of education and research (project WiPro, BMBF; 031A616M). Part of the equipment used in this study was previously purchased through the MoBiDiK project, co-funded by the European Union (European Regional Development Fund) and the German Federal State North Rhine-Westphalia (NRW) (NRWZiel2; 005-1010-0009).

Bayer AG filed several patents regarding the MoBiDiK technology, published and unpublished with multiple authors of this study named as inventors.

ORCID

Laura David http://orcid.org/0000-0002-1683-518X

REFERENCES

Bernshausen, J, Lobedann, M, & Schwan, P. 2016. Process control system for regulating and controlling a modular system for the production of biopharmaceutical and biological macromolecular products. BR112017024373 (A2).

BioPhorum. 2019. Biomanufacturing technology roadmap. Continuous downstream processing for biomanufacturing. https://www.biophorum.com/continuous-downstream-processing-for-biomanufacturing-an-industry-review/ (accessed 06.11.2019).

Bisschops, M., Frick, L., Fulton, S., & Ransohoff, T. (2009). Single-use, continuous-countercurrent, multicolumn chromatography. *BioProcess International*, *7*(6), 18–23.

Bork, C., Holdridge, S., Walter, M., Fallon, E., & Pohlscheidt, M. (2014). Online integrity monitoring in the protein A step of mAb production processes-increasing reliability and process robustness. *Biotechnology Progress*, *30*(2), 383–390.

Bramsiepe, C., Krasberg, N., Fleischer, C., Hohmann, L., Kockmann, N., & Schembecker, G. (2014). Information technologies for innovative process and plant design. *Chemie Ingenieur Technik*, *86*(7), 966–981.

Chumsae, C., Gaza-Bulseco, G., Sun, J., & Liu, H. (2007). Comparison of metheonine oxidation in thermal stability and chemically stressed samples of a fully human monoclonal antibody. *Journal of Chromatography B*, *850*, 285–294.

David, L., Maiser, B., Lobedann, M., Schwan, P., Lasse, M., Ruppach, H., & Schembecker, G. (2019). Virus study for continuous low pH viral inactivation inside a coiled flow inverter. *Biotechnology and Bioengineering*, *116*(4), 857–869.

David, L., Niklas, J., Budde, B., Lobedann, M., & Schembecker, G. (2019). Continuous viral filtration for the production of monoclonal antibodies. *Chemical Engineering Research and Design*, *152*, 336–347.

David, L, Waldschmidt, LM, Lobedann, M, & Schembecker, G. 2019. Effect of low Reynolds numbers on Dean vortices and residence time distribution inside a coiled flow inverter. Currently under review.

Khawli, L. A., Goswami, S., Hutchinson, R., Kwong, Z. W., Yang, J., Wang, X., … Motchnik, P. (2010). Charge variants in IgG1. *mAbs*, *2*(6), 613–624.

Klutz, S., Kurt, S. K., Lobedann, M., & Kockmann, N. (2015). Narrow residence time distribution in tubular reactor concept for Reynolds number range 10-100. *Chemical Engineering Research and Design*, *95*, 22–33.

Klutz, S., Lobedann, M., Bramsiepe, C., & Schembecker, G. (2016). Continuous viral inactivation at low pH value in antibody manufacturing. *Chemical Engineering and Processing: Process Intensification*, *102*, 88–101.

Klutz, S., Magnus, J., Lobedann, M., Schwan, P., Maiser, B., Niklas, J., … Schembecker, G. (2015). Developing the biofacility of the future based on continuous processing and single-use technology. *Journal of Biotechnology*, *213*, 120–130.

Konstantinov, K. B., & Cooney, C. L. (2015). White paper on continuous bioprocessing. May 20-21, 2014 Continuous Manufacturing Symposium. *Journal of Pharmaceutical Sciences*, *104*(3), 813–820.

Lam, X. M., Yang, J. Y., & Cleland, J. L. (1997). Antioxidants for prevention of methionine oxidation in recombinant monoclonal antibody HER2. *Journal of Pharmaceutical Sciences*, *86*(11), 1250–1255.

Lobedann, M, David, L, Borchert, S-O, & Waldschmidt, LM. 2018. Unit operation and use thereof, WO2019063357.

Schwan, P, Kistler, V, & Lobedann, M. 2016. Method for sampling fluid streams for monitoring contaminants in a continuous flow. KR20190079662 (A).

Vlasak, J., & Ionescu, R. (2008). Heterogeneity of monoclonal antibodies revealed by charge-sensitive methods. *Current Pharmaceutical Biotechnology*, *9*, 468–481.

SUPPORTING INFORMATION

Additional supporting information may be found online in the Supporting Information section.

Sustaining an Efficient and Effective CHO Cell Line Development Platform by Incorporation of 24-Deep Well Plate Screening and Multivariate Analysis

Alessandro Mora
Cell Line Development, Process Sciences Dept., AbbVie Bioresearch Center, Worcester, MA

Francis College of Engineering, University of Massachusetts Lowell, Lowell, MA

Sheng (Sam) Zhang
Cell Line Development, Process Sciences Dept., AbbVie Bioresearch Center, Worcester, MA

Gerald Carson
Cell Line Development, Process Sciences Dept., AbbVie Bioresearch Center, Worcester, MA

Bernard Nabiswa
Cell Line Development, Process Sciences Dept., AbbVie Bioresearch Center, Worcester, MA

Patrick Hossler
Cell Culture, Process Sciences Dept., AbbVie Bioresearch Center, Worcester, MA

Seongkyu Yoon
Francis College of Engineering, University of Massachusetts Lowell, Lowell, MA

DOI 10.1002/btpr.2584
Published online December 1, 2017 in Wiley Online Library (wileyonlinelibrary.com)

Efficient and effective cell line screening is paramount toward a successful biomanufacturing program. Here we describe the implementation of 24-deep well plate (24-DWP) screening of CHO lines as part of the cell line development platform at AbbVie. Incorporation of this approach accelerated the identification of the best candidate lines for process development. In an effort to quantify and predict process performance comparability, we compared cell culture performance in and in shake flasks, for a panel of Chinese Hamster Ovary cell lines expressing a monoclonal antibody. The results in 24-DWP screening showed reduced growth profiles, but comparable viability profiles. Slow growers in 24-DWP achieved the highest productivity improvement upon scaling-up to shake flasks. Product quality of the protein purified from shake flasks and 24-DWP were also compared. The 24-DWP culture conditions were found to influence the levels of acidic species, reduce the G0 N-glycan species, and increase the high-mannose N-glycan species. Nevertheless, the identification of undesirable profiles is executed consistently with the scaled-up culture. We further employed multivariate data analysis to capture differences depending on the two scales and we could demonstrate that cell line profiles were adequately clustered, regardless of the vessel used for the development. In conclusion, the 24-DWP platform was reasonably predictive of the parameters crucial for upstream process development activities, and has been adapted as part of the AbbVie cell line development platform. © 2017 American Institute of Chemical Engineers *Biotechnol. Prog.*, 34:175–186, 2018
Keywords: cell line development, scale-down, 24-deep well plate, Chinese Hamster Ovary, cell culture

Introduction

Biopharmaceutical development and production has become a significant part of the global pharmaceutical industry, expanding in terms of clinical molecules available to patients.[1–5] One of the biggest challenges in CMC development is the managing of program timelines for the progression of a particular protein through the various stages of development. Cell line development stands out as commanding a relatively large portion of the cumulative time required for development.[6,7] The selection of Chinese Hamster Ovary (CHO) cell clones that express the desired protein is the mission of cell line development.[8,9] Previous work by others have highlighted opportunities to streamline cell line generation and process development, including the precise screening of clones, the implementation of high-throughput techniques, and consistent scale-up.[10–12]

Various methods are employed for predicting cell line performance as an upstream process transitions from the bench scale to

Correspondence concerning this article should be addressed to S. Yoon at Seongkyu_Yoon@uml.edu.

the lab scale. Shake flasks are an established platform that supports enough volume to allow daily growth and metabolic monitoring. Deep-well plates, in particular 24-deep well plates (24-DWP), enable scale-down development with an increased throughput while reducing the footprint and saving on reagents. 24-DWP and shake flasks offer distinct advantages, and one may adopt one platform over the other for project-specific needs. Other platforms, such as minibioreactors, are amenable toward metabolite monitoring, and can be fully automated.[13,14] Whichever culture vessel is used, there is an apparent need to streamline cell line development activities to ensure the work stream is efficient, and to ensure the cell line development does not have an undue impact on the critical path.

24-DWPs have been used by researchers, although the industry adoption is not yet fully embraced. Barrett et al. reported that shaking kinetics in 24-DWP influence the oxygen transfer and may impact cell culture phenotypes in terms of growth and antibody production.[15] Increased evaporation[16–18] and fluid dynamics intrinsic to the deep-well architecture[19] may affect the culture behavior. Similar challenges are observed for transient transfection, when 24-DWP's are used for high-throughput screening of antibodies. Bos et al. looked at evaporation volume, shape, speed and aeration to identify optimal growth conditions and glycosylation profiles in HEK-293.[20] The 24-DWP used as post-transfection vessel shows both the expression levels[21] and the size of the expressed protein[22] are consistent when compared to shake flasks. Markert and Hansen observed that deep-well plates performance can be replicated at the lab-scale in terms of cellular productivities, phenotypes, and protein quality.[23,24] Rouiller et al described that 96-deep well plate can expedite clonal screening while still providing acceptable scalability.[25] However, despite reports such as these, we believe and prove in this work that 24-DWP do provide for a valuable utility toward high-throughput cell line development, and the predictions from them are reasonably accurate to justify their use.

In recent years, AbbVie has evolved its upstream high-throughput cell line development platform, where the cell line development (CLD) group performs the initial clone screening in 24-DWP and the top candidate cell lines are transferred to process development (PD). In our experience, the 24-DWP screening strategy enables higher throughput, seamless integration with automation, and more accurate cell line decision making, compared to static well plates. Throughout the evolution of our platform, we have observed some differences in process performances in 24-DWP compared to shake flasks and laboratory-scale bioreactors. Over the course of numerous programs, the top cell lines productivity and growth rate might or might not improve upon transfer from CLD to PD, in an unpredictable fashion. We wanted to investigate such erratic behavior and understand how 24-DWP performance translates to larger scale culture.

The degree of discrepancy embodied in the 24-DWP CLD screening, must be properly quantitated in order for this assessment to occur. Late-stage process development has historically utilized tools to identify trends in large datasets. Some of these tools include multivariate analysis (MVA) and process modeling.[26–28] These tools are an important part of continued process verification (CPV) and are an integral part of ensuring consistency of biologics manufacturing. However, there has been little work to incorporate these tools in cell line development.

In this work, we demonstrate the effective implementation of 24-DWP screening in the cell line development for a monoclonal antibody. We approach the investigation by comparing the results from 24-DWP to shake flasks. We report consistent process performance that enabled the precise ranking of 21 duplicate stable CHO cell lines expressing a monoclonal antibody. Product quality was also assessed in the two platforms and cell line profiles are reported for protein size, charge, and glycosylation. The differences that did exist between the culture vessels did not interfere with the ability to respectively rank the cell lines in terms of their overall process performance. Through the use of multivariate data analysis, we were able to capture these differences and we could demonstrate that candidate cell line profiles were adequately clustered, regardless of the vessel used for the development. We further verified the accurate ranking of 24-DWP performances to the 3L bioreactor scale for a subset of cell lines. The 24-DWP platform can be adopted for successful screening of cell lines and provide an early prediction of the cell culture parameters crucial for process development.

Materials and Methods

Development of Chinese Hamster Ovary cell lines

Dhfr-deficient Chinese Hamster Ovary (CHO) cells were transfected with a $dhfr^+$ vector carrying the DNA sequences of the immunoglobulin employed for this study.[29] Stable cell lines were derived from independent pools, cultured in nucleoside-free, animal component-free medium, and isolated as described in the following paragraph.

Post-transfection cellular pools were seeded in 96-well plates and cultured to confluence in a Forma incubator (Thermo Fisher, Waltham, MA, USA) set at 37°C, 80% H_2O, 5% CO_2. Promising cell lines were expanded in 24-well plate and then transferred to 24-DWP (square-well, pyramid bottom, Applikon, Foster City, CA, USA) sealed with a Duetz sandwich cover (EnzyScreen, Heemstede, Netherlands). Throughout the static culture, wells were scanned for cellular confluence on a Clone Select Imager (Molecular Devices, Sunnyvale, CA, USA) with the aid of a fully automated liquid handler (Hamilton Robotics, Reno, NV, USA). The supernatant fraction of the wells was measured for antibody titers on Day 18 (96-WP) and Day 6 (24-WP), on an Octet QK384 equipped with a ProA—Protein A biosensor for the specific binding to the Fc region of the IgG (Pall ForteBio, Menlo Park, CA, USA).

The cultures in 24-DWP were counted by trypan blue exclusion on a CEDEX analyzer (Roche Innovatis, Indianapolis, IN, USA) and passaged every 3 or 4 days. At the time of the first passage, an aliquot of the cell culture was used to seed a shake flask, while still maintaining the 24-DWP culture. In such way, 21 cell lines were duplicated in the two vessels and labeled #1 through #21. The cultures in 24-DWP were seeded in 4 mL and shaken at 225 rpm in a 25 mm throw incubator shaker (Infors-HT, Annapolis Junction, MD, USA). The cultures in shake flasks were seeded in 50 mL of final volume in a 250 mL Erlenmeyer shaker and agitated at 140 rpm. Each cell line was then developed simultaneously at 36°C, 80% H_2O, and 5% CO_2 in the two vessels until ready for the fed-batch experiment.

Fed-batch experiment

On the day of the inoculation, duplicate cultures of each cell line in the two vessels were seeded at 0.45 million viable cells/mL. Cell counting was performed by CEDEX to

measure the viable cell density (VCD), viability, and cell diameter. The supernatant retains were collected on Days 5, 11, 13, and 15 for later titer analysis by Octet. A consistent feeding scheme and glucose supplementation was applied to all cultures. The fed-batch experiment was performed at 35°C, 80% H_2O, 5% CO_2, and terminated on Day 15 or when viability dropped below 50%. Cultures were harvested by precipitating the cells for 30 min at 500*g*, at room temperature and then separating the supernatant from the cell pellet. The harvested supernatant was later used for the subsequent analysis.

Throughout the fed-batch experiment, the integrated viable cell density (IVCD) was calculated from the VCD, as follows[25]:

$$\mathrm{IVCD}_t = \left[\left(\frac{\mathrm{VCD}_t + \mathrm{VCD}_{t-1}}{2}\right) \times \Delta t\right] + \mathrm{IVCD}_{t-1}$$

In equation, IVCD_t represents the IVCD at time point t, and $\mathrm{IVCD}_{t\text{-}1}$ represents the IVCD at the previous cell counting time point (i.e., cell counting Day 1 and Day 0); VCD_t represents the viable cell density at time point t, and $\mathrm{VCD}_{t\text{-}1}$ represents the viable cell density at the previous cell counting time point; Δt represents the difference between time t and t-1. The specific productivity (Q_P) measured in pg/cell/day, expresses the daily amount of antibody produced on a per cell basis, and was calculated as follows:

$$Q_p = \frac{\mathrm{titer}}{\mathrm{IVCD}}$$

Product quality analysis

Fed-batch harvest was clarified, and then purified using a MabSelect Protein A affinity column (2D-HPLC Dionex, Sunnyvale, CA) operating at low pH, step elution gradient and detection at 280 nm. The size was measured by size exclusion chromatography SEC using a TSK-gel Super SW3000 column (Tosoh Bioscience, Tokyo, Japan) operating with 100 mM Na_2SO_4/100 mM Na_2HPO_4 pH 6.8 mobile phase. Charge variants were analyzed by cation exchange chromatography (CEX) using a ProPac WCX-10 analytical column (Dionex, Sunnyvale, CA) operating with 10 mM sodium phosphate/pH 6.0 mobile phase. N-linked oligosaccharides were measured by 2-AB label (ProZyme, Hayward, CA, USA) following the manufacturer's recommended procedure. Briefly, purified antibody samples were digested with N-glycanase (Prozyme, Hayward, CA, USA) and labeled with 2-AB by reductive amination. The labeled glycans were separated and detected by HPLC using a GlycoSepN column (ProZyme, Hayward, CA).

Statistical analysis of cell lines performances in 24-DWP versus shake flask

The growth and titer of cell lines were compared at key time-points throughout fed-batch experiments. The preferred method for assessing statistic dependence was Spearman's Rho (r_s) nonparametric correlation.[30] This analysis was better suited than Pearson's product-moment correlation (R^2) to study the ranking of cell line performances that do not follow normal distribution, as in the case of a cell line development program, where outstanding cell lines shall not be treated as statistical outliers. The absolute value discrepancy between two datasets was assessed by the least square regression (LSR), intended to measure the fit of all cell lines into a model linear regression curve. The slope and the intercept offer an essential metric to assess the distance between 24-DWP and shake flask data.[31] The variation of growth and titer in the two vessels was described by unsupervised principal component analysis [PCA] using SIMCA (UMetrics, MKS Data Analytics Solutions, Malmö, Sweden). A total of 6 growth variables (IVCD at Days 5, 7, 8, 11, 13, and 15) and 4 titer variables (titer at Days 5, 11, 13, and 15) were measured to describe 42 different observations (21 cell lines from 24-DWP and 21 from SF). The dataset consisting of 420 data points was collected and each data point in both vessels was the average of duplicate cultures ($n = 2$). A two-component PCA model was generated and the relationship 24-DWP to shake flask for each cell line was reported in a score scatter plot. Cell lines were then grouped based on hierarchical clustering analysis [HCA] using SIMCA (UMetrics, MKS Data Analytics Solutions, Malmö, Sweden) to identify groups of cell lines that displayed similar patterns in terms of process performance.

Comparison of 24-DWP to 3-L bioreactor scale

A parallel cell line development program was executed for a different antibody (Antibody B), similar in sequence, structure and biological activity to the immunoglobulin analyzed throughout this study. Cell lines developed for antibody B underwent an identical screening methodology and development strategy, with the exception that the top 4 producers (B03, B12, B13, and B27), as identified by 24-DWP screening only, were further scaled-up to the 3 L bioreactor scale. No shake-flask screening was performed as part of the CLD activities for molecule B. The fed-batch conditions were kept consistent between 24-DWP and 3L bioreactors, with the exception of either online, or daily monitoring and control of pH, DO, and glucose. The IVCD and harvest titer were calculated at the end of each culture.

Results and Discussion

Scale-up influences protein expression and growth without affecting the ranking of cell line performance

An essential requirement of any scale-up model is the reproducibility of process performance across the tested platforms. In the context of cell line development, those parameters were typically the protein expression levels and the cellular growth profiles. The cell cultures are compared in progressive platforms: from static (96-WP, 24-WP) to suspension (24-DWP vs shake flask). To ascertain the impact of our scale-up platform toward comparability in cell line process performance, we utilized nonparametric statistics. The ranking of cell lines indicated the similarity of titer and IVCD, and it was compared by Spearman's Rho correlation (r_s). We investigated the relationship between the static culture titer and the scaled-up suspension culture (Figure 1). Protein expression was highly correlated in static cultures of progressively increasing volumes such as from 96-well plate to 24-well plate ($r_s = 0.80$, Figure 1A). Upon transition from static to suspension culture, no correlation was observed for absolute titer ($r_s = 0.18$; Figure 1B). The loss of titer correlation suggested that cellular phenotypes were influenced by the improved growth rate.[32] We pointed at the increased oxygen transfer in shake flasks as a major driver for the phenotype change as reported.[26] The lack of agreement greatly impacts CLD screening ability and reinforced the need of a supplementary screening step for the suspension culture, such as shake flask or 24-DWP. The introduction of 24-

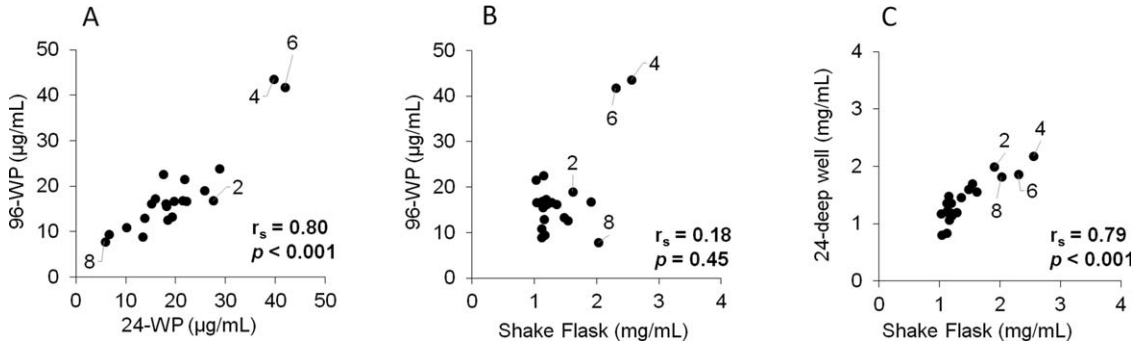

Figure 1. Correlation of protein expression at increasing culture volumes. Static titer measured at confluence: Day 18 (96-WP) and Day 6 (24-WP). Suspension titer measured at the harvest. Cell lines 2, 4, 6, and 8 are labeled and constitute the candidate lines that this work investigates in greater detail.

Table 1. Comparison of Protein Expression in 24-Deep Well Plate Versus Shake Flask Fed-Batch

Day	n	P	r_s	R^2	LSR
5	21	<0.001	0.98	0.96	$y = 1.01x$
11	21	<0.001	0.90	0.71	$y = 0.93x$
13	20	<0.001	0.79	0.69	$y = 0.97x$
15	16	<0.001	0.89	0.77	$y = 0.86x$

Twenty-one duplicate cell lines were compared in the two platforms. Protein expression was measured at Days 5, 11, 13, and 15 and correlated by Spearman's Rho ranking (r_s) and Pearson's (R^2). Absolute values were measured by linear square regression (LSR), where y was the protein expression in 24-deep well and x in shake flask.

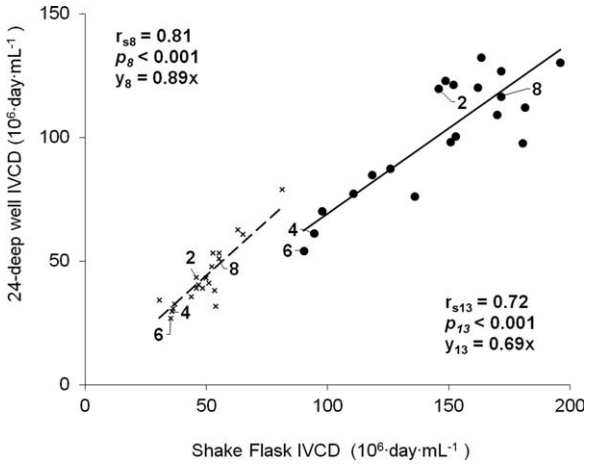

Figure 2. Cumulative progression of IVCD at Day 8 (crosses and dotted line) and Day 13 (dots and solid line).

DWP, allowed a faster transition from static to suspension than shake flasks as result of the smaller working volume enabling the 24-DWP culture. We calculated this time saving as about 7 days for the average cellular doubling time. In contrast to 96-WP, the titers were highly comparable in 24-DWP vs shake flask (Figure 1C) at the tested Days 5, 11, 13, and 15 as reported in Table 1 (r_s of 0.98, 0.90, 0.79, and 0.89). This guided the selection of the candidate cell lines #2, 4, 6, and 8, out of the pool of 21 cell lines screened.

The IVCD cumulative progression was monitored and satisfactory ranking was observed (Figure 2). Cultures demonstrated nearly identical cellular accumulation until day 8 of the fed-batch ($y = 0.89x$, where y was the IVCD in 24-DWP and x in shake flask), with a strong correlation ($r_s = 0.81$). From Day 8 onward, the values showed a significant decline. The reported Day 13 of the fed-batch scored lower r_s (0.72)

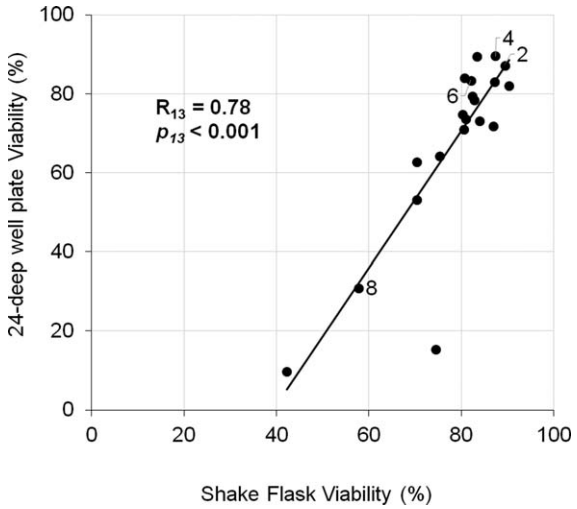

Figure 3. Viability comparison at Day 13 of the fed-batch.

and significant flattening of LSR ($y = 0.69x$). All cell lines showed a decreased IVCD in 24-DWP; and while the slow growers still correlated, most of the rapid growers lost correlation. The most severe loss in correlation was observed at the high end of the Day 13 curve where rapid and very rapid growers showed IVCD above 150 $\times 10^6$·day·mL^{-1} in shake flask but scored about 100 $\times 10^6$·day·mL^{-1} in 24-DWP. We suspected the IVCD reduction to be caused by the physical culture conditions (i.e., water loss through evaporation and increase in osmolality), rather than cell line physiology and we'll discuss it in the following paragraphs. The correlation loss may be consequential to the individual growth characteristics of each cell line, and impacting only rapid growers but not moderate to slow growers.

We hypothesized that the IVCD reduction was caused by lowered growth rate in 24-DWP rather than a premature cellular death.[15,33] In fact, cell lines 2, 4, and 6 showed identical viability at day 13, >80% in the two platforms, despite a significantly reduced IVCD (Figure 3). The remaining lines showed consistent viability decay, reaching 24-DWP values as low as half than the ones in shake flask (i.e., #8). Growth reduction and viability decay appeared uncorrelated events.

Protein expression comparison in different culture vessels

Comparative analysis between the two different culture methods needs to be performed to make a decision on which cell lines to carry forward. The below sections highlight a

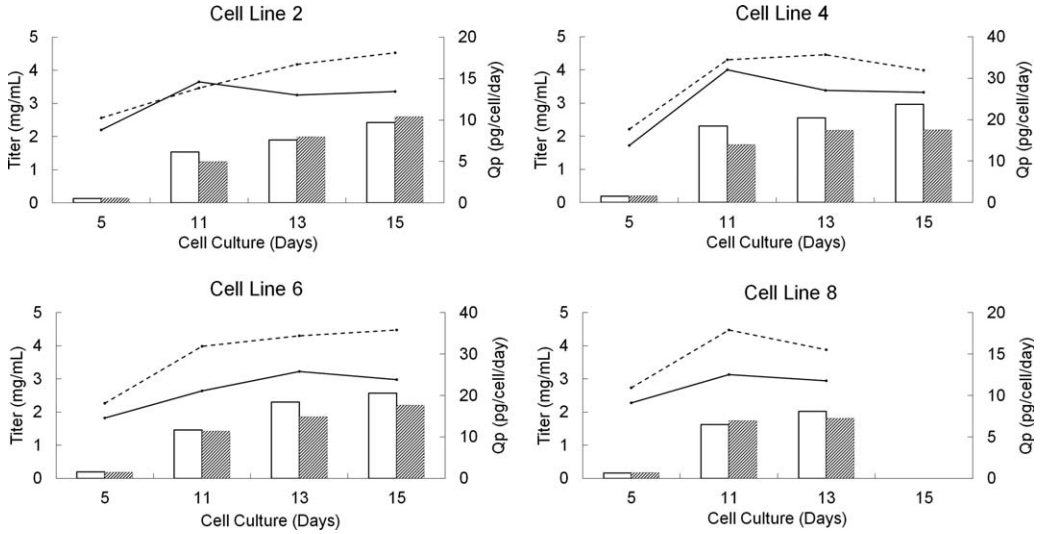

Figure 4. Protein expression and specific productivity of cell lines 2, 4, 6, and 8 in 24-deep well plates versus shake flask. Protein expression in shake flask (white bar) and 24-deep well plate (grey bar). Specific productivity in shake flask (solid line) and 24-deep well plate (dotted line). Cell cultures run duplicate (n = 2) and average values reported.

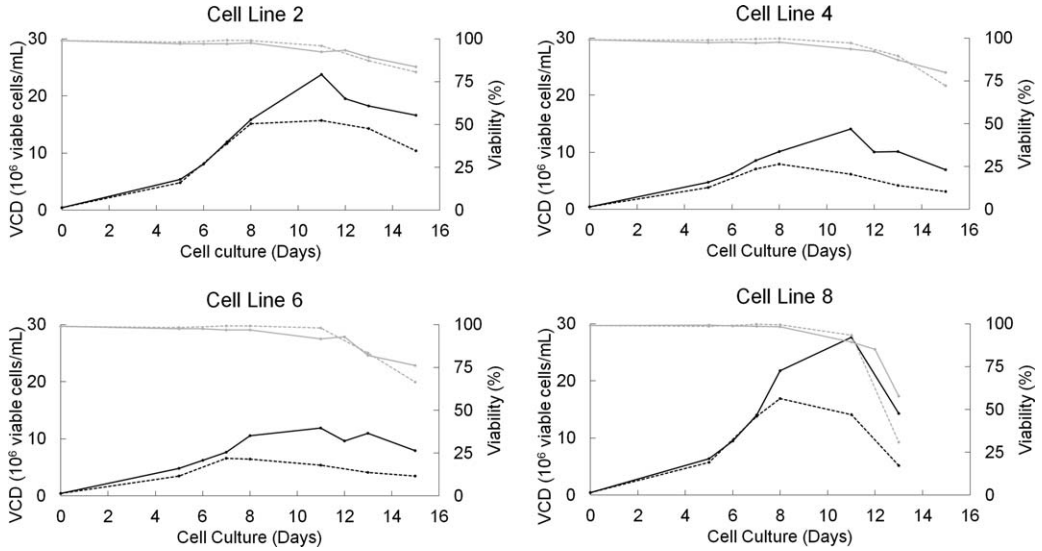

Figure 5. Viable cell density and viability of cell lines 2, 4, 6, and 8 in 24-deep well plates versus shake flask. Viability in shake flask (grey solid line) and 24-deep well plate (grey dotted line). Viable cell density in shake flask (black solid line) and 24-deep well plate (black dotted line). Cell cultures run duplicate (n = 2) and average values reported.

representative mean with which we categorize and select individual cell lines at AbbVie.

Cell lines showed reasonably predictive titers in the two platforms (shake flask vs 24-DWP) at the analyzed days, as reported in Figure 1C. We decided to select the top candidate lines 2, 4, 6, and 8 based on their fed-batch progression, and the titer values achieved at the day of the harvest in both platforms, as reported in Figure 4 and 5 (harvest for cell line #8 occurred on day 13). Harvest titers of cell lines #2 and #8 were 2.60 and 1.81 g/L (24-DWP) and 2.43 and 2.02 g/L (shake flask). This corresponded to titer ratios of 1.07 and 0.90 (Table 2). The harvest titer discrepancy was more pronounced in cell lines #4 and #6 with titer ratios of 0.74 and 0.86, respectively. In those lines, the 24-DWP cultures did not achieve the same titer as the corresponding shake flasks with 2.19 and 2.21 g/L (24-DWP) versus 2.98 and 2.56 g/L (shake flask) for cell lines 4 and 6, respectively.

The screening in 24-DWP allowed an accurate identification of which clones to move forward. Although correlation between vessels was quite good for titer, the absolute values were slightly different. We found that slow growing lines had the biggest difference between the vessels. Regardless of this, the ranking remained consistent and allowed to still select the best candidate lines. Protein expression in 24-DWP greatly correlated to shake flask and could enable successful ranking. Cell lines 4 and 6 emerged as outstanding performers at every stage of the analysis. Cell lines 2 and 8 were clustered in the pool of low producers in the static culture, and upon adaptation to shaking, they improved their protein expression.

All candidate cell lines showed a comparable lag and early exponential phase of the growth curve, followed by a consistent decline in 24-DWP after Day 8, as reported in Figure 5. The viability, differently from the VCD, progressed

Table 2. Titer Values Comparison in 24-Deep Well Plate (24-DWP) Versus Shake Flask (SF), at Days 5, 11, 13, and 15 and Average Relative Ratio (24-DWP/SF)

		Titer (mg/L)			
Cell Line		2	4	6	8
Day 5	24-DWP	139	197	186	175
	SF	133	186	200	161
	Ratio	1.05	1.06	0.93	1.09
Day 11	24-DWP	1239	1750	1424	1746
	SF	1540	2313	1455	1622
	Ratio	0.80	0.76	0.98	1.08
Day 13	24-DWP	1994	2183	1860	1814
	SF	1902	2556	2304	2022
	Ratio	1.05	0.85	0.81	0.90
Day 15	24-DWP	2602	2190	2208	
	SF	2429	2957	2565	
	Ratio	1.07	0.74	0.86	
Average ratio		0.99	0.85	0.89	1.02

Table 3. IVCD Values Comparison in 24-Deep Well Plate (24-DWP) Versus Shake Flask (SF), at Days 5, 11, 13, and 15 and Average Relative Ratio (24-DWP/SF)

		IVCD (10^6•day•m L^{-1})			
Cell Line		2	4	6	8
Day 5	24-DWP	14	11	10	16
	SF	15	14	14	18
	Ratio	**0.90**	**0.82**	**0.75**	**0.89**
Day 11	24-DWP	90	51	45	97
	SF	105	72	69	129
	Ratio	0.85	**0.70**	**0.65**	**0.75**
Day 13	M24-DWP	120	61	54	117
	SF	146	94	90	172
	Ratio	0.82	**0.65**	**0.60**	**0.68**
Day 15	24-DWP	145	69	62	
	SF	181	111	109	
	Ratio	0.80	**0.62**	**0.57**	
Average ratio		0.84	0.70	0.64	0.77

similarly in all cases, including the early decline of line #8. All cultures in 24-DWP reached lower peak VCD than the shake flask cultures, throughout the fed-batch.

Based on their performances, candidate cell lines could be divided into rapid growers (#2 and 8 achieving harvest IVCD of 181 and 172 $\times$ 10^6·day·mL^{-1} in shake flask) or slow growers (#4 and 6 achieving harvest IVCD of 111 and 109 $\times$ 10^6·day·mL^{-1}), as summarized in Table 3. Notably the rapid growers group reached higher 24-DWP/shake flask ratios with average values of 0.99 and 1.02 for titer and 0.84 and 0.77 for IVCD. Contrarily, the slow grower group achieved average ratios of 0.85 and 0.89 for titer and 0.70 and 0.64 for IVCD. Rapid growing cell lines 2 and 8 showed similar titer in the two culture conditions, whereas the slow growing cell lines 4 and 6 showed a significant decrease in the 24-DWP. This suggested that rapid growers could overcome the lowered growth rate in 24-DWP and showed little or no impact on the protein expression. Conversely, slow growers could not overcome the lowered growth rate and this reflected in reduced titer values. This data indicates that compared to rapid growers, slow growing cell lines in the scaled-down culture bear a greater potential to improve their protein expression when scaled-up. To explain the reduced growth, we hypothesized that the higher evaporation in 24-DWP may elevate the culture osmolality,[18] although this parameter was not specifically measured. The 24-DWP manufacturer technical sheet (http://www.enzyscreen.com/oxygen_transfer_rates) reports a daily

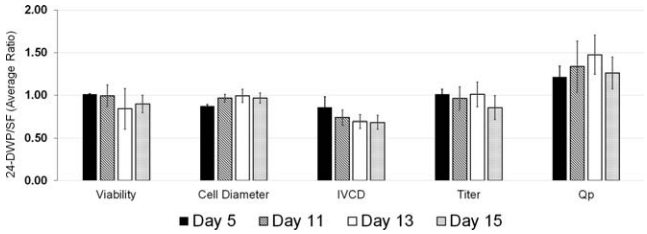

Figure 6. Key parameters: viability, cell diameter, IVCD, titer, and Q_p (specific productivity) measured over the duration of the fed-batch. Bars represent the average ratio of 24-deep well plates (24-DWP) relative to shake flask (SF) values, ± SD (standard deviation), $n = 21$.

water loss of at least 0.6%, accounting for about 10% volume reduction or more, over a 15 day fed-batch. Others report daily evaporation to account up to 5%, translating to 75% volume reduction throughout the fed-batch.[20] In our 24-DWP platform, we measured the water loss only at the end of the fed-batch, and we detected ~30% volume reduction. The hypothesized osmolality increase might be sensed by the cells as a proliferation suppression signal, in a cell-line-dependent fashion.[34,35] Duetz sandwich covers were employed in this study to mitigate such effect, but we suspect that they are not sufficient to completely avoid the problem.[16,17] We speculate that inadequate oxygen transfer may be a secondary cause, known to act in a cell-line-dependent fashion.[26] Barrett et al.[15] confirmed that the deep-well plate reduction in oxygen transfer is a combination of three factors: (a) reduced fluid/air interface, (b) shaking kinetics influencing mass transfer, and (c) culture volume and speed, all intrinsic to the deep-well plate architecture. The physical culture conditions were sufficient to enable VCDs up to 17 million cells/mL in rapid growers (i.e., cell line #2 and #8). Despite all this, it is possible that slow growing lines in 24-DWP have higher oxygen uptake rates and therefore reach oxygen transfer limitations at lower cell numbers. The regulation of cellular proliferation is a complex cellular network and it is also possible that other factors other than oxygen transfer limitations play a role in the lower densities observed in the 24-DWP, specifically for slow growing cell lines.[36] However, further investigation is necessary to completely understand this phenomenon.

A comparative analysis was also executed on the remaining cell lines not identified as candidates. Cellular phenotype of every line was monitored and compared in the two platforms (Figure 6). The analysis corroborated the growth reduction effect in 24-DWP and proved that this phenomenon happens consistently on every cell lines regardless of the individual growth profiles or productivities. The below section describes the results for the two sets of 21 duplicate cultures.

Time course data (Days 5, 11, 13, and 15) from the fed-batch experiment was collected and the duplicate cultures ($n = 2$) were averaged in 24-DWP and in shake flask, with respect to viability, cellular diameter, IVCD, titer, and Q_p (Figure 6). Each data point in 24-DWP was normalized by the corresponding value in shake flask and a relative ratio was obtained. The relative ratios of each data point of all the measured cell lines were averaged and data variation calculated. Viability at Days 5 and 11 scored a ratio close to 1, meaning similar values were achieved in the two cultures during the exponential phase. However, it declined at Day 13 (ratio of 0.84 ± 0.24). Such discrepancy normalized on Day 15 (ratio of 0.90 ± 0.10). The high variation indicated

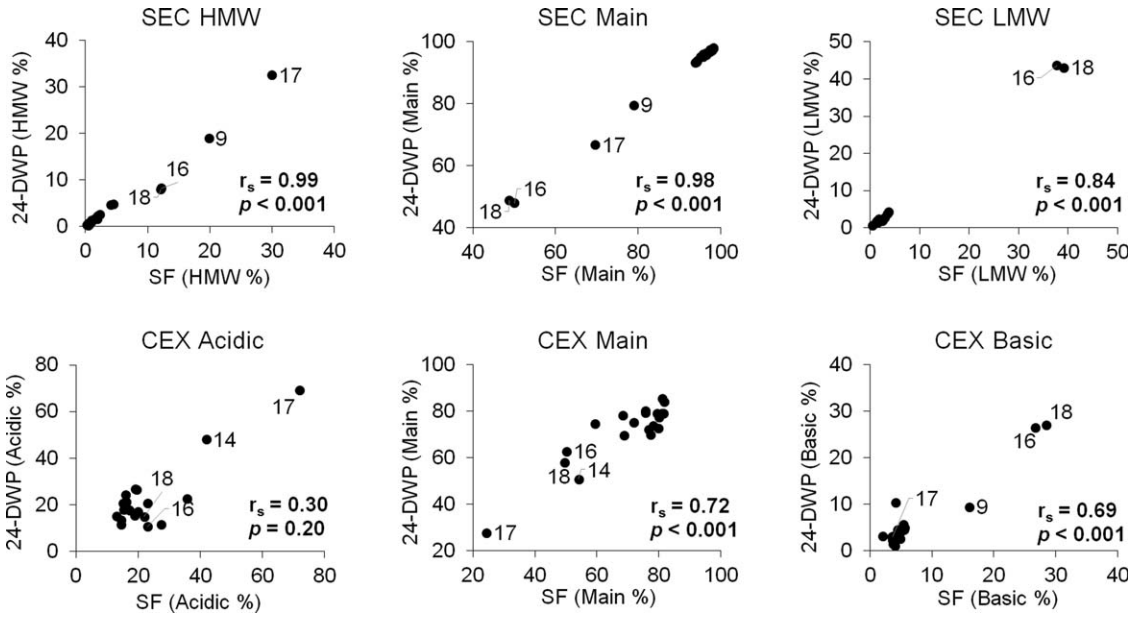

Figure 7. Size exclusion chromatography (SEC, top) and cation exchange (CEX, bottom) in 24-deep well plate (24-DWP) versus shake flask (SF).

that the viability response was dependent on the cell line, as some cell lines started dying earlier than others when grown in 24-DWP. Cellular diameter was comparable throughout the duration of the fed-batch. Cellular size, an indicator of the overall physiology and morphology,[37] was slightly smaller in 24-DWP at day 5 (ratio of 0.87 ± 0.02) and on subsequent days it was similar to shake flasks. The size of a cell reflects the relationship between its growth rate and division frequency,[38] as discussed by Tzur et al. We hypothesize that the 24-DWP architecture may dictate an initial smaller cell size, that tended to increase as result of the reduced cellular growth in 24-DWP, over the course of the fed-batch. IVCD was progressively reduced in every cell line of about 30% with respect to the values achieved in shake flask (ratios of 0.86, 0.74, 0.69, and 0.68 on Days 5, 11, 13, and 15, respectively).

Titer was a highly reproducible parameter with all values in 24-DWP matching the ones in the shake flask (highest variations of 14%). Specific productivity, being a function of decreased growth and unchanged titer, resulted in an improvement with respect to the shake flask control (up to ratio of 1.45 ± 0.23 at day 13). Other factors may contribute to the increased specific productivity, such as the hypothesized osmolality increase in 24-DWP, also described by Shen et al.[39] In terms of protein expression, the 24-DWP platform enabled a successful ranking of cell lines, as well as a satisfactory prediction of the shake flask values. We did not perform any offline gas, pH, and metabolite analysis to minimize the requirement for culture volume, but we are cognizant that the 24-DWP is admittedly not a perfect scale-down model; therefore, some deficiencies exist. In most instances, this is acceptable because we are compromising data for speed and throughput.

Product quality comparison in different culture vessels

A comprehensive quality analysis was performed in an effort to understand the 24-DWP impact on protein processing and post-translational modifications (Figures 7 and 8). Within the framework herein described, the product quality analysis is a fundamental part of the clone screening in CLD. The harvest protein was collected, purified, and analyzed for size (SEC), charge (CEX), and N-glycans (2-AB/HPLC). The product quality in the 24-DWP platform was comparable to that of the shake flask and allowed a precise screening and exclusion of undesirable profiles, which is ultimately the goal of any cell line development program.

SEC analysis (Figure 7, top) showed that all the molecular weight species can be predicted in the 24-DWP platform. The high molecular weight, main peak, and low molecular weight achieved correlations of 0.99, 0.98, and 0.84, respectively. All correlations were statistically significant and the difference in vessel did not affect the percentage of monomer versus other species.

CEX analysis (Figure 7, bottom) was used to measure the charge variants of the expressed protein. The main and the basic species were highly correlated with r_s values of 0.72 and 0.69, respectively. Lower correlation was achieved for the acidic species ($r_s = 0.3$); however, undesirable cell lines #14 and 17 scored identical values (about 45% and 70% of acidic species) and it was still possible to pick out those cells lines.

Many factors can influence acidic species, and reports in literature have shown various ways with which to control their levels.[40] The exact reason for the acidic species differences across the tested cell lines was not specifically known. However, what was known was that some cell lines support higher levels of acidic species when grown in the same exact culture conditions. As a result, those cell lines were excluded from further consideration, and the 24-DWP format enabled this decision-making process. Cell lines #9, 14, 16, 17, and 18 revealed size and charge quality characteristics incompatible with the CLD program acceptance criteria (monomer 80% or lower and high acidic species) and their development was terminated.

Subsets of cell lines were screened for glycan analysis. G0-GlcNAc, G0, and total mannose species collectively accounted for the majority of the measured N-glycan species. The analysis of glycans in the 24-DWP versus shake flask

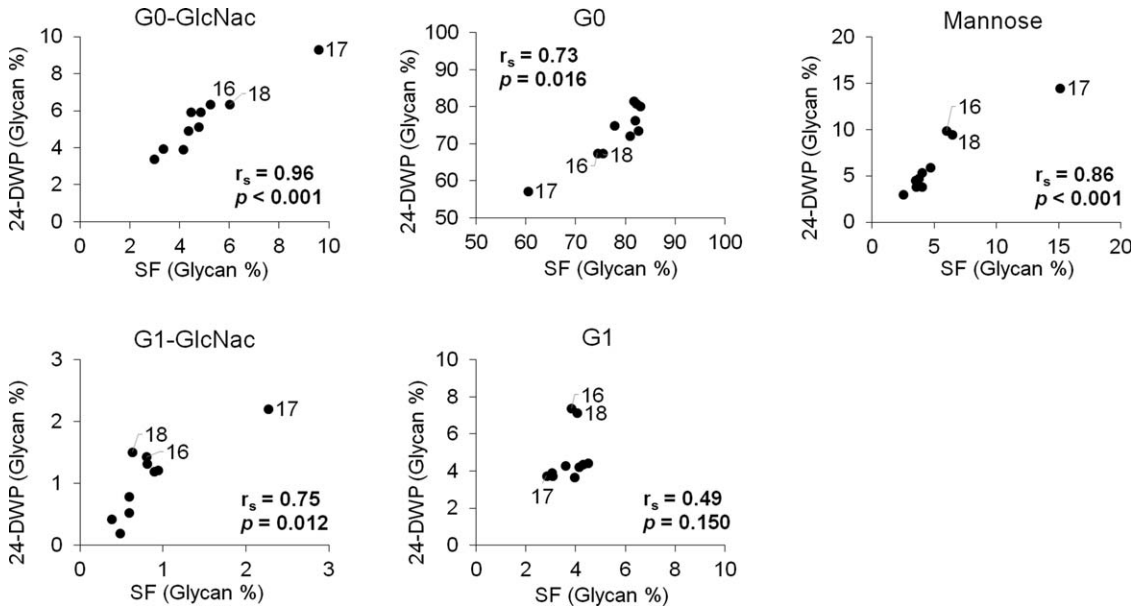

Figure 8. Glycan analysis of G0-GlcNAc, G0, mannose, G1-GlcNAc, and G1 species in 24-deep well plate (24-DWP) versus shake flask (SF).

Table 4. Glycan Analysis Summary Table

	P	r_s	R^2	LSR
GO-G1cNAc	<0.001	0.96	0.81	$y = 1.11x$
GO	0.016	0.73	0.81	$y = 0.79x$
G1-G1cNAc	0.012	0.75	0.60	$y = 1.17x$
G1	0.150	0.49	−0.01	$y = 1.50x$
Mannose	<0.001	0.86	0.77	$y = 1.13x$

Duplicate cell lines were compared in the two platforms with respect of glycan species (G0-GlcNAc, G0, G1-GlcNAc, G1, and mannose). The normalized harvest values correlate in terms of Spearman's Rho ranking (r_s) and Pearson's (R^2) and were statistically significant with the exception of G1. Absolute values were measured by linear square regression (LSR), where y was glycan amount in 24-deep well and x in shake flask.

analysis, showed a sufficient correlation to perform screening of undesirable profiles (Figure 8). G0-GlcNAc, G0, G1-GlcNAc, and total mannose showed respectively r_s values of 0.96, 0.73, 0.75, and 0.86. G1 species were poorly correlated; however, cell lines #16 and 18 were captured by the 24-DWP as undesirable profiles but this cannot be inferred by the SF. The absolute values differed by the amount reported (Table 4) in the form of $Y = aX$. The 24-deep well showed a decreased G0 ($Y = 0.84x$) but increased G0-GlcNAc, G1-GlcNAc, G1, and mannose (a = 1.11, 1.17, 1.50, and 1.13, respectively). The undesirable profiles such as low G0 and high mannose could be captured. We observed that 24-DWP supported a slightly more efficient terminal glycosylation, with a lower amount of G0, and higher amount of G1 species. This may be intrinsic to the scale-down culture condition.[13,28] However, like some of the other process performance variables, the absolute values differed as reported in Table 4. Based on the glycan analysis, cell lines 16, 17, and 18 showed high mannose content and were not carried any further.

While the molecular weight species could be accurately predicted, the charge variants and the glycosylation profiles showed some discrepancy in the two platforms. However, this did not prevent the identification of cell lines presenting undesirable product quality profiles.

Principal component analysis [PCA] and hierarchical clustering analysis [HCA] allow the identification of candidate cell lines while capturing the phenotypic differences depending on the scale

Our current cell line screening platform was effectively improved by the introduction of PCA and HCA as means to capture the relationship among the relative performances of cell lines. Furthermore, such tools simplified the identification of cell line clusters showing similar performances and could efficiently isolate the candidate cell lines from the expanded pool.

PCA was executed on all 21 cell lines in the two production conditions (21 cell lines from 24-DWP and 21 cell lines from shake flask). The scatter plot summarizes the relationship among performances of all cell lines. Most of the variability was well explained by the model. A strong two-component model was built (Figure 9), characterized by good fit (R2X value of 0.894) and good prediction (Q2X value of 0.788). The IVCD variables increased left to right along the horizontal axis. This described the component 1 (R2X of 0.547) of the PCA model. Cell lines with high IVCD localized on the far-right part of the plot. The Titer variables increased bottom to top along the vertical axis. This described the Component 2 (R2X of 0.347) of the PCA model. Cell lines expressing high amount of protein localized on the top part of the plot. The correlation of performances in the 24-DWP (circle) with shake flask (triangle) was expressed in terms of proximity between the two shapes.

PCA enabled the selection of candidate cell lines 2, 4, 6, and 8 regardless of the culture scale. The candidate cell lines demonstrated high proximity meaning high similarity of performance across the two different culture vessels. All shake flask cultures shifted one or more units to the right which was consistent with the greater IVCD achieved versus 24-DWP, with the exception of cell lines #11 and 18. The majority of cell lines don't shift along the vertical axis of titer, indicating no difference in protein expression when scaled-up. Cell lines 4, 6, 16, and 18 show the greatest vertical shift (titer improvement) and localize in the left part of

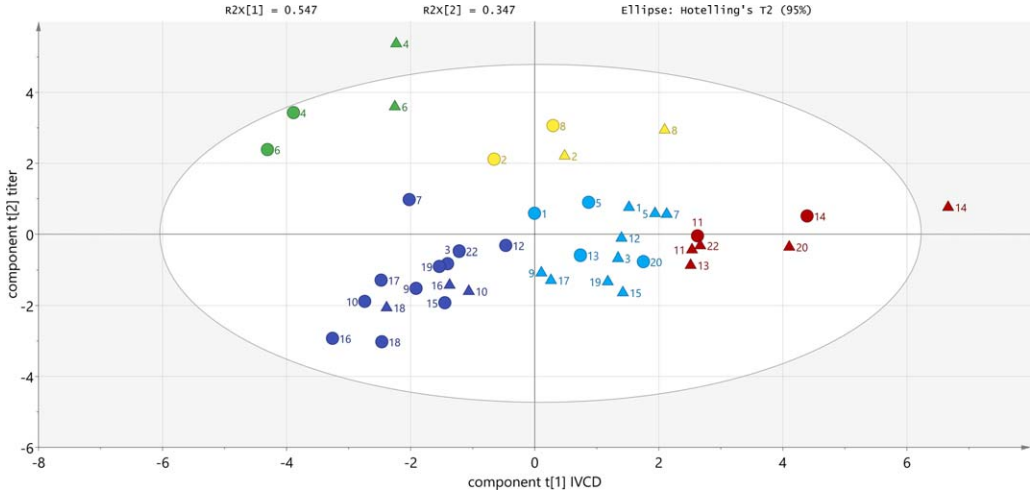

Figure 9. **Score scatter plot of two-component PCA. IVCD variables increase left to right along the horizontal axis (Component 1). Titer variables increase bottom to top along the vertical axis (Component 2). Cell lines developed in 24-deep well plate (circles) localize in proximity of the shake flask (triangle) meaning high similarity of performances in the two vessels. Five cellular profiles were defined by high (H), moderate (M), or low (L) values for titer and IVCD as follows: dark blue (LL), light blue (MM), red (MH), green (HL), and yellow (HM). Most promising cell lines 2, 4, 6, and 8 belong to the green and yellow clusters. The greatest titer improvement upon scale-up belongs to slow growers 4 and 6 when compared to rapid growers 2 and 8.**

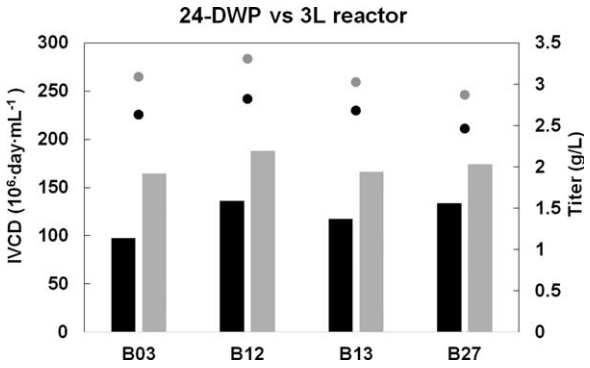

Figure 10. **Comparison of top 4 cell lines in 24-deep well plate versus 3 L reactor. IVCD in 24-deep well plate (black column) and 3 L reactor (grey column). Titers in 24-deep well plate (black dot) and 3 L reactor (grey dot).**

Table 5. Analysis of Top 4 Cell Lines in 24-Deep Well Plate (24-DWP) Versus 3 L Bioreactors

	Cell Line	B03	B12	B13	B27
ICVD (10^6 day mL^{-1})	24-DWP	98	136	117	134
	3L	164	188	166	174
	Rank $_{24\text{-DWP}}$	1	4	2	3
	Rank $_{3L}$	1	4	2	3
	$Ratio_{3L/24\_DWP}$	1.68	0.38	1.42	1.30
Titer (g/L)	24-DWP	2.6	2.8	2.7	2.5
	3L	3.1	3.3	3.0	2.9
	Rank $_{24\text{-DWP}}$	2	4	3	1
	Rank $_{3L}$	3	4	2	1
	$Ratio_{3L/24\_DWP}$	1.17	1.17	1.13	1.16

the PCA score plot (reduced growth area). This indicates that, in the CLD program herein described, low growers benefit the greatest from the improved growth in shake flask and this reflects in a titer improvement, as also suggested by data reported by others.[33]

Groups of cell lines sharing similar global performances were recognized by the SIMCA software, and HCA was used to isolate 5 distinct profiles. Profiles were defined by high (H), moderate (M), or low (L) values for titer and IVCD. Groups HL (green) and HM (yellow) included cell lines with desirable protein expression but low and moderate growth characteristic, when compared to the rest of the pool. Candidate lines 4, 6 and 2, 8 were captured within the same clusters regardless whether the culture was grown in 24-DWP or shake flask. A number of low performers, # 10, 16, and 18 (LL, blue), 1 and 5 (MM, light blue), 11 and 14 (MH, red), showed negligible changes in the global performances when scaled up and were captured in the same cluster. Cell lines localized at the top part of the moderately desirable group (light blue) may be considered as backups for further studies. Remaining low-performing lines show a partial overlap of characteristics upon scaling-up and transitioned into the adjacent group to the right upon improved growth rate in shake flask. Those cell lines are not normally pursued in a cell line development program. The HCA clustering model is effective for screening desirable candidates out of the pool of less desirable ones; therefore, we are not particularly concerned about the lack of co-clustering of those low performing lines.

The PCA and HCA observations explains the behavior of titer values when scaling up 24-DWP to the larger scales and supports the claim that low growers are ideal candidates for scale-up and can be identified during the CLD screening.

Scale-up comparison between 24-DWP and laboratory-scale bioreactors

We lastly wanted to quantify the degree of similarity between 24-DWP values, as captured during the CLD screening, to the 3 L bioreactor scale. To achieve that, we tested the top 4 cell lines from a parallel CLD of a similar molecule B. The development followed the same trajectory as the main immunoglobulin of this study. Cell lines B03, B12, B13, and B27 were selected for further scale-up and advanced to 3 L bioreactor scale. We verified that the larger 3 L scale, delivers slightly higher productivities and

increased growth, perhaps attributed to the pH control, glucose monitoring and better oxygen transfer, when compared to the 24-DWP results (Figure 10). The IVCDs and titers are reported in Table 5 and measured as ratios relative to the 24-DWP values. The average 3 L to 24-DWP ratios corresponded to 1.44 ± 0.14 and 1.16 ± 0.02 for IVCD and titer, respectively. Regardless of the absolute values, the ranking as assessed by spearman's rho, shows nearly identical scores of $r_s = 1.0$ and $r_s = 0.8$, respectively, for IVCD and titer, enabling the satisfactory prediction of performances (Table 5). The limited dataset in 3 L bioreactor did not allow us to investigate any further trend or sample clustering, relative to these top producer cell lines.

These results corroborate the value of scale-down 24-DWP screening and its introduction at multiple stages of upstream development. We are cognizant about the limitations of this system (i.e., lack of pH control, glucose monitoring, metabolite analysis, and daily cell count) and we look forward to the advancements in analytical capabilities to overcome these limitations. The current state of technology can support CLD screening activities, largely based on titer, growth, and product quality assessment. Yet we believe that further improvements can actualize the benefits of 24-DWP into more areas of the development (i.e., process development and characterization, cell line stability study, and others), and perhaps lead to a progressive reduction of shake flask studies. However, the validity of performance prediction was verified across multiple setups, and we conclude that the effective incorporation of the 24-DWP and multivariate data analysis can significantly improve early cell line development screening.

Conclusion

In upstream development, there is a constant requirement to accelerate the clone selection activities. One of the means to achieve a faster timeline is predicting cell line phenotypes and performances, including protein expression, growth profile, and product quality. A successful program is enabled by several aspects including the precise screening of performance post-transfection, the rapid transfer and stable adaptation of the candidate cell lines to suspension culture, and the determination of a desirable quality profile.[8,9]

In this study, we report the analysis of 24-DWP for the production of an industrially relevant biopharmaceutical and its comparison to the industry-standard shake flask. We observed that cell culture evolution in the 24-DWP platform is consistent with shake flasks and enables the successful ranking of process performance. The scale-down platform can be used for screening candidate cell lines as part of the cell line development (CLD) activities, facilitating further upstream process development efforts.

The approach herein described is compatible with early CLD work stream and constitutes a continuously updated process. In our work, we adopted a Process Analytical Technology tool, multivariate data analysis (MVDA), to create an iterative and cumulative dataset to make informed decisions from a statistical basis. The inclusion of the 24-DWP screening in CLD functions is not fully embraced by the industry and few examples are known, mostly describing the scalability of established cell lines.[23,24] In our experience, 24-DWP enabled the transfer to suspension culture, 1 week before shake flasks. Besides the time and reagent saving, the ability to start a production fed-batch in the 24-DWP was advantageous with respect to implementation in an automated system.[23,41] The reduced bench-work also simplified the routine analysis and operations (i.e., multichannel pipetting, plate footprint consistent with automated assays, reduced incubator occupancy), allowing more fed-batch experiments to be executed simultaneously, hence improving the throughput.

While acknowledging the benefits of the deep-well plate, we historically observed a disagreement between the 24-DWP and the shake flask performances. Over the course of multiple biomanufacturing programs, the absolute values of growth and productivity diverged in the two scales when the candidate lines were expanded to the shake flask lab scale. We explored multiple combinations of shaking speeds and culture volumes and the ones here used, achieved the closest comparison to the shake flask culture. The degree of the discrepancy was independent of the well position and hard to predict; therefore, we decided to investigate this phenomenon as part of the 24-DWP screening in CLD. No full comparability study was reported in literature for a large pool of cell lines, therefore we decided to describe our approach to solve this problem. In our analysis, not only were we able to test the 4 candidate lines, but also the additional 17 that were not chosen for process development, attaining a great degree of sample variability, along with the possibility to explore trends and patterns. With this rationale in mind, we executed a comparison of cell line performances in the shake flask versus the 24-DWP as part of the cell line development screening effort.

During CLD screening, the 24-DWP phenotypes achieved cell culture duration and viability comparable to the ones in shake flask. Cellular productivities ranked reasonably well, enabling the selection of promising candidates. Cultures in 24-DWP achieved lower IVCD primarily as a consequence of growth suppression mechanisms, unrelated to early cellular death events. Such effect did not compromise the productivity of rapid growing lines, as opposed to slow growing lines that bore a greater potential to improve their productivity upon scaling-up. We could not extrapolate this specific trait in the 3 L bioreactor because the sample size was limited and any effort to study trends would have been not statistically significant.

The product quality, size, and charge of the protein are the supplementary screening criteria to enable the identification of undesirable profiles. The 24-DWP showed high relative ranking and good absolute prediction of values for size and charge; therefore, it is suitable as supplementary screening criteria during cell line development. When looking at glycans, we observed decreased G0 and increased high-mannose species in 24-DWP compared to shake flask. This may be caused by the distinct culture conditions although it did not compromise the selection of cell lines that matched the program requirements, showing acceptable relative ranking. Overall the 24-DWP offered a reliable platform for delivering comparable performances and quality of the therapeutic protein.

Multivariate statistical analysis showed that 24-DWP cultures delivered similar performance to shake flask. Cell lines were clustered based on their mutual relationships and upon scaling up to shake flasks we reported two phenomena. On the one hand, all the cell lines consistently improved their growth rate. On the other hand, only slow growers improved their productivities. The 24-DWP platform identified the

desirable profile of candidate lines 2, 4, 6, and 8 that stand out when compared to all the developed cell lines, regardless of the scale. This observation and the associated multivariate analysis methodology should help facilitate the identification of lines to move forward in the pipeline. We further verified the accurate ranking of 24-DWP performances to the 3 L bioreactor scale for a subset of cell lines. In conclusion, the 24-DWP scale can be successfully implemented in cell line screening and enabled an efficient selection of cell lines suitable for future manufacturing campaigns, while saving development time and reducing cost and labor.

Acknowledgment

The authors thank Georgeen Gaza-Bulseco, Chelsey Mattison, and David Winarta of AbbVie for their help on product quality analysis; Falguni Patel and Stephanie Rieder of AbbVie for their contributions to the development of 24-deep well culture parameters; and John Burns of AbbVie for Octet support. The authors also thank Li Malmberg and Ralph Lambalot of AbbVie for their support.

Disclosures

The design, study conduct, and financial support for the study were provided by AbbVie. The authors participated in the interpretation of data, review, and approval of the publication; all authors contributed to the development of the publication and maintained control over the final content. AM, SZ, GC, BN, and PH have or had a financial interest in AbbVie. GC, BN, and PH are AbbVie employees. AM and SZ are former employees of AbbVie. SY serves as a PhD advisor to AM. All authors have no conflict of interest to declare.

Literature Cited

1. Reichert JM. Antibodies to watch in 2015. *MAbs*. 2015;7:1–8. doi:10.4161/19420862.2015.988944.
2. Walsh G. Biopharmaceutical benchmarks 2014. *Nat Biotechnol*. 2014;32:992–1000. doi:10.1038/nbt0910-917.
3. Reichert JM. Marketed therapeutic antibodies compendium. *MAbs*. 2012;4:413–415. doi:10.4161/mabs.19931.
4. Aldeghaither D, Smaglo BG, Weiner LM. Beyond peptides and mAbs - Current status and future perspectives for biotherapeutics with novel constructs. *J Clin Pharmacol*. 2015;55:S4–S20. doi:10.1002/jcph.407.
5. Beck A, Reichert JM. Antibody-drug conjugates present and future. *MAbs*. 2014;6:15–17. doi:10.4161/mabs.27436.
6. Lai T, Yang Y, Ng SK. Advances in mammalian cell line development technologies for recombinant protein production. *Pharmaceuticals*. 2013;6:579–603. doi:10.3390/ph6050579.
7. Butler M, Meneses-Acosta a. Recent advances in technology supporting biopharmaceutical production from mammalian cells. *Appl Microbiol Biotechnol*. 2012;96:885–894. doi:10.1007/s00253-012-4451-z.
8. Estes S, Melville M. Mammalian cell line developments in speed and efficiency. *Adv Biochem Eng Biotechnol*. 2014;123:127–141. doi:10.1007/10.
9. Kim JY, Kim YG, Lee GM. CHO cells in biotechnology for production of recombinant proteins: current state and further potential. *Appl Microbiol Biotechnol*. 2012;93:917–930. doi:10.1007/s00253-011-3758-5.
10. Lewis AM, Abu-Absi NR, Borys MC, Li ZJ. The use of 'Omics technology to rationally improve industrial mammalian cell line performance. *Biotechnol Bioeng*. 2016;113:26–38. doi:10.1002/bit.25673.
11. Kang S, Ren D, Xiao G, Daris K, Buck L, Enyenihi A. a, Zubarev R, Bondarenko PV, Deshpande R. Cell line profiling to improve monoclonal antibody production. *Biotechnol Bioeng*. 2014;111:748–760. doi:10.1002/bit.25141.
12. Dickson AJ. Enhancement of production of protein biopharmaceuticals by mammalian cell cultures: the metabolomics perspective. *Curr Opin Biotechnol*. 2014;30:73–79. doi:10.1016/j.copbio.2014.06.004.
13. Janakiraman V, Kwiatkowski C, Kshirsagar R, Ryll T, Huang Y-M. Application of high-throughput mini-bioreactor system for systematic scale-down modeling, process characterization, and control strategy development. *Biotechnol Prog*. 2015;31:1623–1632. doi:10.1002/btpr.2162.
14. Rameez S, Mostafa SS, Miller C, Shukla AA. High-throughput miniaturized bioreactors for cell culture process development: reproducibility, scalability, and control. *Biotechnol Prog*. 2014;30:718. doi:10.1002/btpr.1874.
15. Barrett TA, Wu A, Zhang H, Levy MS, Lye GJ. Microwell engineering characterization for mammalian cell culture process development. *Biotechnol Bioeng*. 2010;105:260–275. doi:10.1002/bit.22531.
16. Duetz WA. Microtiter plates as mini-bioreactors: miniaturization of fermentation methods. *Trends Microbiol*. 2007;15:469–475. doi:10.1016/j.tim.2007.09.004.
17. Duetz WA, Witholt B. Effectiveness of orbital shaking for the aeration of suspended bacterial cultures in square-deepwell microtiter plates. *Biochem Eng J*. 2001;7:113–115. doi:10.1016/S1369-703X(00)00109-1.
18. Silk NJ, Denby S, Lewis G, Kuiper M, Hatton D, Field R, Baganz F, Lye GJ. Fed-batch operation of an industrial cell culture process in shaken microwells. *Biotechnol Lett*. 2010;32:73–78. doi:10.1007/s10529-009-0124-0.
19. Micheletti M, Lye GJ. Microscale bioprocess optimisation. *Curr Opin Biotechnol*. 2006;17:611–618. doi:10.1016/j.copbio.2006.10.006.
20. Bos AB, Luan P, Duque JN, Reilly D, Harms PD, Wong AW. Optimization and automation of an end-to-end high throughput microscale transient protein production process. *Biotechnol Bioeng*. 2015;112:1832–1842. doi:10.1002/bit.25601.
21. Abbott WM, Middleton B, Kartberg F, Claesson J, Roth R, Fisher D. Optimisation of a simple method to transiently transfect a CHO cell line in high-throughput and at large scale. *Protein Expr Purif*. 2015;116:113–119. doi:10.1016/j.pep.2015.08.016.
22. Barnard GC, Hougland MD, Rajendra Y. High-throughput mAb expression and purification platform based on transient CHO. *Biotechnol Prog*. 2015;31:239–247. doi:10.1002/btpr.2012.
23. Markert S, Joeris K. Establishment of a fully automated microtiter plate-based system for suspension cell culture and its application for enhanced process optimization. *Biotechnol Bioeng*. 2017;114:113–121. doi:10.1002/bit.26044.
24. Hansen HG, Nilsson CN, Lund AM, Kol S, Grav LM, Lundqvist M, Rockberg J, Lee GM, Andersen MR, Kildegaard HF. Versatile microscale screening platform for improving recombinant protein productivity in Chinese hamster ovary cells. *Sci Rep*. 2016;5:18016. doi:10.1038/srep18016.
25. Rouiller Y, Bielser J-MM, Brühlmann D, Jordan M, Broly H, Stettler M. Screening and assessment of performance and molecule quality attributes of industrial cell lines across different fed-batch systems. *Biotechnol Prog*. 2016;32:160–170. doi:10.1002/btpr.2186.
26. Tescione L, Lambropoulos J, Paranandi MR, Makagiansar H, Ryll T. Application of bioreactor design principles and multivariate analysis for development of cell culture scale down models. *Biotechnol Bioeng*. 2015;112:84–97. doi:10.1002/bit.25330.
27. Ahuja S, Jain S, Ram K. Application of multivariate analysis and mass transfer principles for refinement of a 3-L bioreactor scale-down model-when shake flasks mimic 15,000-L bioreactors better. *Biotechnol Prog*. 2015;31:1370–1380. doi:10.1002/btpr.2134.
28. Tsang VL, Wang AX, Yusuf-Makagiansar H, Ryll T. Development of a scale down cell culture model using multivariate analysis as a qualification tool. *Biotechnol Prog*. 2014;30:152–160. doi:10.1002/btpr.1819.

29. Urlaub G, Chasin L. a. Isolation of Chinese hamster cell mutants deficient in dihydrofolate reductase activity. *Proc Natl Acad Sci USA*. 1980;77:4216–4220.
30. Spearman C. The proof and measurement of association between two things. *Am J Psychol*. 1904;15(1):72–101.
31. Sprent P, Smeeton NC. *Applied Nonparametric Statistical Methods*. 2001.
32. Porter AJ, Racher AJ, Preziosi R, Dickson AJ. Strategies for selecting recombinant CHO cell lines for cGMP manufacturing: improving the efficiency of cell line generation. *Biotechnol Prog*. 2010;26:1455–1464. doi:10.1002/btpr.443.
33. Chaturvedi K, Sun SY, O'Brien T, Liu YJ, Brooks JW. Comparison of the behavior of CHO cells during cultivation in 24-square deep well microplates and conventional shake flask systems. *Biotechnol Rep*. 2014;1–2:22–26. doi:10.1016/j.btre.2014.04.001.
34. Dmitrieva NI, Michea LF, Rocha GM, Burg MB. Cell cycle delay and apoptosis in response to osmotic stress. *Comp Biochem Physiol Mol Integr Physiol*. 2001;130:411–420. doi:10.1016/S1095-6433(01)00439-1.
35. Saito H, Posas F. Response to hyperosmotic stress. *Genetics*. 2012;192:289–318. doi:10.1534/genetics.112.140863.
36. Kumar N, Gammell P, Clynes M. Proliferation control strategies to improve productivity and survival during CHO based production culture: a summary of recent methods employed and the effects of proliferation control in product secreting CHO cell lines. *Cytotechnology*. 2007;53:33–46. doi:10.1007/s10616-007-9047-6.
37. Ginzberg MB, Kafri R, Kirschner M. On being the right (cell) size. *Science*. 2015;348:1245075–1245075. doi:10.1126/science.1245075.
38. Tzur A, Kafri R, LeBleu VS, Lahav G, Marc WK. Cell growth and size homeostasis in proliferating animal cells. *Science*. 2009;325:167–171. doi:10.1126/science.1174294.Cell.
39. Shen D, Kiehl TR, Khattak SF, Li ZJ, He A, Kayne PS, Patel V, Neuhaus IM, Sharfstein ST. Transcriptomic responses to sodium chloride-induced osmotic stress: a study of industrial fed-batch CHO cell cultures. *Biotechnol Prog*. 2010;26:1104–1115. doi:10.1002/btpr.398.
40. Hossler P, Wang M, McDermott S, Racicot C, Chemfe K, Zhang Y, Chumsae C, Manuilov A. Cell culture media supplementation of bioflavonoids for the targeted reduction of acidic species charge variants on recombinant therapeutic proteins. *Biotechnol Prog*. 2015;31:1039–1052. doi:10.1002/btpr.2095.
41. Lindgren K, Salmén A, Lundgren M, Bylund L, Ebler A, Fäldt E, Sörvik L, Fenge C, Skoging-Nyberg U. Automation of cell line development. *Cytotechnology*. 2009;59:1–10. doi:10.1007/s10616-009-9187-y.

Manuscript received Apr. 23, 2017, and revision received Nov. 5, 2017.

SARTORIUS

Application Note

May 20, 2021

Keywords or phrases:
Process Development, Process Efficiencies, Quality Control, Binding Capacity, Dynamic Binding Capacity, Bio-Layer Interferometry, Bioprocessing, Downstream Bioprocessing, Protein Quantitation

Enhancing Efficiency and Economics In Process Development and Manufacturing of Biotherapeutics

Rashi Takkar, Sriram Kumaraswamy

Correspondence
Email: octet@sartorius.com

Abstract

The high costs of discovery, development and production of therapeutic drugs necessitate the need for improved process efficiencies and economics. Analytical tools that circumvent traditional biologics analysis processes such as the need for labeling of reagents while allowing for real time visualization of data can help save development time and facilitate improved efficiencies during process development. Octet® instruments are used in a wide range of applications in process development and biotherapeutics manufacturing; including in early bioprocess development applications such as cell line development and clone selection and in downstream applications such as the determination of dynamic binding capacity for affinity purification columns. The technology's ability to monitor binding interactions in real-time coupled with its capability to analyze samples in their crude matrix and in high throughput can help shorten development and analysis times dramatically lead-ing to significant cost savings. In this application note, insights from Octet ® instrument adopters at GlaxoSmithKline and Aragen Biosciences illustrate multiple examples where the Octet® system has been used to improve process efficiencies and highlights its advantages over HPLC and ELISA in various segments of process development.

Find out more: www.sartorius.com

Introduction

Analytical techniques that measure protein quantity and quality are used in nearly all stages of research, process development and manufacturing of biotherapeutics. UV spectroscopy, ELISA and HPLC have been in use for decades for protein quantitation in physiological and process samples, and continue to be the workhorses despite their many limitations. To characterize the functional activity of proteins during biotherapeutic development, label-free biosensor-based binding assays are increasingly being utilized. The high cost and lengthy times associated with drug discovery and development have forced biopharm companies to improve the efficiency and economics in all stages of development. These key drivers have fueled the search for innovative analytical techniques that provide improved performance and speed without increasing costs. Biopharmaceutical companies have enthusiastically adopted Sartorius' Octet® systems due to their broad utility in protein quantitation and functional characterization combined with enhanced throughput, decreased sample preparation requirements, and low cost of operation. This white paper describes the use of Octet® instruments for protein quantitation, particularly in the areas of process development and quality control.

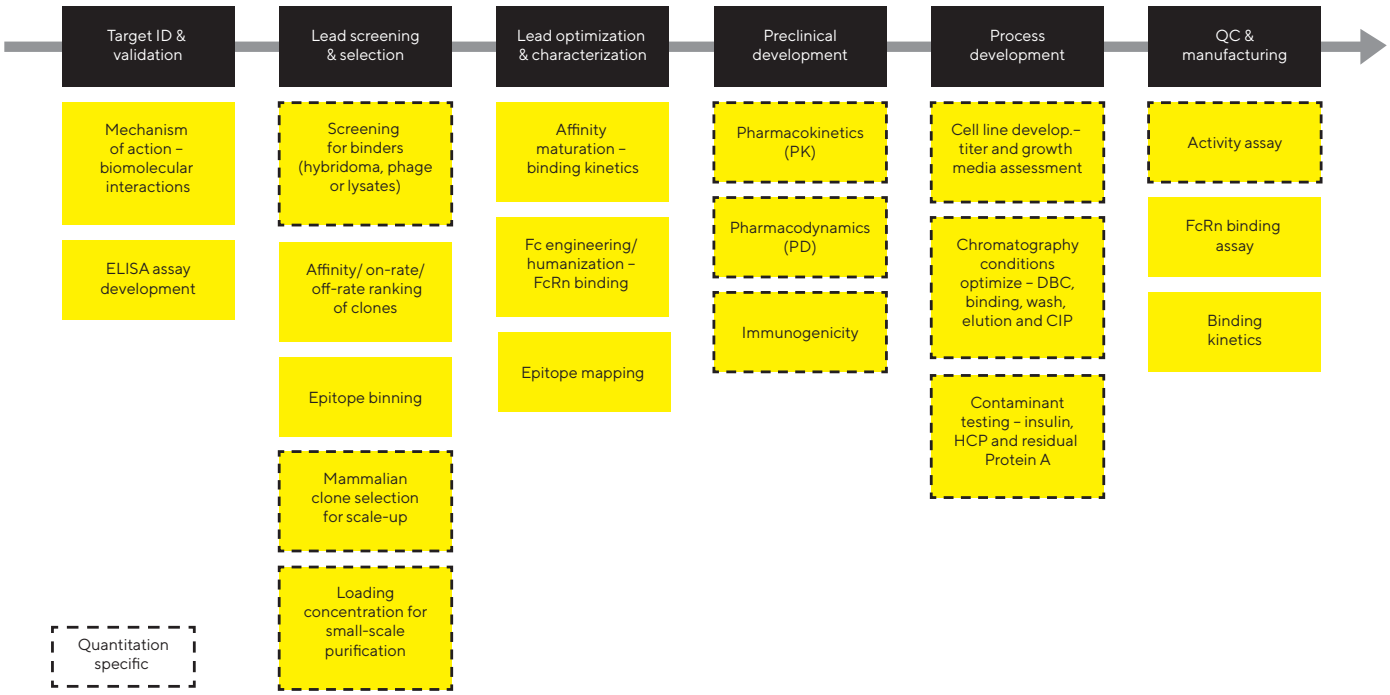

Figure 1: Applications of Octet® instruments in the drug research and development process.

Advantages over ELISA and HPLC

The principles of concentration measurement with an Octet® system are similar to established immunoassays such as ELISA and HPLC. However, protein quantitation protocols on the Octet® platform provide several advantages. The Octet® platform monitors binding of proteins from solution to a biosensor surface in real time, without need for labels or other detection reagents. This real-time monitoring of binding interactions enables clear discrimination between specific and non-specific binding signals, which can shorten assay development times dramatically. Octet® assays are also much faster: quantitation of a 96-well plate requires 15–30 minutes, or 60 minutes for a 384-well plate, depending on the instrument model. Figure 2 provides a comparison of analysis times. Analysis of 70 samples on an Octet® R8 system requires as little as 55 minutes including operator hands-on time, whereas ELISA or HPLC assays require at least 22 hours including several hours of analyst involvement. Samples run on Octet® systems are also recoverable, so that researchers may save and reuse precious sample for other experiments. In addition, Octet® assays are not affected by absorption interferences in colored samples or by light scattering with turbid samples, enabling measurement of analyte concentration in crude matrices such as cell culture supernatant, cell lysate and serum. Octet® concentration assays are complemented by the platform's ability to measure functional activity. For example, titer for a monoclonal antibody (mAb) can be determined using biosensors coated with Protein A, while the functional activity of the mAb can be assessed in a second assay step involving binding to its specific antigen. In contrast, HPLC and A280 spectroscopy can determine only the total protein concentration of a sample, and separate assays must be used to measure biological activity.

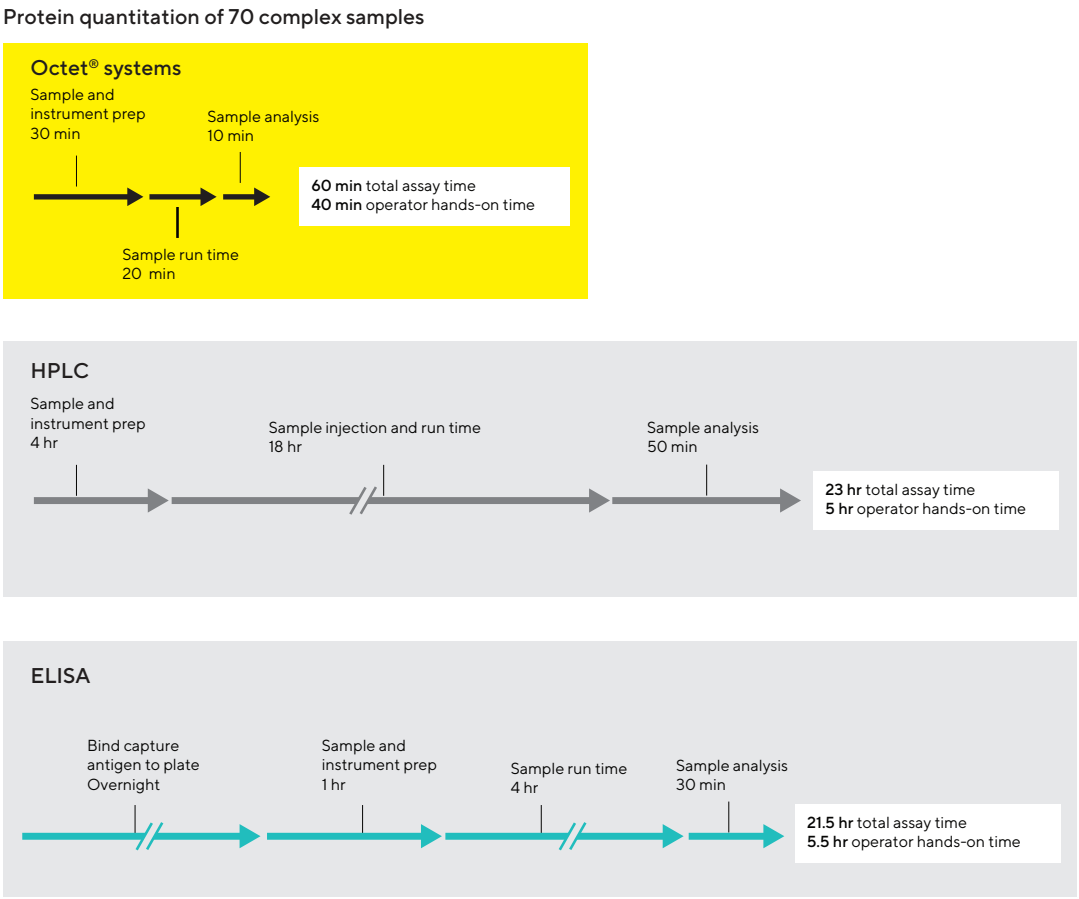

Figure 2: Comparison of protein quantitation in complex matrices using Octet® systems and alternative methods.

Bio-Layer Interferometry Technology (BLI)

BLI technology monitors and analyzes the interference pattern generated from the reflection of white light from two different surfaces: a layer of immobilized protein on the biosensor tip and an internal reference layer (Figure 3). Any increase or decrease in the number of binding molecules to the biosensor surface produces a change in optical thickness that causes a shift in the interference pattern. Unbound molecules in complex matrices and changes in the refractive index of the surrounding medium have minimal effect on the interference pattern. BLI technology simplifies protein quantitation by enabling specific measurement in complex samples. The one-step Dip and Read assay format uses native proteins, without need for labels or secondary reagents.

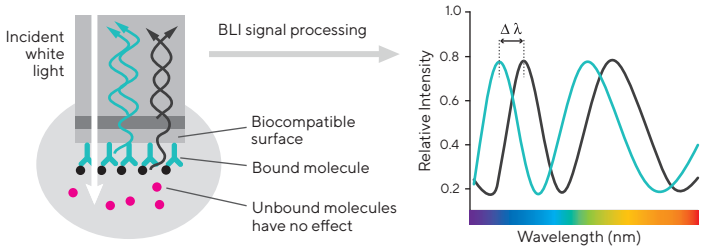

Figure 3: Bio-Layer Interferometry is an optical analytical technique that analyzes the interference pattern of white light reflected from two surfaces. Changes in the number of molecules bound to the biosensor causes a shift in the interference pattern that is measured in real time.

Concentration Measurement

Accurate determination of biologically relevant protein concentrations is essential to several areas in the biopharmaceutical industry including research, bioprocessing, quality control and manufacturing. The Octet® platform uses a simple Dip and Read approach for rapid analysis of samples in 96 and 384-well microplate formats. The concentration of the target protein or antibody in a sample is determined via a direct binding or sandwich assay. Biosensors coated with a capture molecule, called the ligand, are dipped into solutions containing the analyte in a highly parallel, automated method to measure binding interactions. In a typical quantitation assay, a standard curve is generated using known amounts of the protein analyte, and unknown sample concentrations are interpolated from the standard curve (Figure 4). Concentration can be calculated from the initial binding rate of the interaction which is based on the initial slope or from the binding rate at equilibrium.

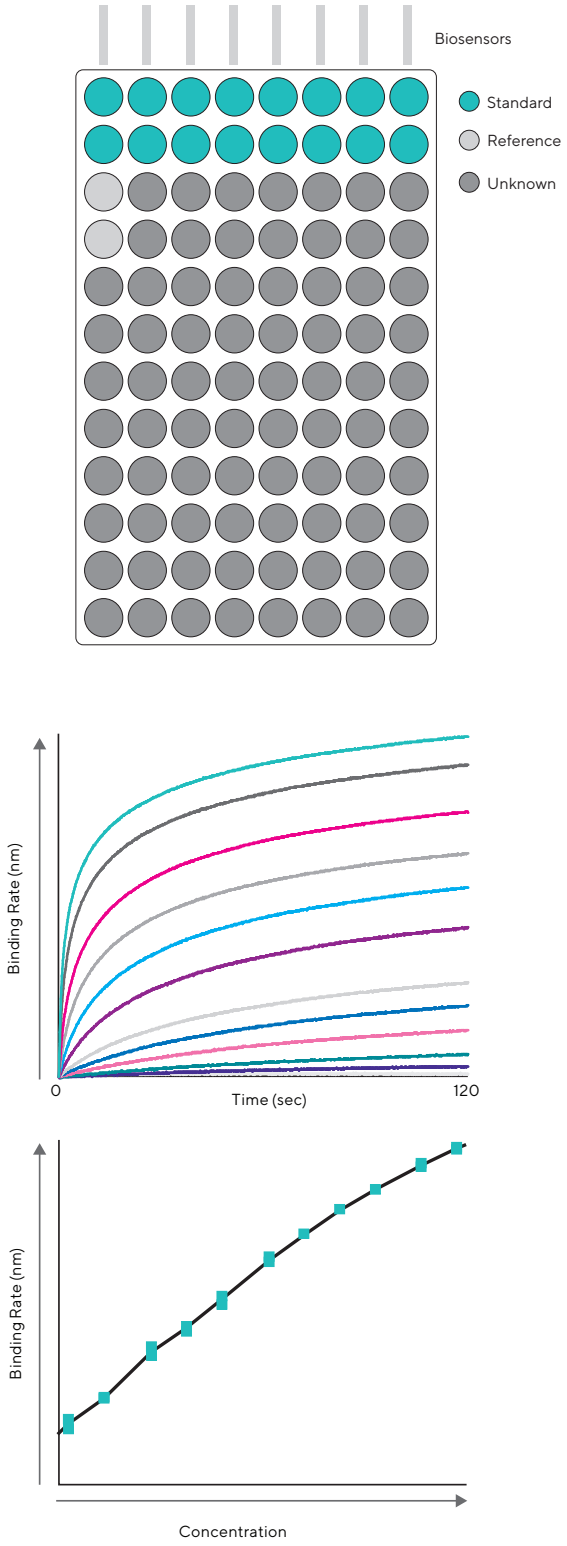

Figure 4: A typical quantitation assay setup. Biosensors dip into standards run in duplicate to obtain binding rate (nm) vs. time (sec) curves. The initial slope of the interaction is used to create the standard curve of the binding rate vs. concentration. The concentration of an unknown sample is then interpolated from the standard curve.

Quantitation Applications for Drug Development

Research and Early Bioprocess Development

The Octet® platform is a useful tool for cost-effective protein expression screening in research and early bioprocess development with several significant benefits.

Octet® platform advantages

- Antibody and protein concentrations can be determined in crude matrices, such as cell lysates or hybridoma supernatants, saving time and resources when processing a large number of samples.
- Octet® assays have a dynamic range of greater than two orders of magnitude, enabling a single quantitation assay to be utilized across all development stages – from early cell culture to production bioreactors.
- Octet® systems perform rapid quantitation with minimal user involvement. 96 samples are analyzed in as little as 20 minutes, and 384 samples in 70 minutes. With additional plate handling automation, Octet® RH16 systems can process more than 1200 samples per day.
- Samples are analyzed in a non-destructive method and are fully recoverable, which is advantageous when working with low sample volumes and precious samples.
- Octet® systems are easy to learn and operate. Multiple analysts can operate the instrument with minimal training, allowing rapid integration of these systems into laboratory workflows.

Early clone selection

In clone selection, thousands of hybridoma or phage clones are screened to determine positive binding clones and their protein secretion levels. Titer measurements are used to select high-producing clones and to normalize the functional activity of these clones in crude matrices. Integration of an Octet® system into the antibody discovery workflow affords increased screening throughput. With Octet® RH16 and Octet® RH96 instruments, automated plate handling can also be added to achieve even higher throughput. Octet® quantitation assays are also used to determine loading levels of chromatography columns for small-scale purification.

Cell line development

Harvest samples are screened on Octet® systems to select high-expressing clones during various scale-up procedures involving 96-, 48-, 24- and 6-well plates, fed batch shake flasks, and bioreactors (Figure 5). Octet® assays also are used to determine protein levels during media development for fed-batch and bioreactor processes (Figure 5). This is performed by comparing protein secretion levels fol-

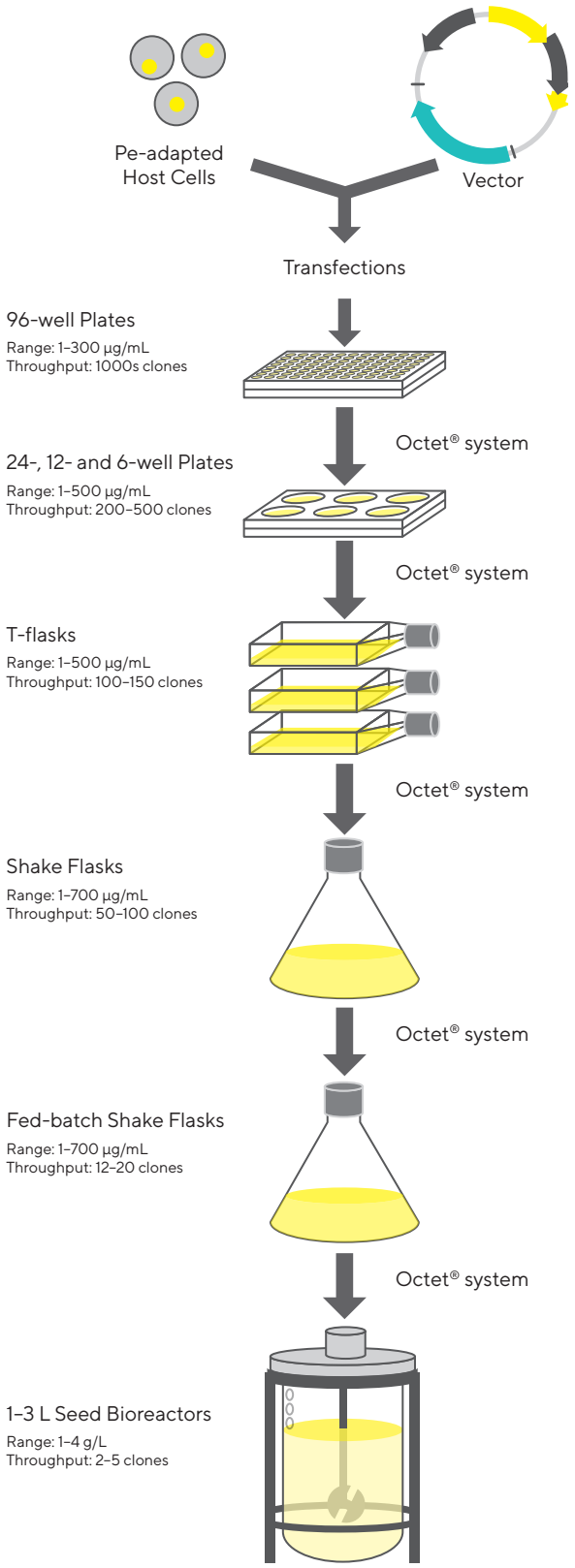

Figure 5: Protein titer assessment and growth media optimization using the Octet® system at different stages of cell line development.

lowing variations in feeding regimes, strategies and concentrations. Data acquisition and subsequent data analysis can be performed rapidly for hundreds of samples, bypassing traditional processing bottlenecks. Please see Sartorius Application Note "Fc-Fusion Protein Quantitation in Cell Culture Supernatants" for more information.

Downstream Process Development

Efficient development of manufacturing processes for antibodies and recombinant proteins is a critical need for biopharmaceutical companies. Increasingly stringent regulatory requirements targeting better understanding and control of manufacturing processes are expected to impact product quality and performance. The Octet® platform can quickly determine the impact of multiple process variables at different stages of the purification process, and help identify optimal conditions that provide protein product with the desired yield, binding specificity and potency (Figure 6). Pre-configured reagents and protocols are available for rapid quantitation of protein products, host cell proteins (HCP), and residual Protein A levels during purification processes.

Octet® platform advantages

- One Octet® instrument can be used to measure protein titer, host cell proteins and residual Protein A contaminant levels.
- Octet® assays are faster to develop and run than ELISA and HPLC assays.
- Octet® assays can be automated with robotic and liquid handling systems for complete, walk-away screening.

Dynamic binding capacity (DBC) of chromatography columns

Affinity chromatography often is the first major purification procedure performed on harvested cell culture samples in downstream bioprocessing. The dynamic binding capacity (DBC) of an affinity chromatography column is defined as the amount of protein that will bind to the column resin under a defined condition. DBC is determined by continuously loading a sample containing a known concentration of target protein and monitoring this protein in the flow-through fractions. Quick determination of DBC using HPLC or A280 spectroscopy is hampered by the presence of large amounts of host cell proteins in the flow-through fractions. Specific detection of the protein of interest among contaminants is straightforward with Octet® systems, reducing the time required to optimize purification conditions (Figure 6).

Binding, wash and elution conditions

Numerous chromatography binding and elution conditions are tested during optimization studies, including different buffer compositions, salt, pH, operating temperature and sample injection volume. High-throughput tools, such as mini columns and 96-well filter plates, often are used to screen these process variables. The impact of different conditions on product titer and quality can be analyzed rapidly and effectively on Octet® systems, speeding identification of optimal chromatography conditions (Figure 6).

Contaminant testing

Downstream purification processes must remove host cell proteins, residual Protein A and residual DNA impurities. According to guidance from regulatory authorities, host cell

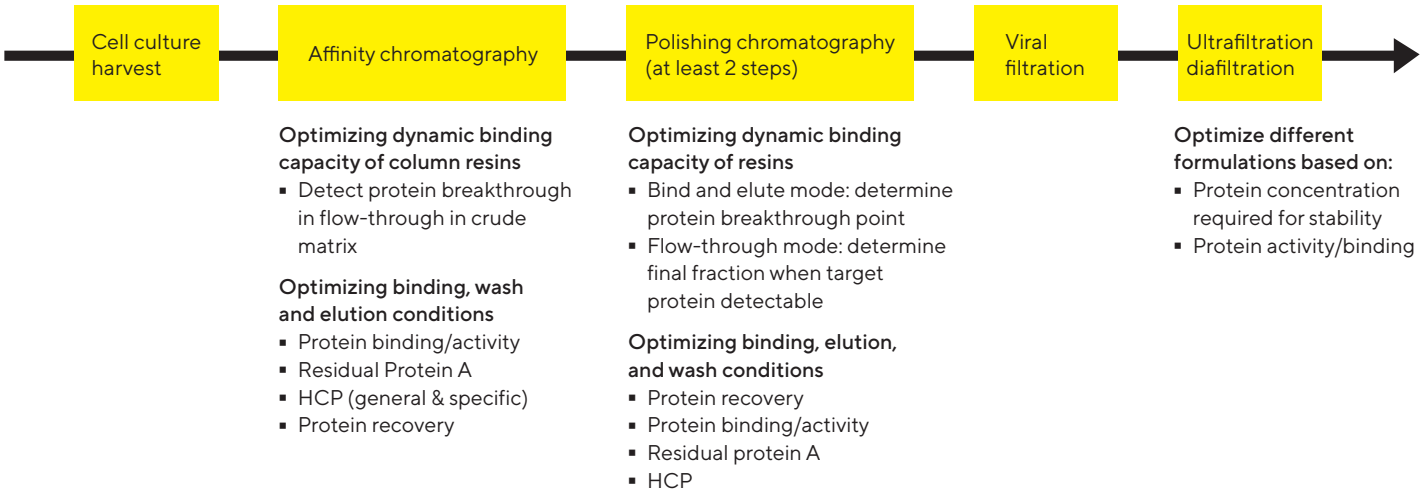

Figure 6: Use of Octet® systems in the downstream purification process of proteins and antibodies.

proteins in a drug substance should be below detectable levels using a highly sensitive analytical method, and as a rule this level should not exceed 100 ppm. The type of assay required for HCP determinations depends on the phase of clinical studies for which the material is produced. For earlier clinical phases, a generic assay may be sufficient. However, a process-specific HCP assay generally is required for phase 3 and later studies. Leached Protein A is another contaminant of concern in process development. The elution of antibodies during Protein A chromatography requires acidic conditions, which in turn can accelerate leaching of Protein A from the column. Residual Protein A levels should not exceed 10 ppm in the final drug product.

Customer Highlight: GlaxoSmithKline

The analytical lab at GlaxoSmithKline incorporated a generic HCP assay on the Octet® QK384 system to streamline their workflow in process development. The automated Octet® HCP assay required minimal analyst intervention and provided more accurate and precise results than their manual ELISA assay (Table 1). Hands-on time for preparation and processing of 1–3 assay plates was reduced to 30 minutes from the previous 2.5 hours with manual ELISA, and antibody consumption decreased by 40%.

More information on the development of the HCP assay on Octet® systems can be found in Technical Note, Host Cell Protein Dectection on the Sartorius website.

Process development assays for residual Protein A and product titer can be fully automated on Octet® RH16 systems using external liquid handling platforms. The Octet® assay for leached Protein A is highly sensitive with a LLOQ of 0.20 ppm, has >2.5 logs of dynamic range, and is faster than competing methods. A residual Protein A assay on the Octet® RH16 system can be completed in 1 hour and 45 minutes per plate with minimal analyst involvement, compared to a minimum of 3.5 hours for ELISA (including significant analyst hands-on time). For more information on the Octet® residual Protein A quantitation protocol, see Technical Note, Dip and Read Residual Protein A Detection Kit on the Sartorius website.

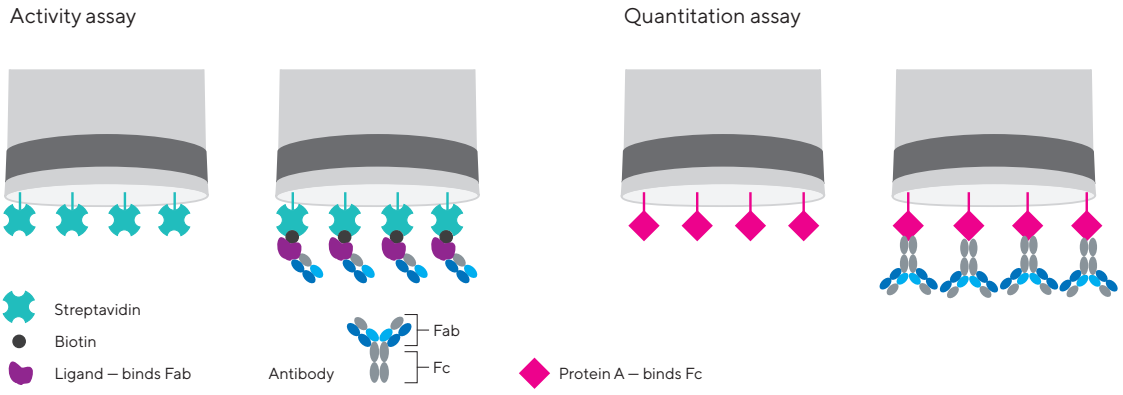

Figure 7: An activity assay can be developed on the Octet® platform by immobilizing a specific biotinylated ligand on the biosensor and then detecting binding of an analyte, Fab or protein. In the quantitation assay, mAb titer is determined using Protein A-loaded biosensors, which does not measure mAb activity towards its target.

Quality Control

Octet® systems provide robust and highly reproducible assays for protein concentration and functional activity, and are suitable for operation in quality control and manufacturing environments. Protein activity and various kinetic assays are used to support in-process testing, drug potency, lot-to-lot variability and stability studies.

Octet® platform advantages

- Octet® systems are designed for GLP/GMP environments, and provide 21 CFR Part 11 compliance tools.
- Octet® assays provide detailed information about the binding behavior of protein products, and reveal subtle differences in binding activity between production lots.

Customer Highlight: Aragen Biosciences

Aragen Biosciences created a stable and scalable CHO cell line, purification platform and manufacturing process for a particular product in a GMP environment. They developed an Octet® assay to compare the activity and quality of a new product lot (Lot 2) with a reference lot (Lot 1) throughout their bioprocess and manufacturing processes. The assay involved loading a biotinylated ligand on Streptavidin Biosensors, and measuring binding interaction of the ligand with the protein analyte. As seen in Figure 8, Lot 2 contained a large second peak that was absent in the Lot 1 reference material. The second peak in Lot 2 exhibited a slower on-rate and much faster off-rate, indicative of a less-active fraction (Figure 9). Octet® system activity data results were confirmed with a cell-based assay, and Aragen was able to modify their production conditions to significantly reduce this second peak fraction.

- Octet® quantitation assays provide a direct measure of the biological activity of the analyte(s) (Figure 7).
- Octet® assays can be easily transferred to manufacturing operations.

Activity assays

An activity assay is generally utilized during process development, QC and manufacturing to compare various prepared lots of the drug molecule, as well as its stability. Activity assays are critical because they differentiate active protein from inactive or clipped variants, as those species will not bind the ligand. Active protein concentration can be determined using a binding assay on the Octet® platform by immobilizing a specific ligand against the target analyte onto the biosensor, and then measuring its binding interaction with the analyte as shown in Figure 7.

Benefits of automated Octet® CHO HCP assay compared to manual ELISA

Benefit	Details
Precision	Liquid handling robot reduces pipetting variation inherent in manual pipetting
Reliability	Method performed exactly the same each time
Streamlined process	Worklist drives robotic method and creates sample plate importation files Robotic method automatically creates and executes Octet® method file
Walk away	No analyst intervention needed to complete method after instrument loaded and diluent volumes are checked
Washing steps	No washing steps needed and plate washer integration not required
Analysts involvement	Automated Octet® → ~30 minutes for 1–3 assay plates Manual ELISA → ~2.5 hours per assay plate
Throughput	3 assay plates can be run in ~5 hours 38 samples/plate in duplicate wells > 108 samples in 3 plates
Antibody consumed	Re-use of coating antibody can significantly reduce consumption over multiple assay plates

Table 1: Benefits of automated Octet® CHO HCP assay compared to manual ELISA summarized by GSK.

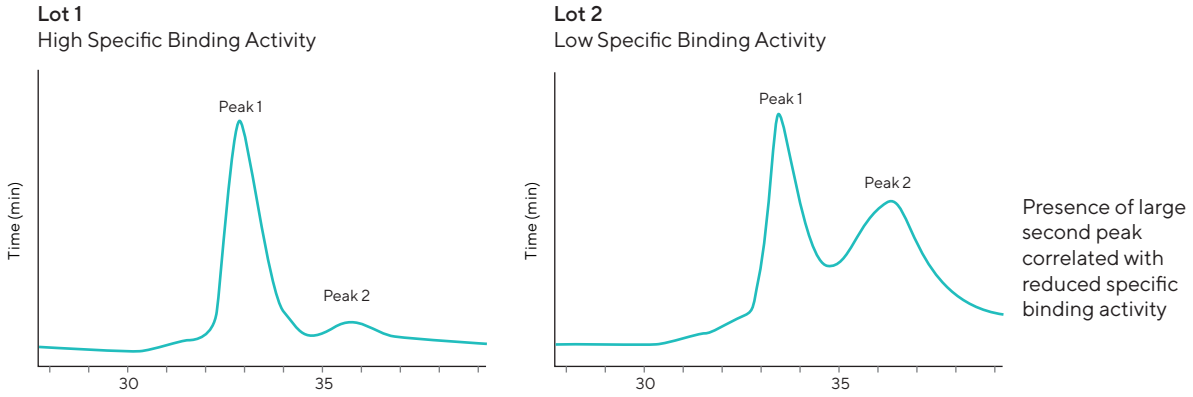

Figure 8: HPLC spectra of Lot 1 and Lot 2 of a drug molecule. Lot 2 was made by Aragen Biosciences and had an additional peak (Peak 2) compared to the reference lot (Lot 1) provided by their customer. Data provided courtesy of Aragen Biosciences.

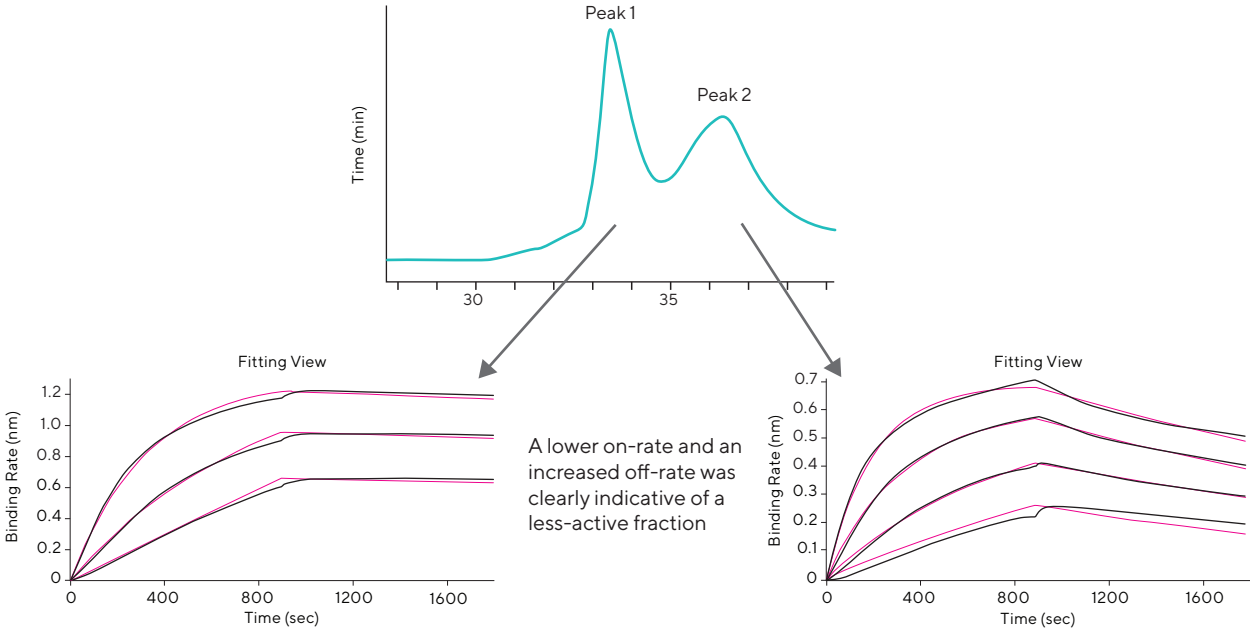

Figure 9: The Octet® binding kinetics or functional assay demonstrated that Peak 1 was the active fraction. Peak 2 was the less-active fraction, with a lower on-rate and a much faster off-rate in a binding experiment. Data provided courtesy of Aragen Biosciences.

Conclusion

Octet® systems deliver comprehensive characterization of biotherapeutics, as well as rapid and reproducible determination of protein concentrations during different stages of the development process. Titer and functional activity assays on Octet® systems are useful for a broad array of applications in target identification, lead selection, process development, formulation development, quality control, and manufacturing. In early stages of drug development, Octet® systems provide the high throughput needed to screen through large libraries of candidate drug molecules.

In later stages of process development and manufacturing, Octet® systems provide the required reliability, robustness and measurement accuracy. The broad utility of this single platform makes the Octet® instrument unique in its ability to deliver high value across a wide range of application needs in biopharmaceutical discovery, development and manufacturing processes.

Germany
Sartorius Lab Instruments GmbH & Co. KG
Otto-Brenner-Strasse 20
37079 Goettingen
Phone +49 551 308 0

USA
Sartorius Corporation
565 Johnson Avenue
Bohemia, NY 11716
Phone +1 888 OCTET 75
Or +1 650 322 1360

For further contacts, visit
www.sartorius.com/octet-support

AN-4011 Rev C